Doctoral Dissertation

Reconfigurable Multi-layer and Multi-granular Photonic Transport Network Design

KADOHATA Akihiro

Department of Electrical Engineering and Computer Science
Graduate School of Engineering
Nagoya University

2016

Acknowledgments

This dissertation completes my achievements of research activities at Department of Electrical Engineering and Computer Science, Graduate School of Engineering, Nagoya University, under the supervision of Prof. Ken-ichi Sato and Associate Prof. Hiroshi Hasegawa. I would like to express my deepest gratitude to Prof. Ken-ichi Sato and Associate Prof. Hiroshi Hasegawa for fruitful suggestions and continuous encouragements.

I would like to express my sincere gratitude to Prof. Masaaki Katayama at Nagoya University and Prof. Eiji Oki at the University of Electro-Communications for reviewing this dissertation carefully and providing valuable advices.

This dissertation was supported by NTT Network Innovation Laboratories. I would like to appreciate my supervisors, Mr. Akira Hirano and Mr. Atsushi Watanabe for providing a lot of valuable advices and supports. I also would like to appreciate Dr. Ryutaro Kawamura and Mr. Mitsuhiro Teshima for giving me an opportunity to receive Ph. D. degree at Nagoya University while working for NTT. I also would like to appreciate my former supervisor, Dr. Wataru Imajuku for instructing various knowledges and experiences.

Furthermore, I would like to thank to my colleagues of the Networking Systems Research Group, Mr. Fumikazu Inuzuka, Mr. Yoshiaki Sone, Mr. Takafumi Tanaka and Mr. Takuya Oda for valuable discussion. I am grateful to all the members of the Photonic Transport Network Laboratory for giving me comfortable environments.

Finally, I would like to thank my beloved family and wife, Mami, for their kind supports and encouragements.

Contents

Glossary of Acronyms

ATM	Asynchronous Transport Mode
CAPEX	CAPital EXpenditure
CDC-less	Color-less, Direction-less, Contention-less
DXC	Digital Cross Connect
EDFA	Erbium Doped Fiber Amplifier
FEC	Forward Error Correction
FF	First Fit
IF	InterFace
IP	Internet Protocol
IRWA	Impairment awareness Routing and Wavelength Assignment
LSP	Label Switched Path
MPLS-TP	Multi-Protocol Label Switching - Transport Profile
NMS	Network Management System
NNI	Network Node Interface
OAM	Operation, Administration, and Maintenance
OCh	Optical Channel
ODU	Optical channel Date Unit
OEO	Optical-Electrical-Optical
OMS	Optical Multiplex Section
OPEX	OPerational EXpenditure
OSNR	Optical Signal to Noise Ratio
OTN	Optical Transport Network
OTU	Optical channel Transport Unit
PDH	Plesiochronous Digital Hierarchy
PTS	Packet Transport System
3R	Reshaping, Retiming and Regenerating
ROADM	Reconfigurable Optical Add/Drop Multiplexer
RWA	Routing and Wavelength Assignment
SDH	Synchronous Digital hierarchy
STM	Synchronous Transport Module
TDM	Time Division Multiplex
ILP	Integer Linear Programming
UNI	User Node Interface
WDM	Wavelength Division and Multiplexing
WSS	Wavelength Selective Switch
WXC	Wavelength Cross Connect

List of Parameters

Symbol	Description
C	Set of combination of failure status for nodes and links, $c \in C$.
C_{CI}	Cost of OCh-IF (=0.22).
C_{DI,c_S}	Cost of ODU-IF for ODU paths, $C_{DI,2.5G(ODU-1)}$=0.25, $C_{DI,10G(ODU-2)}$=0.67, $C_{DI,40G(ODU-3)}$=1.67.
C_{DX}	Cost of ODU-XC (=26.6).
C_F	Cost parameter of wavelength fragmentation, $0 \leq C_F \in \mathbb{R}$.
C_{FI}	Cost of fiber expansion, $0 \leq C_{FI} \in \mathbb{R}$.
$CI^w_{(i,j)}$	Number of OCh-IF with wavelength channel w in link (i, j), binary.
C_{MI}	Cost of OTM-IF (=8.99).
C_S	Set of capacity of sub-lambda path, $c_S \in C_S$.
C_T	Cost of transponder (=3.75).
C_W	Capacity of wavelength path.
C_{WX}	Cost of the WXC (=2.50).
C_{WR}	Cost parameter of wavelength path reconfiguration, $0 \leq C_{WR} \in \mathbb{R}$.
$DI_{(m,n),c_S}$	Number of ODU-IF of ODU types c_S between (m, n), binary.
D_S	Set of sub-lambda path demands, $d_S \in D_S$.
D_W	Set of wavelength path demands, $d_W \in D_W$.
DX_m	Number of ODU-XC in node m.
E	Set of links, $\{e, (i, j), (j, k)\} \in E$.
$f(e)$	Number of fibers in the link e or (i, j), $0 < f(e) \in \mathbb{Z}$.
F	Set of fibers, $f \in F$.
F_0	Set of used fibers for a wavelength path d_W before reconfiguration in wavelength w and link (i, j), $f \in F_0 \subset F$.

Symbol	Description
$G(V, E)$	Physical network topology.
K	Set of routes from source to destination, $k \in K$.
$M_{m,f}$	Number of multiplexer/demultiplexer capability connecting fiber f in node m, $1 \leq M_{m,f} \in \mathbb{Z}$.
$MI_{(i,j)}$	Number of OTM-IF is connected to link (i, j).
N_{DPM}	Maximum number of ODU-IF ports (=32)
N_{DP,c_S}	Number of ODU-IF slots that use ODU path, $N_{DP,2.5G(ODU-1)}$=1/16, $N_{DP,10G(ODU-2)}$=1/4, $N_{DP,40G(ODU-3)}$=1.
N_{WM}	Number of wavelengths multiplexed in a fiber.
$p_{(m,n),w}$	Binary, $p^{(m,n),w} = 1$, if wavelength path is assigned between (m, n) using any wavelength w, otherwise 0.
$p_{(i,j)}^{(m,n),w}$	Binary, $p_{(i,j)}^{(m,n),w} = 1$, if wavelength path is assigned wavelength w in link (i, j) between (m, n), otherwise 0.
$p_{0(i,j)}^{(m,n),w}$	Binary, $p_{0(i,j)}^{(m,n),w} = 1$, if an existing wavelength path between (m, n) routed through fiber link (i, j) on wavelength w, otherwise 0.
$p_{(i,j),f}^{(m,n),w,d_W}$	Binary, $p_{(i,j),f}^{(m,n),w,d_W} = 1$ if wavelength path d_W between (m, n) uses wavelength w in link (i, j) and fiber f; otherwise, 0.
$p_k^{(m,n),w}$	Binary, $p_k^{(m,n),w} = 1$ if wavelength path is accommodated between (m, n) uses wavelength w in the kth route in the wavelength w; otherwise, 0.
$p_{0\ k}^{(m,n),w}$	Binary, $p_{0\ k}^{(m,n),w} = 1$ if existing wavelength path is accommodated between (m, n) uses wavelength w in the kth route in the wavelength w; otherwise, 0.
P_S	Set of source and destination nodes for an end-to-end sub-lambda path, $(s, d) \in P_S$.
P_W	Set of originating and terminating nodes for a wavelength path, $(m, n) \in P_W$.
RR_n	Number of receivers at node n.
$s_{(m,n)}^{(s,d),c_S,d_S}$	Number of c_S low-speed sub-lambda path d_S between (s, d) employing wavelength path between (m, n) as an intermediate virtual link.
$s_{0(m,n)}^{(s,d),c_S,d_S}$	Number of existing c_S low-speed sub-lambda path d_S between (s, d) employing wavelength path between (m, n) as an intermediate virtual link.

Symbol	Description
T_m	Number of transponder exists in node m.
TR_m	Number of transmitters at node m.
$v_{(m,n)}$	Number of wavelength paths between (m, n) in virtual topology.
$v^w_{(m,n)}$	Number of wavelength paths between (m, n) on wavelength w.
V	Set of nodes, $\{i, j, k, m, n, s, d\} \in V$.
w_e	Number of wavelengths in link e.
w_r	Number of wavelengths required.
W	Set of wavelength, $w \in W$.
X	Set of link and node, $x \in X$.
Y	Set of route, $y \in Y$.
$\delta^{(m,n)}_{k,e}$	Binary, $\delta^{(m,n)}_{k,e} = 1$ if the kth route includes link e between (m, n); otherwise, 0.
$\lambda^w_{(m,n)}$	Binary, $\lambda^w_{(m,n)}$ =1, if wavelength path is assigned between (m, n) using any wavelength w, otherwise 0.
$\lambda^{w,d_W}_{(m,n)}$	Binary, $\lambda^{w,d_W}_{(m,n)}$ =1, if wavelength path d_W is assigned between (m, n) using any wavelength w, otherwise 0.
$\Lambda_{(m,n)}$	Number of wavelength path demands between (m, n).
$\sigma^{c_S,d_S}_{(s,d)}$	Number of sub-lambda path d_S having capacity c_S between (s, d).
$\phi(c)$	Communication status of combination of failure status c between source and destination nodes.

List of Figures

List of Tables

Chapter 1

Introduction

To assist the reader in understanding the value of this dissertation, this chapter presents the background and includes present and future traffic trends, and the history of transmission technology as well as path layer technology including standardization activities. The target and assumption of transport path are explained. After that, the goals and the contributions of this study are described. Finally, organization of the dissertation is shown.

1.1 Background

The Internet can be accessed from any where in the world thanks to the proliferation of broadband services such as inexpensive Asymmetric Digital Subscriber Line (ADSL), high capacity Fiber To The Home (FTTH), and high mobility wireless access. The Internet has become one of the most indispensable social infrastructures as it allows humans to communicate with each other, to enjoy movies and games, to conduct business, to acculturate our society and so on. Recent video technologies such as Internet Protocol (IP) TV and high-definition and ultrahigh-definition TV continue to advance and have gained wide acceptance. More advanced video applications that include 3D TV and cutting-edge applications including e-science, all of which need enormous bandwidth, have been conceived [1]. The amount of Internet traffic in the backbone network has drastically increased with the different communications and recent video technologies.

Figure 1.1 shows the amount of a forecast of global Internet traffic (2014 to 2018) [2, 3]. Figure 1.1 (a) shows the global consumer IP traffic for the key categories of online gaming, file sharing, web, email, and data, and Internet video. Internet video streaming and downloads are beginning to consume a larger share of the bandwidth and will grow to more than 80 percent of all consumer Internet traffic. As another forecast, Figure 1.1 (b) shows the global data center IP traffic. Data center IP traffic by 2018 will drastically increase to about 8,000 Exabytes with the enhancement of cloud application services, and more than three-fourths of the entire workloads will be processed in cloud data centers due to the faster delivery of services and data. Data center traffic will continue to dominate Internet traffic for the foreseeable future. Recent advances in cellular phone technology

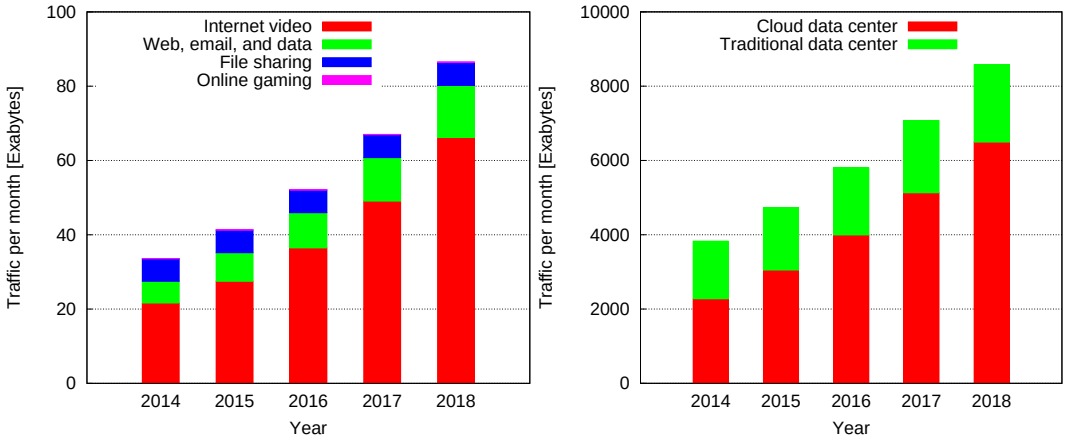

(a) Global consumer IP traffic. (b) Global data center traffic.

Figure 1.1. The amount of global Internet traffic.

such as Long Term Evolution (LTE) will also support another traffic trend by high mobility and heavy loads [4]. These changes of relentless increases tendencies in quasi-dynamic and multi-granular traffic will certainly continue in the future.

1.1.1 Digital Transmission Technology

Digital transmission technology has been developed to realize higher capacities and longer transmission distances [5–7]. A brief history of digital transmission technology is given here [8]. Digital transmission started with the invention of Pulse Code Modulation (PCM) by A. H. Reeves in 1937 [9]. PCM based transmission using Time Division Multiplexing (TDM) was achieved for the first time in the world by Bell Labs in 1962 using balanced pair cable [10]. In Japan, a 1.5 Mbit/s commercial system, PCM-24, was deployed by NTT in 1965. After that, a 400 Mbit/s commercial system, DC-400M, was deployed in 1975 on coaxial cable. A significant event was the proposal of optical fiber communication over a glass rod by Seki and Negishi in 1936. The next advancement was proposal by K. C. Kao in 1966 to establish optical fiber communication on low loss optical fiber made of purified silica glass [11]. Practical optical fiber with loss under 0.2 dB/km was a major advance in implementation techniques in 1976 [12].

Figure 1.2 shows the history of optical fiber transmission technology as it impacts the capacity of optical networks. Three key technologies are now used to achieve higher capacity and longer distance. Electrical time division multiplexing (ETDM), the first generation of optical fiber communication technology, bundles multiple lines into one shared line. F-32M, a 32 Mbit/s commercial system, was deployed for short distance communication in 1981 [13, 14]. The combination of single-mode optical fiber and long wavelength lasers yielded F-400M, which was deployed between Asahikawa and Kagoshima. 600 Mbit/s, 2.4 Gbit/s and 10 Gbit/s commercial systems based on the interface of 156 Mbit/s were developed in conjunction with the standardization of the Synchronous Digital hierarchy (SDH).

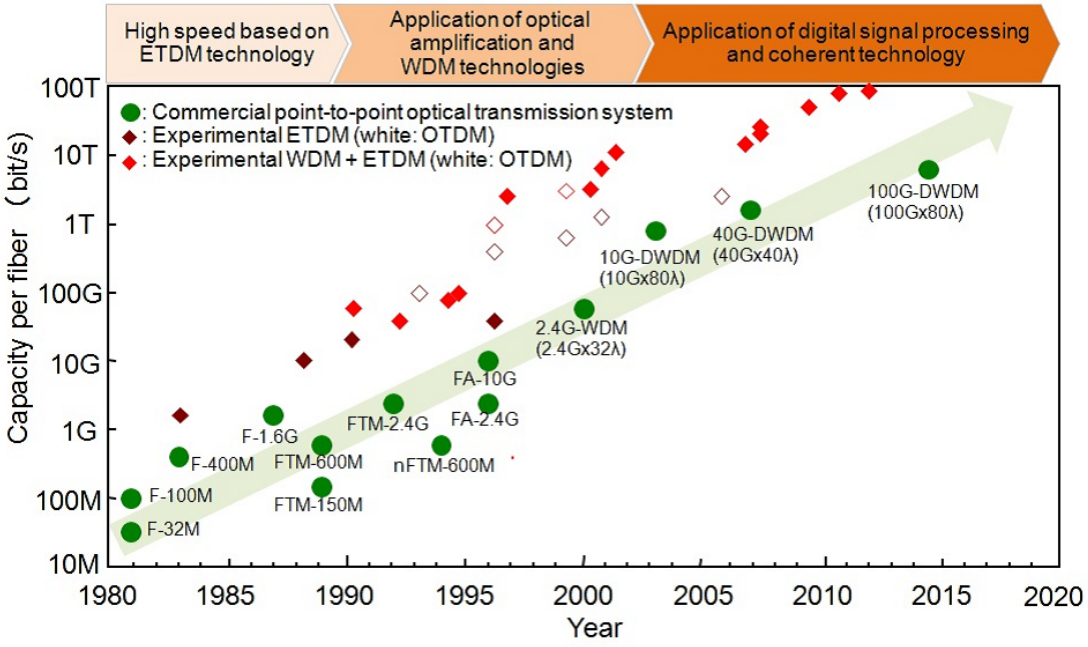

Figure 1.2. Developments in transport technologies for enhancing speed and capacity.

The second generation of optical fiber communication technology is dominated by dense wavelength division multiplexing (DWDM) and optical amplifiers such as the erbium-doped fiber amplifier (EDFA), which adds erbium ions to the optical fiber core. 2008 saw th release of a 1.6 Tbit/s DWDM transmission system that multiplexes 40 λ each carrying a 40 Gbit/s signal, and an 800 Gbit/s (10 Gbit/s $\times$ 80 λ) reconfigurable optical add/drop multiplexer (ROADM) transmission system used to construct 10 Gbit/s optical signal add/drop optical ring networks [15]. The third generation of optical fiber communication technology revolves around digital signal processing and coherent detection, called digital coherent technology, which improves receiver sensitivity and spectral efficiency while also significantly improving dispersion-compensation performance before and after long-distance transmission. In 2015, a 100 Gbit/s packet transport system (100G-PTS) was developed by NTT as the next generation optical transport system [16]. 100G-PTS can achieve a maximum capacity of 8 Tbit/s by multiplexing 80 λ, each carrying a 100 Gbit/s signal.

1.1.2 Path Layer Technology

Path layer technology has been developed with digital transmission technology. The history of this is described in Fig. 1.3. In the 1980s, the Plesiochronous Digital Hierarchy (PDH) using staff multiplexing was deployed that allows the streaming of data to synchronize the signal exchanges. There were three main issues. First, there was no international agreement as to the three different hierarchies so interconnecting countries was difficult. Second, it could not demultiplex directly from high speed signal to low speed signal less than two layer. Third,

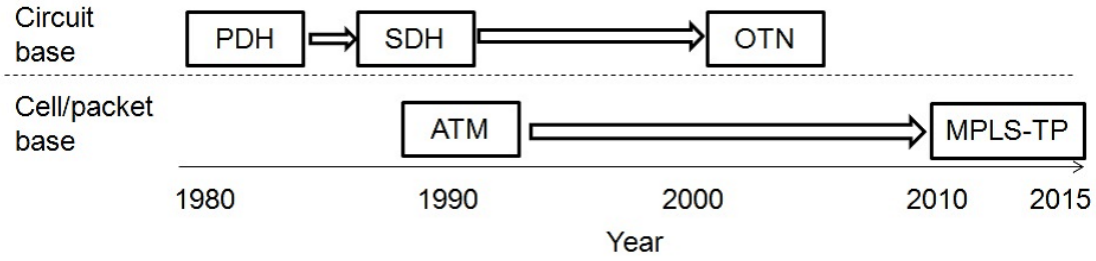

Figure 1.3. Developments of path layer technologies.

Operation, Administration, and Maintenance (OAM) had some constraints due to the paucity of overhead bits. To cope with those issues, SDH was standardized in 1988 [17]. It was originally designed to establish circuit mode communications where two network nodes established a dedicated communications channel (circuit) through the network. The hierarchy was internationally unified based on Synchronous Transport Module Level One (STM-1) of 155.52 Mbit/s. It permitted the direct multiplexing or demultiplexing low speed digital paths and made cross-connection easier to achieve. The network operation function was strengthened to have overhead each section and path layer, which allowed transmission and quality to be controlled in each layer. The Optical Transport Network (OTN), based on the idea of SDH was standardized for Layer 1 in 2001, [18]. The structure of OTN is similar to that of SDH. The biggest difference between OTN and SDH is that SDH was defined with fixed frame rates, while OTN was defined with fixed frame sizes. This fundamental change makes mapping IP-based traffic into OTN much more efficient than is possible with SDH and so provide a practical way to cope with the change in traffic from voice or telephone centric to data one. In another development, the cell based transport protocol called Asynchronous Transfer Mode (ATM) was standardized in 1990. Compared to circuit switching style of SDH, ATM of store & forward has a strong point that different bit rates and burst traffic could be accommodated more efficiency and a weak point that delay occurs according to increasing size of cell. In 2012, Multi-protocol Label Switching - Transport Profile (MPLS-TP) was standardized for Layer 2 as a next generation packet based transport protocol to cope with increasing IP/Ethernet-based traffic [19]. MPLS-TP will provide with a reliable packet-based technology that is based upon circuit-based transport networking and accommodate from low granularity traffic and high one.

1.1.3 Standardization of OTN and MPLS-TP

The OTN provides optical communication technologies suitable for the WDM systems adopted by ITU-T [20]. In 2001, three bit rates, Optical channel Date Unit (ODU)-1 (2.5 Gbit/s), ODU-2 (10 Gbit/s), and ODU-3 (40 Gbit/s), were specified in the OTN standard to match SDH bit rates. An additional bit rates, ODU-4 (100 Gbit/s) was specified in 2007. The network architecture defined in [21] that is composed of the Optical Channel (OCh), Optical Multiplex Section

(OMS) and Optical Transmission Section (OTS). The interface of OTN was defined in ITU-T Rec. G.709 to implement OCh by means of a digital framed signal with digital overhead that supports management requirements [18]. Two digital layer networks, ODU and Optical Transport Unit (OTU), were introduced. The intention was that all client signals would be mapped into the OCh via the ODU and OTU layer networks. The principal information containment relationships are described in Figure 1.4.

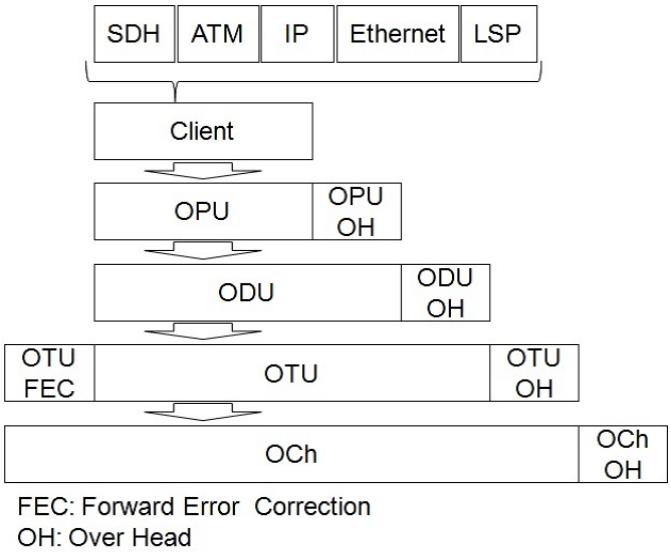

Figure 1.4. Frame structure of OTN

A packet-based technology that can accommodate packet-based data more efficiently than current SDH or OTN has been an urgent requirement because packet-based traffic has become dominant in these networks as the number of IP-based services [22]. However, traditional packet network technologies are problematic for adoption by telecommunication carriers because of a lack of sufficient OAM functions, fault localization, and fast switching in the event of a failure. Thus, a new packet-based transport network technology that has the same operation and maintenance capabilities as traditional transport network technology is required [19, 23, 24]. MPLS has been standardized in IETF to make it possible to explicitly determine the path route of IP packets by attaching a label to each IP packet and forwarding each packet by inspecting only the label instead of the IP address header on the label-switched path (LSP) [22]. MPLS, however, does not have ofter all of the maintenance functions required in transport networks. Some conventional MPLS functions including penultimate hop popping (PHP), equal cost multi-path (ECMP), and label merging could disrupt the management of a connection-oriented path because of a lack of traceability. Moreover, MPLS can be controlled by the control plane through a soft state procedure that any fault occurs during the exchange of control messages in the data plane even though they are not experiencing a failure. It is difficult to secure user data traffic.

To modify weakness features and extend conventional MPLS, MPLS-TP em-

phasizes operation and maintenance capabilities by improving the data plane control mechanism, introducing static and central operations by the management plane, and implementing various OAM functions and high-speed protection switching as shown in Fig. 1.5 [22]. A generic associated channel label (GAL) is newly defined in the MPLS header stack for identifying the OAM packet, and each OAM function is differentiated by an associated channel (ACH). Existing functions such as Pseudo Wire Emulation Edge-to-Edge (PWE3) and MPLS forwarding are also available in MPLS-TP.

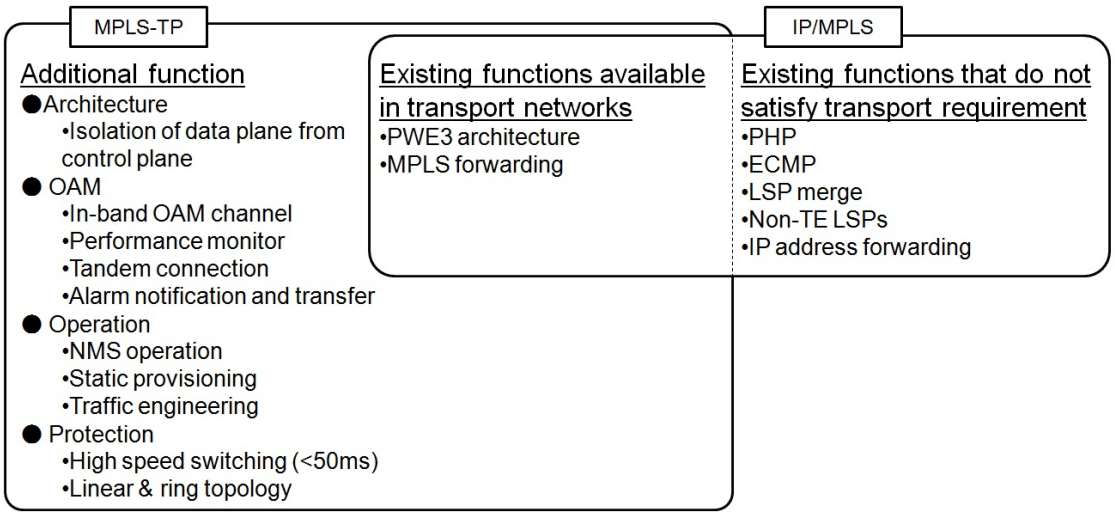

Figure 1.5. Difference between MPLS-TP and IP/MPLS.

1.1.4 Transport Path for WDM Networks

In the wavelength layer, there are two optical path schemes: wavelength path scheme and virtual wavelength path scheme [25]. The wavelength path uses the same wavelength between source and destination nodes. Therefore, assigning wavelengths is complicated due to the wavelength continuity constraint [26]. On the other hand, the virtual wavelength path assigns wavelengths link-by-link. Therefore, virtual wavelength paths offer greater accommodation efficiency than wavelength paths. However, virtual wavelength paths demand the use of wavelength converters or Optical-Electrical-Optical (OEO) conversion which increases equipment cost. This dissertation targets the wavelength path scheme as optical path in wavelength layer.

In the sub-lambda (or electrical) layer, which sub-lambda path corresponds to ODU path and LSP in MPLS-TP, it is cost effectively that traffic less than the bandwidth of a wavelength path is accommodated to sub-lambda paths. The accommodation of wavelength path combined with sub-lambda path is cost effective solution for multi-granular traffic. This dissertation targets sub-lambda path over wavelength path multi-layer transport networks.

1.2 Purpose of This Study

The optical reach without OEO conversion has been extended as a result of the introduction of digital coherent technology [5–7]. Therefore, a lot of 3R (Reshaping, Retiming and Regenerating) transponders can be reduced. However, the wavelength continuity constraint for wavelength path states that the same wavelength must be assigned from the source to the destination node. Figure 1.6 shows the wavelength channel to fiber link that occurs wavelength fragmentation in some wavelength channels [27,28]. Wavelength fragmentation, which is similar to storage fragmentation, increases and the wavelength accommodation efficiency degrades.

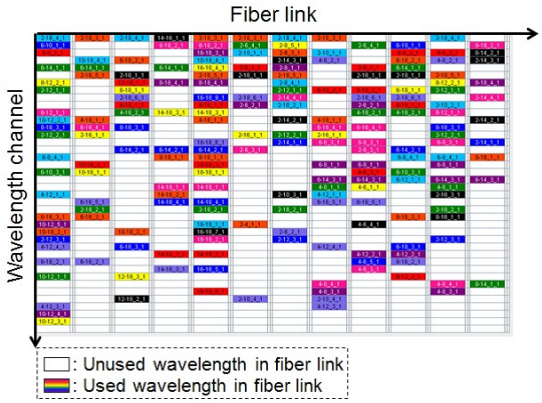

Figure 1.6. Image of wavelength fragmentation.

On the other hand, to simplify path layer and to decrease the number of electrical switch such as IP router, ODU over WDM and MPLS-TP over WDM have been proposed that IP, Ethernet, ATM, and SDH are mapped into ODU or LSP in MPLS-TP [16, 29]. Those can be reduced process of upper layer than ODU layer or MPLS-TP layer and also reduced electrical consumption. However, the virtual topology for cost minimization in the sub-lambda layer is changing according to traffic fluctuations [30]. Figure 1.7 shows the image of sub-lambda path and wavelength path accommodation. The figure at left shows that sub-lambda paths are accommodated in multiple wavelength paths, i.e., a multi-hop sub-lambda path. The figure at right shows that sub-lambda paths are accommodated in a single wavelength path, i.e., a single-hop sub-lambda path. Figure 1.7 (a) shows an example when the volume of traffic is small and traffic emerges from different locations. As shown in Fig. 1.7 (a) at left, the number of wavelength paths is 2 and the number of wavelengths in link is 4. As shown in Fig. 1.7 (a) at right, the number of wavelength paths is 2 but the number of wavelengths in link is 5 larger than that in multi-hop sub-lambda path. In this example, multi-hop sub-lambda path can reduce the number of wavelengths in link. Figure 1.7 (b) shows an example when the traffic volume increases at the same source and destination nodes. As shown in Fig. 1.7 (b) at left, the number of wavelength paths is 2 and the number of wavelengths in link is 4. As shown in Fig. 1.7 (b) at right, the number of wavelength paths is 1 smaller than that in multi-hop sub-lambda path and the number

of wavelengths in link is 4 as same as that in the multi-hop sub-lambda path. In this example, single-hop sub-lambda path can reduce the number of wavelength paths. Thus, optimized virtual topology in sub-lambda layer, i.e., accommodation design for cost minimization as single-hop or multi-hop, is changing according to how much the amount of traffic and where between nodes traffic emerge.

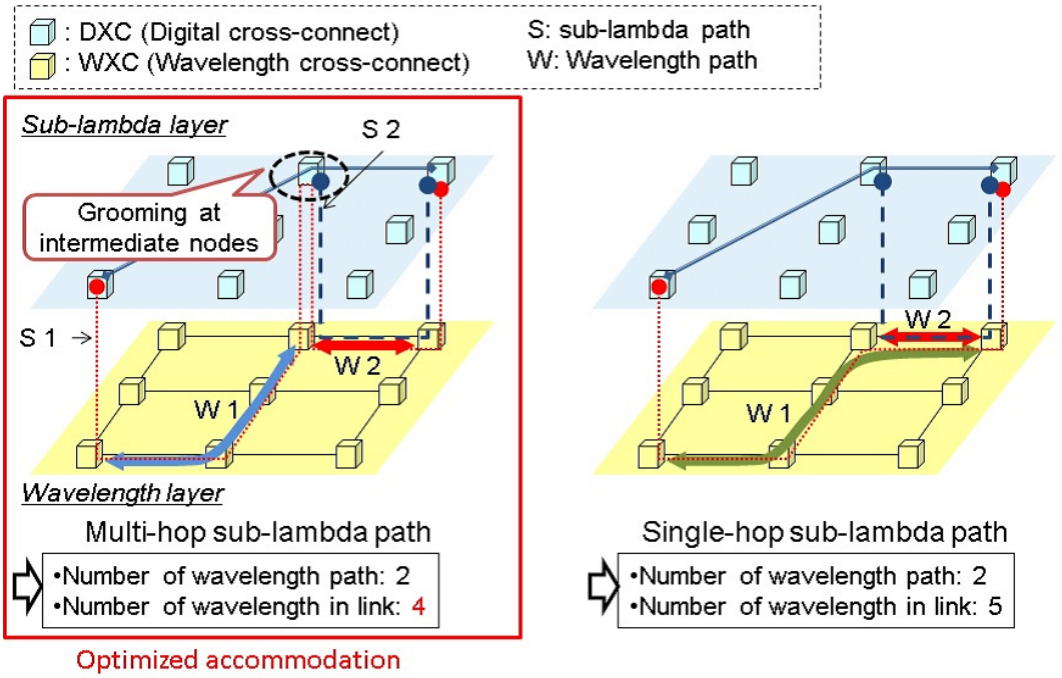

(a) Example when the volume of traffic is small and traffic emerges from different locations.

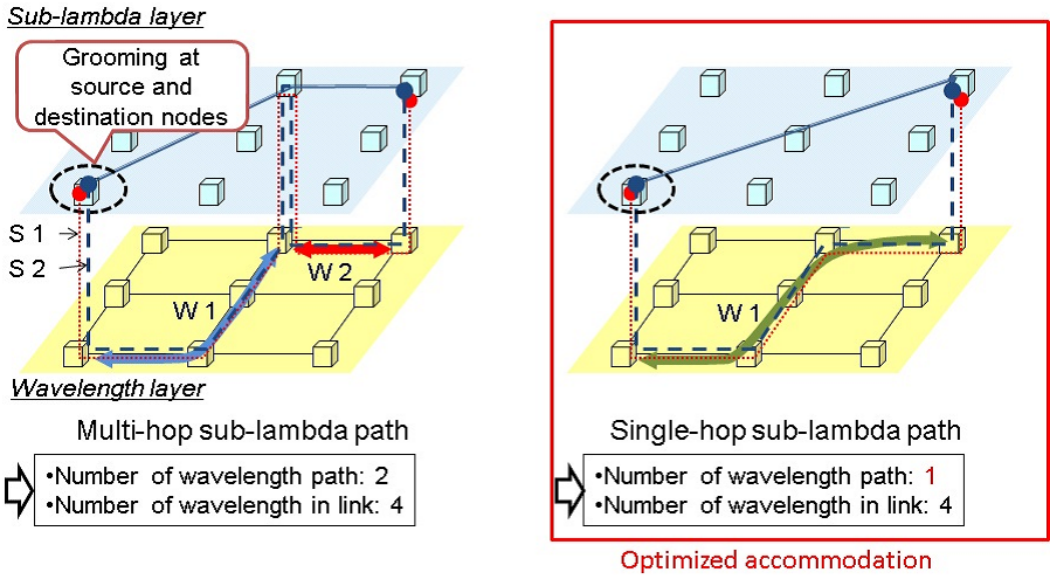

(b) Example when the traffic volume increases at the same source and destination nodes.

Figure 1.7. Multi-hop and single-hop sub-lambda path.

To achieve more efficient path accommodation in the sub-lambda path over wavelength path multi-layer transport networks, reconfiguration of wavelength path combined with sub-lambda path is one of the promising candidates method. Following study challenges need to be resolved:

1. Wavelength path accommodation design and reconfiguration considering wavelength continuity constraint.
2. Sub-lambda path regrooming.
3. Reduction of migrating sequence from old path set to new one when reconfiguring.
4. Path accommodation design and reconfiguration for different reliability classes considering trade-off of reconfiguration between cost effectiveness and disruption risk.

The purposed of this dissertation is to resolve the above challenges, and main contributions are as follows:

1. Proposed optical path accommodation design and management schemes in Chapter 3.
2. Proposed reconfiguration schemes with three phases: reconfiguration trigger, design and migrating sequence in Chapters 4 and 5.
3. Proposed mathematical formulation and heuristic algorithms for reconfiguration with wavelength defragmentation in Chapters 4 and 5.
4. Proposed accommodation design and reconfiguration schemes for virtualized multi-layer transport networks based on different service classes in Chapter 6.

1.3 Organization of This Dissertation

This dissertation presents research-derived proposals for and analysis of the reconfigurable multi-layer and multi-granular optical transport network design. The dissertation includes 7 chapters. Chapter 1 provides an introductory background. Chapter 2 presents related work. Relationship between study challenges and Chapters 3 to 6 is shown in Fig. 1.8. To answer study challenge 1, Chapter 3 presents optical path accommodation design and management. Chapter 3 follows the study paper of [31]. To answer study challenges 1 and 3, Chapter 4 deals with wavelength path reconfiguration to minimize fragmentation and reconfiguration costs. Chapter 4 extends the study papers of [27, 32–35]. To answer study challenges 1, 2 and 3, Chapter 5 presents sub-lambda path regrooming with wavelength defragmentation. Chapter 5 is also based on the study papers published in [36–38]. To answer for study challenge 4 based on the established reconfiguration studies in Chapters 3, 4 and 5, Chapter 6 presents multi-layer reconfiguration schemes considering differentiated reliable classes defined as a combination of including or excluding a secondary path and allowing or not allowing reconfiguration. Chapter 6 is an extension of the study papers published in [39, 40]. Finally, Chapter 7 is conclusion of this dissertation. Main contents of chapters in the dissertation are organized as follows.

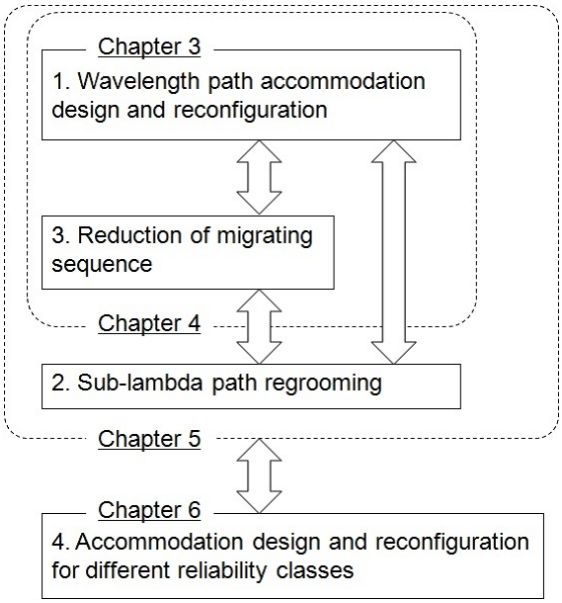

Figure 1.8. Relationship between study challenges and chapters.

Chapter 1 : Introduction presents the introductory background that includes present and future traffic trends, and the history of transmission technology as well as path layer technology including standardization activities. It clarifies the purposes and contributions of this dissertation.

Chapter 2 : Multi-layer and Multi-granular Photonic Transport Networks presents a comprehensive review of related work. Sub-lambda over wavelength path in the multi-layer node architecture is introduced. Each problem for the wavelength path, the sub-lambda path and reconfiguration is addressed, respectively. Finally, conventional studies are summarized.

Chapter 3 : Pre-planning and Reconfiguration on the Wavelength-grouped Transmission Guaranteed Link presents optical path accommodation design and resource management schemes in optical transparent WDM networks. This chapter proposes the pre-planning based wavelength path reconfiguration scheme. There are two stages: pre-planning stage and operation stage. In the pre-planning stage, optical path is designed in advance based on demand prediction and reserved on calculated routes as path group. In the operation stage, optical path is accommodated and virtually reconfigured routes and wavelengths in the logical end-to-end link if demand prediction is different from the actual demand. The effectiveness of the proposed scheme is evaluated in the view point of the number of fibers and accommodation efficiency.

Chapter 4 : Wavelength Defragmentation presents a reconfiguration study of wavelength paths with the goal of reducing wavelength fragmentation. This chapter presents a wavelength path reconfiguration scheme that reduces wavelength fragmentation in three phases: i) reconfiguration trigger phase; ii) reconfiguration design phase; and iii) migrating sequence phase from old path set to new path set. Two cost models are introduced: wavelength fragmentation cost and

reconfiguration cost, and the reconfiguration design using integer linear programming (ILP) is shown that can reduce the number of changed wavelengths while retaining the effectiveness of wavelength defragmentation. For the migration phase, a migrating sequence algorithm is proposed that prevents service disruption by using spare wavelengths to break the dependency cycles that may be formed in moving to the new path set. For large-scale networks, heuristic algorithms are also proposed. Employing the proposed heuristic algorithms can suppress the number of fibers and increase the accommodation efficiency.

Chapter 5 : Sub-lambda Path Reconfiguration with Wavelength Defragmentation presents sub-lambda path regrooming after wavelength defragmentation. This chapter proposes two steps reconfiguration scheme using ILP which performs sub-lambda path regrooming after wavelength defragmentation. An adaptive reconfiguration scheme based on wavelength path resource management is also presented including a heuristic sub-lambda path regrooming algorithm. Employing the proposed scheme, network can be designed to reduce not only the number of fiber but also the number of network devices.

Chapter 6 : Differential Reliability Classes Based Path Accommodation Design and Reconfiguration presents differentiated reconfiguration to address the trade-off relationship between accommodation efficiency and disruption risks in virtualized multi-layer transport networks that considers service classes defined as a combination of including or excluding a secondary path and allowing or not allowing reconfiguration. A multi-layer redundant path accommodation design scheme and a reconfiguration algorithm are proposed. An evaluation algorithm for reliability is also introduced. The proposed reconfigurable networks are shown to be a cost effective solution that maintains reliability.

Chapter 7 : Conclusions presents a summary of this dissertation and describes future prospects.

Chapter 2

Multi-layer and Multi-granular Photonic Transport Networks

This chapter presents a comprehensive review of related work done on reconfiguration problems. Sub-lambda over wavelength path in the multi-layer node architecture is introduced. Each problem for the wavelength path, the sub-lambda path and reconfiguration is addressed, respectively. Finally, conventional studies are summarized.

2.1 Introduction

In the wavelength layer, transparent optical WDM networks can be reduced to 3R transponders with OEO conversion as a result of the digital coherent technology. However, the wavelength continuity constraint states that the same wavelength must be assigned from the source to the destination node. Wavelength fragmentation increases and the wavelength accommodation efficiency degrades. In the sub-lambda layer, it is cost effectively that traffic less than the bandwidth of a wavelength path is accommodated to sub-lambda paths. The accommodation of wavelength path combined with sub-lambda path is cost effective solution for multi-granular traffic. However,the optimized virtual topology in sub-lambda layer, i.e., accommodation design for cost minimization as single-hop or multi-hop, is changing according to traffic fluctuations. For further efficient path accommodation in the sub-lambda path over wavelength path multi-layer transport networks, reconfiguration of wavelength path combined with sub-lambda path is one of the promising candidates method.

This chapter presents the hierarchical multi-layer transport node architecture and each problem for the wavelength path, the sub-lambda path and reconfiguration is addressed, respectively.

2.2 Multi-layer Node Architecture

Figure 2.1 shows the multi-layer node architecture in which each node is equipped with multiple digital cross connects (DXCs) and a wavelength (or optical) cross

connect (WXC) without wavelength-conversion capability, so that a wavelength path set between DXC nodes must keep the wavelength unchanging along the path. The WXC has wavelength multiplex or demultiplex capabilities and through the use of wavelength selective switches (WSS) is color-less, direction-less, and contention-less (CDC-less); this permits the setup of arbitrary wavelengths and directions [41]. Bidirectional wavelength paths are also possible: the same wavelength can travel in both directions simultaneously. Each WXC is connected to multiple DXCs in parallel such as ODU cross connects or MPLS-TP routers, and the wavelength path in wavelength layer can be provided routing that pass through that node. The sub-lambda path in sub-lambda layer are also groomed and switched as multi-hop or single-hop by DXC. The multi-hop sub-lambda path can be defined such that a connection can traverse multiple wavelength paths before it reaches the final destination; this means that a connection may be groomed using different connections on different wavelength paths. On the other hand, the single-hop sub-lambda path is defined as a connection that can traverse only a single wavelength path, i.e., only end-to-end traffic grooming is allowed [42]. The DXC is assumed to have a delay adjustment capability so that switch to the new path creates no service disruption [43].

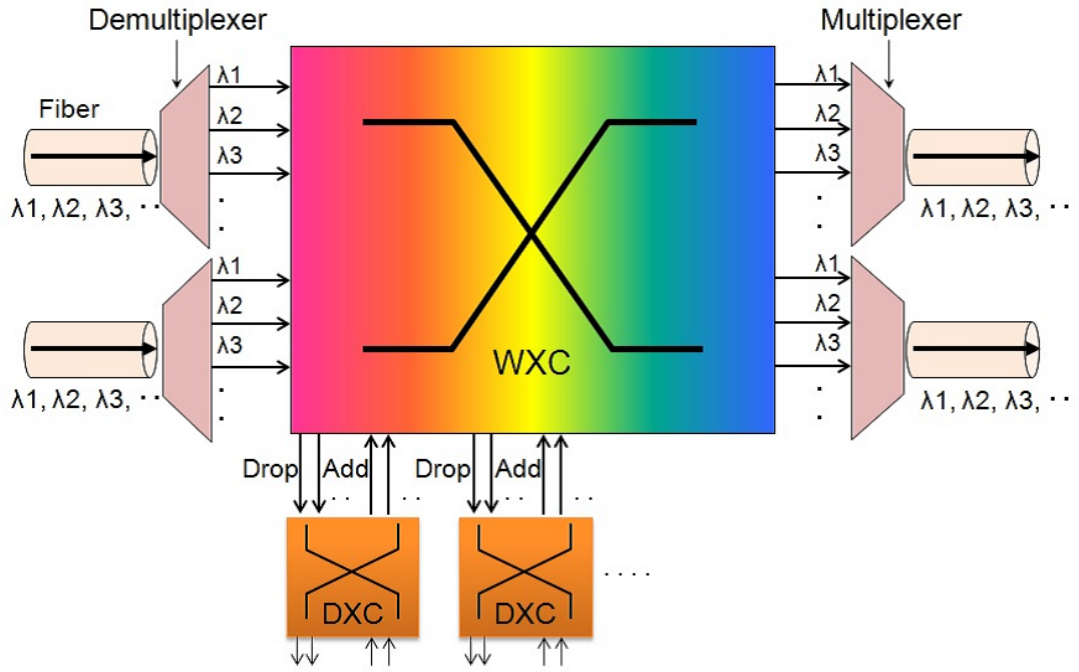

Figure 2.1. Multi-layer node architecture.

2.3 Routing and Wavelength Assignment Problem

The problem of establishing wavelength paths by routing and assigning a wavelength to each connection is called the RWA problem [26, 44]. The quality of an optical signal for wavelength paths degrades as it travels through fibers and intermediate node devices. Then, the problem considering transmission impairment constraint which limits the route selection is also called Impairment awareness Routing and Wavelength Assignment (IRWA) problem. There are two main traffic cases: static, and incremental or quasi-dynamic. The static traffic case assumes that all wavelength paths are established at the same time. The set of connections is known in advance, and the problem is then to establish wavelength paths for these connections in a global fashion while minimizing the network resources used such as the number of wavelengths multiplexed in a fiber or the number of fibers in the network. In realistic optical networks, traffic is incremental and some wavelength paths will be released after a few days, month or years. In the incremental or quasi dynamic case, new connection requests arrive sequentially, and a wavelength path should be established for each connection.

The problem of establishing a static traffic design is known as to be NP-complete [45]. The objective function is to minimize the flow in each link, which, in turn, corresponds to minimizing the number of wavelength paths passing through a particular link. Mathematical formulation is presented for the problem to minimize the number of wavelengths required as follows.

- Given: $\Lambda_{(m,n)}$.
- Variables: $p_{(i,j)}^{(m,n),w}$, w_r and $\lambda_{(m,n)}^{w}$.

The objective function is as follows.

$$\text{Minimize }: w_r. \tag{2.1}$$

The constraints are based on the principle of conservation of flows as follows.

$$w_r \geq \sum_{(m,n)\in P_W, w\in W} p_{(i,j)}^{(m,n),w} \ \forall (i,j) \in E. \tag{2.2}$$

$$\sum_{i\in V} p_{(i,j)}^{(m,n),w} - \sum_{k\in V} p_{(j,k)}^{(m,n),w} = \begin{cases} \lambda_{(m,n)}^{w};\ \text{If } m = j \\ -\lambda_{(m,n)}^{w};\ \text{If } n = j \ \forall (m,n) \in P_W, w \in W. \\ 0;\ \text{Otherwise} \end{cases} \tag{2.3}$$

$$\sum_{w\in W} \lambda_{(m,n)}^{w} = \Lambda_{(m,n)} \ \forall (m,n) \in P_W. \tag{2.4}$$

$$\sum_{(m,n)\in P_W} p_{(i,j)}^{(m,n),w} \leq 1 \forall (i,j) \in E, w \in W. \tag{2.5}$$

Equation (2.2) ensures that the summation of wavelengths used in link (i, j) is less than or equal to the number of wavelengths required. Equations (2.3) - (2.5) decide the route and wavelength for each wavelength path demand.

A lot of heuristic wavelength assignment algorithms have been studied for incremental or quasi-dynamic traffic demands such as First Fit (FF), Random (R), Most-Used (MU), and Least Fragmentation (LF) algorithms [26, 46, 47]. The FF algorithm choses a lower numbered wavelength before a higher-numbered wavelength when all wavelengths are numbered. The idea behind this scheme is to pack all in-use wavelengths in the lower end of the wavelength space so that continuous longer paths toward the higher end of the wavelength space will have a higher probability of being available. The R algorithm chooses, at random, one of all wavelengths available. The MU algorithm selects the wavelength that used most often in the network. MU slightly outperforms FF, doing a better job of packing connections into fewer wavelengths and conserving the spare capacity of less-used wavelengths. The LF algorithm was proposed to achieve higher accommodation efficiency; to decrease the wavelength fragmentation, it assigns wavelength of the least fragmentation value calculated from each wavelength index around required routes. The LF algorithm was shown that accommodation efficiency is higher than the other algorithms [46, 47].

2.4 Traffic Grooming Problem

The bandwidth of a optical path (i.e., a wavelength path) in WDM backbone network is quite high (100 Gbit/s, today), and expected to grow to 400 Gbit/s or 1 Tbit/s in the future [48]. Many services will generate much lower demands, e.g., ODU-1 (2.5 Gbit/s), ODU-2 (10 Gbit/s) and ODU-3 (40 Gbit/s). Since high-bandwidth optical paths will carry many low-speed traffic streams, it is necessary to accommodate low-speed traffic efficiently, which is known as the traffic-grooming problem [44, 49]. Its objective is to minimize the network cost or to maximize the network throughput. There are two main traffic cases: static, incremental or quasi-dynamic. In this section, the static traffic case is examined. The traffic grooming problem is usually divided into three sub-problems, which are not necessarily independent: (1) determining the virtual (or logical) topology, (2) routing and wavelength assignment over the physical topology, (3) routing the traffic on the virtual topology.

The problem of designing the virtual topology can be formulated as ILP, which is known to be NP-hard [42]. This subsection shows a mathematical formulation for static traffic in which a connection can traverse multiple wavelength paths before it reaches its destination and that a connection may be groomed with different connections on different wavelength paths. All nodes are assumed to be equipped with tunable transceivers, which can be tuned to any of a fixed number of wavelengths w. Mathematical formulation is presented for the problem to maximize the total successfully-routed low-speed traffic demands as follows.

- Given: C_S, C_W, D_S, $f_{(i,j)}$, N_{WM}, RR_m and TR_m.
- Variables: $p_{(i,j)}^{(m,n),w}$, $s_{(m,n)}^{(s,d),c_S,d_S}$, $v_{(m,n)}$, $v_{(m,n)}^{w}$ and $\sigma_{(s,d)}^{c_S,d_S}$

The objective function is following.

$$\text{Maximize}: \sum_{(s,d)\in P_S, c_S\in C_S, d_S\in D_S} c_S \cdot \sigma_{(s,d)}^{c_S,d_S} \tag{2.6}$$

The constraints are based on the conservation of flows and resources. They are also divided three parts: constraints for virtual topology connections, and constraints for physical route, constraints for virtual topology traffic.
Constraints for virtual topology connections:

$$\sum_{n\in V} v_{(m,n)} \leq TR_m \ \forall m \in V \tag{2.7}$$

$$\sum_{m\in V} v_{(m,n)} \leq RR_n \ \forall n \in V \tag{2.8}$$

$$\sum_{w\in W} v_{(m,n)}^w \leq v_{(m,n)} \ \forall (m,n) \in P_W \tag{2.9}$$

Constraints for physical route:

$$\sum_{i\in V} p_{(i,n)}^{(m,n),w} = v_{(m,n)}^w \ \forall (m,n) \in P_W, w \in W \tag{2.10}$$

$$\sum_{j\in V} p_{(m,j)}^{(m,n),w} = v_{(m,n)}^w \ \forall (m,n) \in P_W, w \in W \tag{2.11}$$

$$\sum_{i\in V} p_{(i,m)}^{(m,n),w} = 0 \ \forall (m,n) \in P_W, w \in W \tag{2.12}$$

$$\sum_{j\in V} p_{(n,j)}^{(m,n),w} = 0 \ \forall (m,n) \in P_W, w \in W \tag{2.13}$$

$$\sum_{i\in V} p_{(i,k)}^{(m,n),w} - \sum_{j\in V} p_{(k,j)}^{(m,n),w} = 0 \text{ If } k \neq m,n \ \forall (m,n) \in P_W, w \in W \tag{2.14}$$

$$\sum_{(m,n)\in P_W} p_{(i,j)}^{(m,n),w} \leq f_{(i,j)} \ \forall (i,j) \in E, w \in W \tag{2.15}$$

Constraints for virtual topology traffic:

$$\sum_{m\in V} s_{(m,d)}^{(s,d),c_S,d_S} = \sigma_{(s,d)}^{c_S,d_S} \ \forall (s,d) \in P_S, c_S \in C_S, d_S \in D_S \tag{2.16}$$

$$\sum_{n\in V} s_{(s,n)}^{(s,d),c_S,d_S} = \sigma_{(s,d)}^{c_S,d_S} \ \forall (s,d) \in P_S, c_S \in C_S, d_S \in D_S \tag{2.17}$$

$$\sum_{m\in V} s_{(m,s)}^{(s,d),c_S,d_S} = 0 \ \forall (s,d) \in P_S, c_S \in C_S, d_S \in D_S \tag{2.18}$$

$$\sum_{n\in V} s_{(d,n)}^{(s,d),c_S,d_S} = 0 \ \forall (s,d) \in P_S, c_S \in C_S, d_S \in D_S \tag{2.19}$$

$$\sum_{m\in V} s_{(m,k)}^{(s,d),c_S,d_S} - \sum_{n\in V} s_{(k,n)}^{(s,d),c_S,d_S} = 0$$

$$\text{If } k \neq s,d \ \forall (s,d) \in P_S, d_S \in D_S, c_S \in C_S \tag{2.20}$$

$$\sum_{(s,d)\in P_S, c_S\in C_S, d_S\in D_S} c_S \cdot s_{(m,n)}^{(s,d),c_S,d_S} \leq C_W \cdot v_{(m,n)} \; \forall (m,n) \in P_W \qquad (2.21)$$

The above equations are explained below.

- Equations (2.7) and (2.8) ensure that the number of wavelength paths between (m, n) is less than or equal to the number of transmitters at node m and the number of receivers at node j.
- Equation (2.9) shows that the wavelength paths between (m, n) are composed of wavelength paths with different wavelengths.
- Equations (2.10) - (2.14) are the multi-commodity equations (for flow conservation) that determine the routing of a wavelength path from its origin to its termination.
- Equation (2.15) ensures that wavelength w on fiber link (i, j) can only be present in at most wavelength path of number of fiber link in the virtual topology.
- Equations (2.16) - (2.20) are the multi-commodity equations (for flow conservation) that determine the routing of sub-lambda path demands on the virtual topology.
- Equation (2.21) ensures that the aggregate sub-lambda path flowing through wavelength paths cannot exceed the overall wavelength channel capacity.

Several heuristic algorithms have been studied to resolve the traffic-grooming problem such as Maximizing Single-hop Traffic (MST) and Maximizing Resource Utilization (MRU) [42]. Let $T(s, d)$ denote the aggregate traffic between node pair s and d, which has yet to be assigned. Let $t(s, d)$ denote one connection request between s and d, which has yet to be assigned.

The basic idea of the MST algorithm was introduced to resolve the virtual-topology design problem. This simple heuristic attempts to establish wavelength paths between source and destination pairs with the highest $T(s, d)$ values, subject to constraints on the number of transceivers at the two end nodes, and the availability of a wavelength in the path connecting the two end nodes. The connection requests between s and d will be carried as much as possible on the latest wavelength path to be established. If there is enough capacity in the network, every connection will traverse a single wavelength path. If there are too few resources to establish enough wavelength paths, the algorithm will try to carry the blocked connection requests using currently available spare capacity of the virtual topology.

The MRU algorithm operates as follows. Let $H(s, d)$ denote the hop distance on the physical topology between node pair (s, d). Define $T(s, d)/H(s, d)$ as the connection resource utilization value, which represents the average traffic per wavelength link. This quantity shows how efficiently the resources are used to carry the traffic requests. This heuristic tries to establish the wavelength paths between the node pairs with the maximum resource utilization values. When no wavelength path can be set up, the remaining blocked traffic requests will be routed on the virtual topology based on their connection resource utilization value $t(s, d)/H'(s, d)$, where $H'(s, d)$ denotes the hop distance between source and destination pairs on the virtual topology.

2.5 Reconfiguration Problem

The reconfiguration of wavelength paths and that of sub-lambda path must be considered the RWA problem and the traffic grooming problem respectively. Additionally, these reconfiguration problems consist of three phases: i) determination of whether reconfiguration should be conducted; ii) design based on a certain optimization objective; and iii) migrating from old path set to the new path set. This subsection presents a comprehensive review of related work on each phase of the reconfiguration problems [33].

For the first phase, there are two main reconfiguration triggers: a regular interval and an interval determined by the traffic fluctuation. The former is periodic, such as every week, every month, or at some fixed threshold based on the number of path demands. The latter includes reconfiguration when unbalanced traffic is detected on wavelength paths [30] and reconfiguration with time varying traffic based on blocking and time windows [50].

For the second phase, there are two schemes: Passive rerouting design and Intentional rerouting design [51]. The former dynamically reconfigures paths in response to changing traffic demands between each node pair. The latter reconfigures paths in advance based on some objective functions or weight functions. The wavelength path reconfiguration problem mentioned above has been studied in different scenarios. Passive rerouting design has been studied as follows: shortest available wavelength path rerouting [51], dynamic rerouting considering fairness [52], and alternate rerouting to minimize propagation delay, link load, and the number of paths changed based on a genetic algorithm [53]. Intentional rerouting design has been studied as follows: rerouting an existing wavelength path to the k-shortest path with the highest weight value [51] and reconfiguration for working and backup paths [54]. The reconfiguration objectives for intentional rerouting design include minimization of average packet hop distance [55], minimization of rejected new demands and rerouted existing wavelength paths [56], and maximization of connection requests [42]. Reconfiguration algorithms to reduce fragmentation have been studied such as the push-pull algorithm [57], and the greedy algorithm-based defragmentation algorithm [58]. In multi-layer reconfiguration, virtual topology designs have been reported such as maximizing the carried traffic of connections without service disruption [59], heuristic algorithm for virtual topology reconfiguration to reduce the number of wavelength paths changed while ensuring that the network congestion is low in optical ring networks [60], minimizing the average packet hop distance while minimizing the number of changes needed from the existing virtual topology [55], and reducing the maximum link load [61]. Grooming algorithms for static traffic have been reported, such as MST and MRU [42].

Work on the third phase includes: an algorithm for minimizing the number of simultaneously disrupted connections [62], and a migration algorithm to minimize disruption duration or the number of disruptions [63–65].

Many reconfiguration algorithms in different scenarios have been studied for each three phase. For effective accommodation of traffic, it is necessary to reconfigure wavelength paths in cooperation with sub-lambda paths. Additionally, since

Internet carriers have many clients with different service level agreements, service disruption must not occur and the number of migrating sequences needs to be reduced as much as possible to reduce the risk of reconfiguration. However, there are no reconfiguration studies considering all three phases and reducing disruption risk in multi-layer transport networks. Given this background, this dissertation targets all three of the above mentioned phases and incremental quasi-dynamic traffic in multi-layer transport networks. This dissertation assumes that wavelength path demands are changed at intervals in excess of a week. Thus reconfiguration is assumed to be performed every few weeks or few months.

2.6 Summary

This chapter presented a comprehensive review of related work. The sub-lambda over wavelength path in the multi-layer node architecture was also introduced. Two problems for path accommodation design were shown: routing and wavelength assignment in the wavelength layer and traffic grooming problems in the sub-lambda layer. After that, path reconfiguration directed towards these two problems as described.

The reconfiguration problem consists of three phases: i) determination of whether reconfiguration should be conducted; ii) design based on a certain optimization objective; and iii) migrating from old path set to new path set. For effective accommodation of traffic, it is necessary to reconfigure wavelength paths in cooperation with sub-lambda paths. This dissertation targets all three of the above mentioned phases and incremental quasi-dynamic traffic in multi-layer transport networks.

Chapter 3

Pre-planning and Reconfiguration on the Wavelength-grouped Transmission Guaranteed Link

This chapter presents optical path accommodation design and resource management schemes in optical transparent WDM networks. In optical path accommodation design, there are the simple classes of post-planning and pre-planning schemes considering wavelength continuity constraints. This chapter proposes the pre-planning based wavelength path reconfiguration scheme. There are two stages: pre-planning stage and operation stage. In the pre-planning stage, optical path is designed in advance based on demand prediction and reserved on calculated routes as path group. In the operation stage, optical path is accommodated and virtually reconfigured routes and wavelengths in the logical end-to-end link if demand prediction is different from the actual demand. The effectiveness of the proposed scheme is evaluated in the view point of the number of fibers and accommodation efficiency.

3.1 Introduction

In core and metro transparent optical WDM networks, all optical paths should be established from the source node to destination node implementing optical switches to eliminate expensive OEO conversions at each intermediate node. However, optical path accommodation design has two constraints: the wavelength continuity constraint and the transmission impairment constraint. Therefore, implementing a design to accommodate optical paths is more difficult than implementing a design to dispose of OEO conversion in opaque networks. The wavelength continuity constraint includes the constraints on wavelength channel selection and on route selection in order to avoid wavelength collision. The same wavelength must be assigned from source node to destination node. The optical path scheme to deal with this wavelength continuity constraint was proposed as the Wavelength Path as described in Section 2.3. The transmission impairment constraint limits the route selection because the quality of an optical signal degrades as it travels through fibers and intermediate node devices.

Optical path accommodation design schemes that consider these constraints are simply classified into post-planning and pre-planning schemes. In the post-planning scheme, the route and wavelength are calculated using a heuristic algorithm to address the Impairment awareness Routing and Wavelength Assignment (IRWA) problem in real time, and accommodates one-by-one an optical path [66,67]. The post-planning scheme flexibly accommodates an optical path as long as the resources in the network are available. However, this scheme cannot achieve optimal accommodation throughout the network because it depends on the order of the wavelength assignment. Moreover, it takes time to establish an optical path, because a route is designed when the path is established and the design for transmission is not employed at that time. On the other hand, in the pre-planning scheme, the route and wavelength are calculated off-line in advance according to the optical path demand prediction, and are accommodated one-by-one in an optical path when request for establishing the optical path is caused. The management and control scheme for transparent optical networks in the pre-planning scheme was proposed, that is called a Wavelength-grouped Transmission-Guaranteed Link (λTGL) [68]. The λTGL is a logical end-to-end link that directly connects the source and destination nodes with multiple wavelengths using a route in which optical reachability is guaranteed. The optical reachability is guaranteed by the physical layer transmission design, which is completed in advance. The wavelengths in each λTGL are also determined in advance considering wavelength continuity constraints. Optical path accommodation design scheme based on to λTGL concept is needed considering virtualized reconfiguration of routes and wavelengths on path management table according to the change of the optical path demand prediction.

This chapter presents the Pre-planning and Reconfiguration of Wavelength Path (PRW) scheme based on the λTGL management and control scheme, which achieves a fast and flexible optical path accommodation design. A mathematical formulation for the PRW is also introduced. Numerical evaluations show that proposed PRW is cost effectiveness design in the view of the number of fiber required and accommodation rate.

3.2 Pre-planning and Reconfiguration of Wavelength Path and Resource Management

3.2.1 Pre-planning and Reconfiguration of Wavelength Path

The pre-planning scheme is more effective than the post-planning scheme as long as the optical path demand prediction matches the real optical path demand from the viewpoint of both capital expenditure (CAPEX) and operational expenditure (OPEX). However, in the pre-planning scheme, there are some problems that need to be addressed in addition to the IRWA problem. The first problem is how to plan or prediction the optical path demand. The second problem is how and when to reconfigure routes and wavelengths when there is a mismatch in the optical path demand prediction. In regard to the first problem, the optical path demand

prediction is assumed to be given, and to resolve second problem, the PRW scheme is used. The scheme is achieved in four steps as follows.

- Step 1: Optical path design in the pre-planning stage
- Step 2: Reservation of wavelengths on calculated routes for each between node pair in the pre-planning stage
- Step 3: Optical path accommodation in the network operation stage
- Step 4: Virtualized reconfiguration of routes and wavelengths in the λTGL

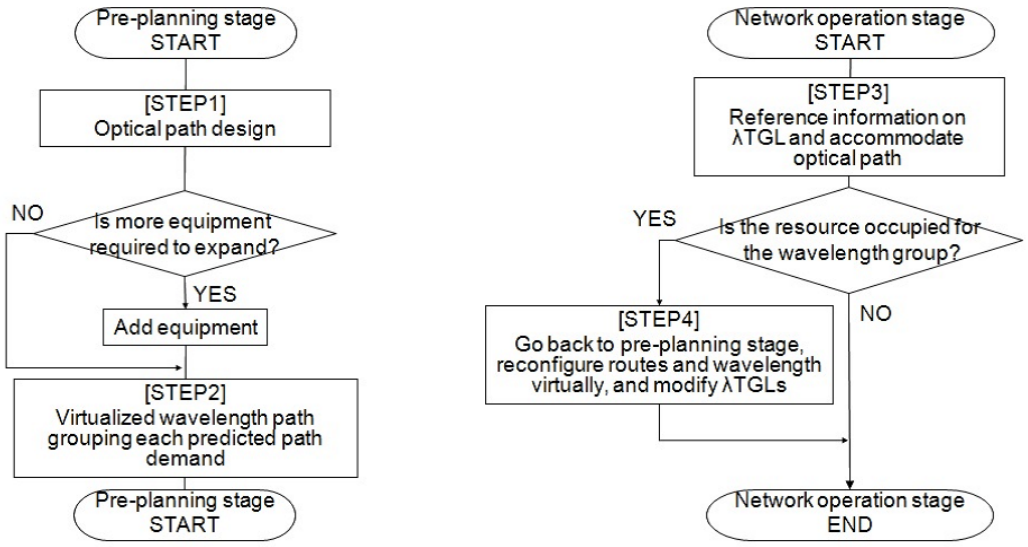

(a) Flow in the pre-planning stage.

(b) Flow in the network operation stage.

Figure 3.1. PRW scheme flow.

In the Step 1, routes and wavelengths are designed with the physical topology and initial equipment as inputs, i.e., the number of fibers in each link, the number of wavelengths multiplexed in a fiber, and the optical path demand prediction for all optical paths. Based on calculations, if additional fiber equipment is required in a link, then it is implemented. If this is not the case, then the initial amount of equipment is used. In the Step 2, the wavelengths are reserved on calculated routes for each between node pair in the λTGL. The flow of the algorithm for Step 1 and Step 2 is shown in Fig. 3.1 (a). When establishing the optical path is requested, an pre-planed optical path in the secured λTGL with requested source and destination node pair is selected, and a wavelength is assigned to the optical path. If the optical path demand prediction is different from the actual optical path demand and a resource in the λTGL is occupied, this scheme proceeds to Step 4. In the Step 4, and routes and wavelengths are reconfigured virtually in the λTGL according to an updated optical path demand prediction. In this step, reconfiguration target is optical paths not accommodated. The λTGLs must modify each path between each node pair. The flow for the algorithm for Step 3 and Step 4 is shown in Fig. 3.1 (b). Thus, optical paths can be fast and flexibly accommodated.

3.2.2 Resource Management

The resource management for optical path based on the PRW scheme is presented. For instance, as shown in Fig.3.2, when initial optical path demand prediction is three each nodes between A-B, and between A-C, and between B-C, it assumes that in the Step2, λTGL reserved between A-B are λ1, λ2, λ3, and λTGL reserved between A-C and between B-C are λ4, λ5, λ6, from design of Step 1. When the optical path is requested in Step 3, the available wavelength can be searched from the management table having information of λTGL, and the optical path is accommodated at the actual wavelength. While Step 3 is repeated, available wavelength is nothing in the group A-C. Then, this scheme goes to Step 4, routes and wavelengths are reconfigured without interrupting optical path accommodated, while minimizing any increase in the number of fibers in the Step 1. Thus, the λTGLs are modified that group A-C is λ1, λ2, λ3, and λ5, group A-B and group B-C is λ4, λ6.

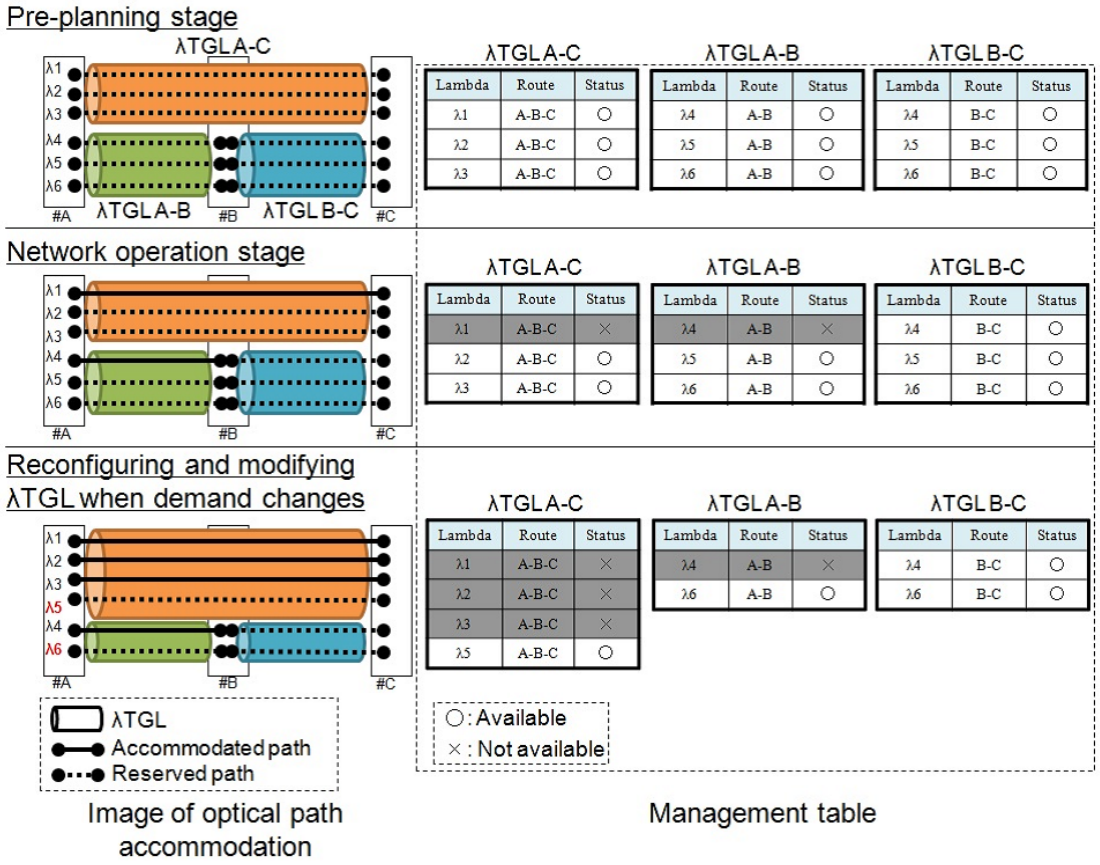

λTGL A-C		
Lambda	Route	Status
λ1	A-B-C	○
λ2	A-B-C	○
λ3	A-B-C	○

λTGL A-B		
Lambda	Route	Status
λ4	A-B	○
λ5	A-B	○
λ6	A-B	○

λTGL B-C		
Lambda	Route	Status
λ4	B-C	○
λ5	B-C	○
λ6	B-C	○

λTGL A-C		
Lambda	Route	Status
λ1	A-B-C	×
λ2	A-B-C	○
λ3	A-B-C	○

λTGL A-B		
Lambda	Route	Status
λ4	A-B	×
λ5	A-B	○
λ6	A-B	○

λTGL B-C		
Lambda	Route	Status
λ4	B-C	○
λ5	B-C	○
λ6	B-C	○

λTGL A-C		
Lambda	Route	Status
λ1	A-B-C	×
λ2	A-B-C	×
λ3	A-B-C	×
λ5	A-B-C	○

λTGL A-B		
Lambda	Route	Status
λ4	A-B	×
λ6	A-B	○

λTGL B-C		
Lambda	Route	Status
λ4	B-C	○
λ6	B-C	○

Figure 3.2. Example of PRW scheme.

3.3 Mathematical Formulation in The Pre-planning Stage

To realize the PRW scheme, mathematical formulation based on the ILP is presented. The problem for PRW scheme is stated as follows.

- Given: C_{FI}, f_{0e}, N_{WM}, $p_{0k}^{(m,n),w}$, $\delta_{k,e}^{(m,n)}$, and $\Lambda_{(m,n)}$
- Variables: f_e, $p_k^{(m,n),w}$ and w_e.
- Determine: Design of optical path as shortest route for predicted optical path demands to minimize the number of fiber required.

The mathematical formulation assumes that transmission impairment constraints are not considered. The optical signal to noise ratio (OSNR) is calculated by assigning a gain or loss power to all optical components such as the Erbium Doped Fiber Amplifier (EDFA) or switch [69]. Then, the hop constraint is determined. Alternative methods for determining the hop constraint are given in [67]. Optical cross connect is assumed to be colorlessly add/drop an arbitrary wavelength at an arbitrary UNI port, and directionless output to an arbitrary NNI port. Thus, wavelengths do not collide in any of the nodes and it only has to consider about the wavelength collision in the fibers.

Following formulation is also described not multi-commodity equations described in Section 2.4 but physical route search based [70]. Then, routes are searched between source and destination nodes all pairs, in advance. The objective function is formulated to minimize the sum of the number of wavelengths used in all links and the number of all fibers multiplied by the cost of fibers in the network as

$$\text{Minimize} : \sum_{e \in E} \Big(w_e + C_{FI} \cdot f_e \Big). \tag{3.1}$$

The cost of fiber expansion, C_{FI}, in Equation (3.1) assumes a much higher cost than that for the number of wavelengths. In other words, the route takes a detour as long as the resources in the fibers are unused and the number of additional fibers is minimized. Constraints are formulated as follows.

$$\sum_{w \in W, k \in K} p_k^{(m,n),w} = \Lambda_{(m,n)} \forall (m,n) \in P_W. \tag{3.2}$$

$$\sum_{k \in K, (m,n) \in P_W} \delta_{k,e}^{(m,n)} p_k^{(m,n),w} \leq f_e \forall e \in E, w \in W. \tag{3.3}$$

$$\sum_{k \in K, (m,n) \in P_W, w \in W} \delta_{k,e}^{(m,n)} p_k^{(m,n),w} \leq w_e \forall e \in E. \tag{3.4}$$

$$w_e \leq N_{WM} f_e \forall e \in E. \tag{3.5}$$

Explanation of those equations is as follows.

- Equation (3.2) ensures that the optical path demand each between source and destination is satisfied the sum of the number of wavelengths for all routes.

- Equation (3.3) ensures the wavelength continuity.
- Equation (3.4) and (3.5) ensure that the sum of the number of wavelengths is less than or equal to the number of wavelengths multiplexed in a fiber multiplied by the number of fibers.

When there is a change in the optical path demand prediction, the existing optical paths are not reconfigured. Following constraint must be added

$$p_{0k}^{(m,n),w} \leq p_{k}^{(m,n),w} \forall\ k \in K, (m,n) \in P_W, w \in W. \tag{3.6}$$

In Step 1, each network link with a fiber was equipped. The number of equipped fibers was not decreased even if an optical path did not pass through that fiber. Following constraint must be added

$$f_{0e} \leq f\ _{e} \forall e \in E. \tag{3.7}$$

3.4 Numerical Evaluation for Pre-planning and Reconfiguration of Wavelength Path

The PRW scheme is compared to the post-planning scheme in terms of the number of required fibers and accommodation rate of the optical path in fibers. The rate of change in the optical path demand prediction is defined as the difference between the initial optical path demand prediction and the actual optical path demand, assumed to be equal to the updated optical path demand prediction. This simulation is assumed that the updated optical path demand prediction is not changing and all updated optical path demands are accommodated. The sum of all the initial optical path demands prediction is assumed to be equal to the sum of all updated optical path demand prediction, and the rate of increase is equal to the rate of decrease. For example, when the initial optical path demand prediction is 10 between each node pair in a physical topology with 9 nodes (total demand is 360 for ${}_9\mathrm{C}_2\times$ 10) and the rate of change in the demand prediction is 10 %, both the rates of increase and decrease in the demand are 5 % and both the increase and decrease in optical path demand are 18 demands for 360 $\times$ 5 %.

3.4.1 Simulation Conditions

In the PRW scheme, wavelengths are assigned as a whole according to the initial optical path demand prediction using the ILP described in Section 3.2.2, and routes and wavelengths are reconfigured virtually in the λTGL about paths between each node pair more than initial optical path demand prediction according to an updated optical path demand prediction considering Equations (3.6) and (3.7). On the other hand, in the post-planning scheme, optical paths are accommodated sequentially one by one from the source to destination node each an optical path demand. To obtain an exact optimal solution would take an exponential amount of time. Thus, the optimization calculation using ILP is terminated within a

few percent of the optimized result of the real number linear programming (LP) result. These demands between node pairs are randomly changed 10 times, and the average of the results is calculated. Physical topology is used 3×3 grid as shown in Fig. 3.3. Number of Wavelengths multiplexed in a fiber (N_{WM}) are changing 24, 40, or 56.

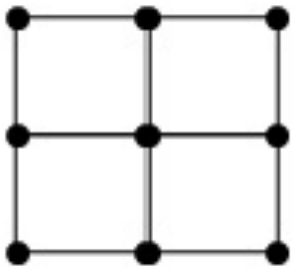

Figure 3.3. Physical topology in simulation.

3.4.2 Results and Discussion

The reduction rate of number of fibers for the PRW to the post-planning in terms of the rate of change in the initial demand prediction is shown in Fig. 3.4. The number of required fibers for the PRW can be reduced from 15 % to 28 % compared to post-planning. The reduction rate of number of required fibers for the PRW to the post-planning decreases with an increase in the rate of change in the demand prediction. The reason is because the route and wavelength of the PRW is close to that of the post-planning according to increasing demand fluctuation. Figure 3.5 shows the same evaluation measure with respect to changing the initial optical path demand prediction from 10 to 40 when the rate of change in the initial demand prediction is 30 %. The reduction rate of number of required fibers for the PRW to the post-planning remains constant with an increase in demand. Based on Figs. 3.4 and 3.5, the PRW scheme can be used to design economical networks compared to using the post-planning scheme regardless of the increase in the optical path demand.

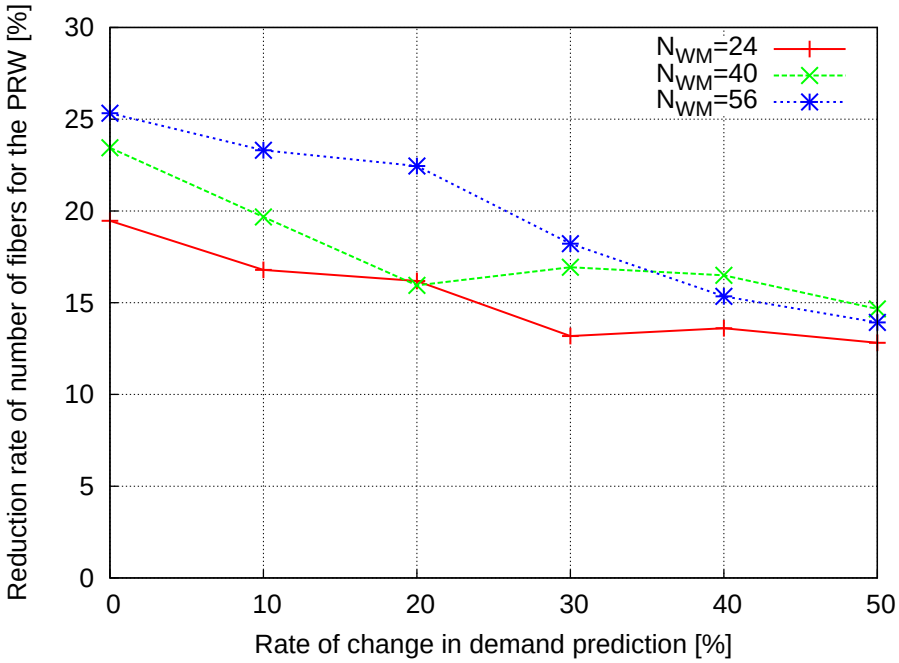

Figure 3.4. Reduction rate of number of fibers for the PRW to the post-planning in terms of the rate of change in the initial demand prediction.

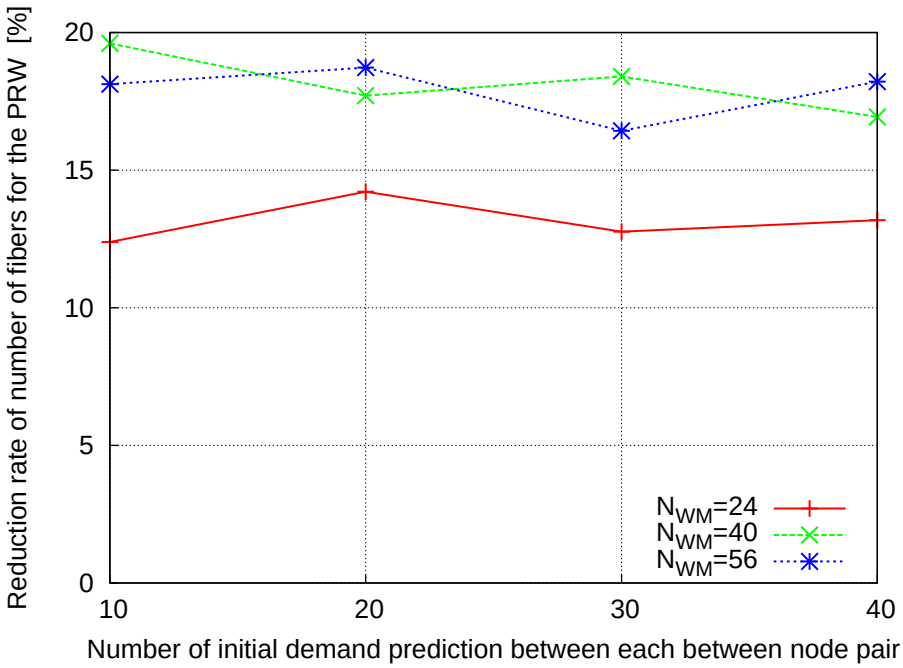

Figure 3.5. Reduction rate of number of fibers for the PRW to the post-planning when the rate of change in the initial demand prediction is 30 %.

The accommodation rates in the fibers for the PRW and the post-planning schemes when the rate of change in the initial demand prediction is 30 % are shown in Fig. 3.6. The accommodation rate is defined as the sum of wavelength in all links to N_{WM} times the sum of fibers:

$$A = \frac{\sum_{e \in E} w_e}{N_{WM} \sum_{e \in E} f_e}. \tag{3.8}$$

The gap between the accommodation rate for the post-planning scheme and that for the PRW scheme is small with an increase in demand. When the initial optical path demand prediction between each node pair is low, as a higher number of wavelength multiplexed is employed, the accommodation rate of the post-planning becomes worse. In this simulation, the PRW scheme achieves a higher accommodation rate than the post-planning scheme.

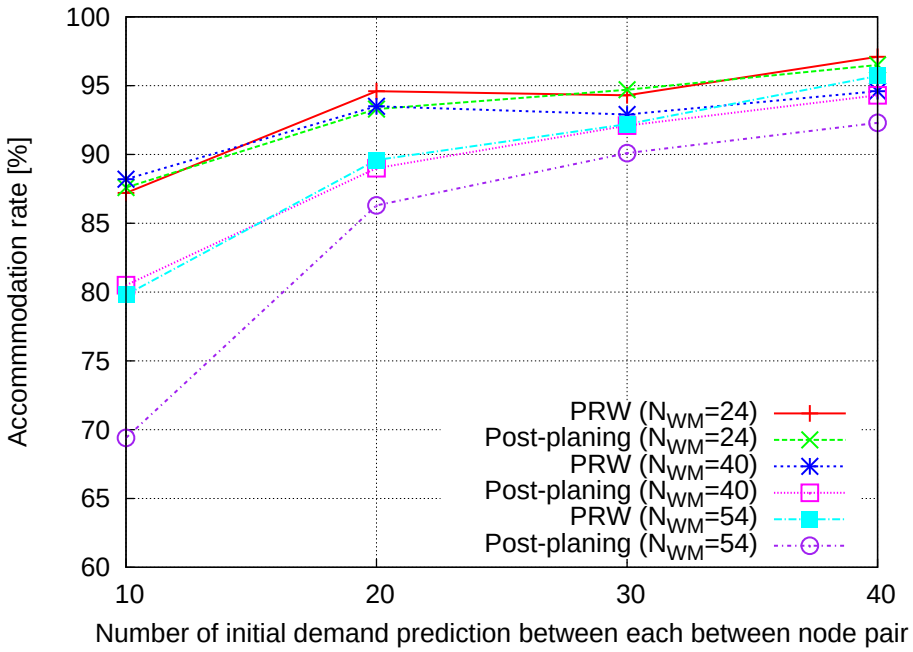

(a) Results of post-planning.

Figure 3.6. Comparison of accommodation rate for the PRW and post-planning.

3.5 Summary

This chapter presented optical path accommodation design and resource management schemes in optical transparent WDM networks. This chapter proposed the PRW scheme based on the concept of λTGL, which is logical end-to-end link that directly connects the source and destination nodes with multiple wavelengths using a route in which optical reachability is guaranteed. Numerical evaluations showed in 3×3 grid that the number of required fibers for the PRW can be reduced from 15 % to 28 % compared to post-planning, and that the PRW scheme achieves a higher accommodation rate than the post-planning scheme.

Chapter 4

Wavelength Defragmentation

This chapter presents a reconfiguration study of wavelength paths with the goal of reducing wavelength fragmentation. This chapter presents a wavelength path reconfiguration scheme that reduces wavelength fragmentation in three phases: i) reconfiguration trigger phase; ii) reconfiguration design phase; and iii) migrating sequence phase from old path set to new path set. Two cost models are introduced: wavelength fragmentation cost and reconfiguration cost, and the reconfiguration design using ILP is shown that can reduce the number of changed wavelengths while retaining the effectiveness of wavelength defragmentation. For the migration phase, a migrating sequence algorithm is proposed that prevents service disruption by using spare wavelengths to break the dependency cycles that may be formed in moving to the new path set. For large-scale networks, heuristic algorithms are also proposed. Employing the proposed heuristic algorithms can suppress the number of fibers and increase the accommodation efficiency.

4.1 Introduction

The optical reach that can be achieved without OEO conversion has been extended as a result of advances in long-distance and high capacity transmission technologies [6]. The wavelength continuity constraint of optical transparent WDM networks states that the same wavelength must be assigned from the source to the destination node [25]. To enhance the accommodation efficiency, there have been studied routing and wavelength assignment algorithms such as FF algorithm, MU algorithm and so on for an incoming wavelength path [26]. The LF algorithm was proposed to achieve higher accommodation efficiency; to decrease the wavelength fragmentation [46,47]. However, when it is difficult to predict where future incoming traffic will emerge between source and destination nodes, overall optimization is limited to only route design and wavelength assignment for a wavelength path. Therefore, repetitive reconfiguration for wavelength defragmentation is important for optimizing all accommodated paths.

Figure 4.1 shows an image of wavelength defragmentation in which wavelength paths are reconfigured to minimize the wavelength or spectrum fragmentation. There are two examples of reconfiguration design as shown to the right in Fig. 4.1.

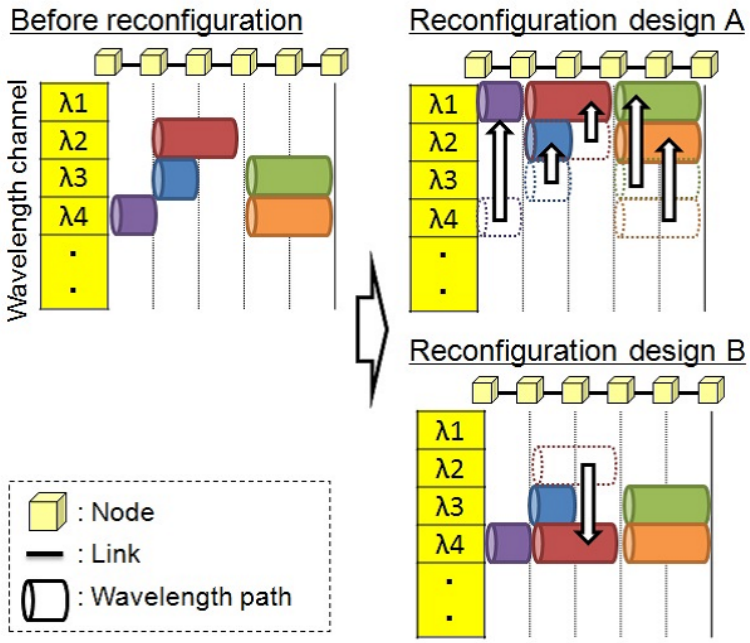

Figure 4.1. Image of wavelength path reconfiguration.

Reconfiguration design A shows that wavelength paths are reconfigured to a lower frequency or number. The number of wavelength channels used is 2 and the number of migrating sequences is 5. On the other hand, reconfiguration design B shows that a wavelength path in λ 2 is reconfigured to λ 4. The number of wavelength channels used is 2, which is the same result as that from reconfiguration design A, and the number of migrating sequences is only 1, which is less than that in reconfiguration design A. Namely, by engineering a reconfiguration design algorithm, the number of migrating sequences can be reduced the number of migrating sequences while retaining the effectiveness of the wavelength defragmentation.

This chapter focuses on the three phases for intentional rerouting design in the wavelength layer. As for the first phase, two scheme are considered: trigger that the number of paths accommodated exceeds some some threshold number and that wavelength path resources is less than the threshold value set. As for the second phase, a mathematical formulation for reconfiguration design is proposed employing fragmentation and reconfiguration costs to decrease both wavelength blocking for future traffic demand and the number of sequences that needed to be migrated to the new path set. Heuristic algorithms are also proposed to reduce calculation time of ILP based design. As for the third phase, a migrating sequence algorithm is introduced with eliminates service disruption by using spare wavelength to break the dependency cycles. Numerical evaluations show that the number of fibers for ILP-based reconfiguration design can be suppressed compared to the design without employing fragmentation cost while reducing the number of changed wavelengths. Additionally, employing proposed heuristic algorithms, the number of fibers can be suppressed and the accommodation efficiency is increased compared to when reconfiguration is not performed.

4.2 Problem Statements and Assumptions for Wavelength Defragmentation Design

A network of V nodes connected by bidirectional E links forming an arbitrary physical topology is considered. All links in the physical topology have at least one fiber, and the number of fibers is increased when a wavelength path cannot be established. Each fiber carries as many wavelength channels as the number of wavelengths multiplexed in a fiber. Each node is equipped with a WXC without a wavelength-conversion capability so that a wavelength path must be set up with the same wavelength. The node comprises an OTM-IF with a WDM function, an OCh-IF, an ODU-IF and WDM transponders. The WXC has wavelength multiplexing or demultiplexing capabilities and is CDC-less through the use of wavelength selective switches. This permits the establishment of arbitrary wavelengths and directions.

In the second phase, i.e. reconfiguration design, there are some assumptions that reconfiguration design is calculated off-line, and wavelength path demands are changed at intervals in excess of a week. In the third phase, i.e. migrating phase, it is assumed that there are some spare (or vacant) wavelength channels to setup 1+1 protection and so break the dependency graph. The network equipment and fiber are assumed to be expanded so as to keep this assumption. The reconfiguration design problem is stated as follows.
Given:

- A physical network topology graph, $G(V, E)$.
- Number of wavelengths multiplexed in a fiber.
- Number of fibers on a link.
- Number of wavelength paths between each node pair.
- Set of routes and wavelengths for all wavelength paths accommodated before reconfiguration.

Determine:

- Reconfiguration design that reduces wavelength blocking for subsequent incoming traffic
- Reduction of the number of fibers required
- Reduction of the number of changed paths in the new path set.

4.3 ILP-based Wavelength Defragmentation

The reconfiguration design is stated using ILP. Reconfiguration is performed when the number of wavelength paths accommodated exceeds some threshold number. First, the costs of fragmentation and reconfiguration are introduced for multi-fiber WDM networks. Then the objective function and constraints are described. Given parameters and variables are following.

- Given: C_F, C_{WR}, $f_{(i,j)}$, $M_{m,f}$ and N_{WM}.
- Variables: $p_{(i,j),f}^{(m,n),w,d_W}$ and $\lambda_{(m,n)}^{w,d_W}$

Wavelength fragmentation cost is introduced. When there are some usable wavelengths in a link that has multiple fibers, $f_{(i,j),w}$ in link (i,j) and wavelength channel w shows 0; otherwise 1. $f_{(i,j),w}$ can be written as

$$f_{(i,j),w} = \left\lfloor \frac{\sum_{(m,n)\in P_W, d_W \in D_W, f\in F} p_{(i,j),f}^{(m,n),w,d_W}}{f_{(i,j)}} \right\rfloor. \tag{4.1}$$

For instance, Fig. 4.2 shows an image of wavelength fragmentation in a simple network. When there are two fibers in link $e(i,j) = (2,3)$, $\lambda 1$ or $\lambda 3$ cannot be used, $f_{e=(2,3),w=1}$ or $f_{e=(2,3),w=3}$ is equal to 1. On the other hand, $\lambda 2$ or $\lambda 4$ is available, so $f_{e=(2,3),w=2}$ or $f_{e=(2,3),w=4}$ is equal to 0. Wavelength fragmentation cost for wavelength channel F_w is determined by calculating $f_{(i,j),w}$ for each wavelength channel, w, for all links (i,j). F_w is 0 if the wavelength is completely occupied or vacant through all physical links; otherwise, the function shows 1. The mathematical formulation is given as

$$F_w = \left\lceil \frac{\sum_{(i,j)\in E} f_{(i,j),w}}{|E|} \right\rceil - \left\lfloor \frac{\sum_{(i,j)\in E} f_{(i,j),w}}{|E|} \right\rfloor. \tag{4.2}$$

Reconfiguration cost is introduced to satisfy two objectives; reducing the number of migrating sequences, and reducing the number of wavelength cross connections between source and destination nodes that need to be reset. Reconfiguration cost for a wavelength path d_W between nodes pair (m,n), $R_{(m,n),d_W}$ is formulated as

$$R_{(m,n),d_W} = \sum_{(i,j)\in E, w\in W, f\in F\setminus F_0} p_{(i,j),f}^{(m,n),w,d_W}. \tag{4.3}$$

The reconfiguration cost represents the number of wavelengths that must be switched to unused wavelength or fiber route before reconfiguration. Figure 4.3 shows an example of reconfiguration in single fiber in a 3×3 grid. Left figure shows the accommodation of wavelength paths in $\lambda 1$, and right figure shows that in $\lambda 2$; three wavelength paths are accommodated. Figure 4.3 (a) shows the reconfiguration from $\lambda 2$ to $\lambda 1$, Fig. 4.3(b) shows the reconfiguration from $\lambda 1$ to $\lambda 2$. In Fig. 4.3(a), $\sum_{(m,n),d_W} R_{(m,n),d_W}$ is equal to 5, and in Fig. 4.3 (b), $\sum_{(m,n),d_W} R_{(m,n),d_W}$ is equal to 7. The reconfiguration cost in case 1 is less than that in case 2; thus the number of changed wavelengths or the number of reset wavelength cross connections for case 1 is less than that for case 2.

The objective function and constraints are shown for the reconfiguration design based on ILP. The objective function is given as

$$\begin{aligned}\text{Minimize}: \quad & \sum_{(i,j)\in E, f\in F, (m,n)\in P_W, w\in W, d_W\in D_W} p_{(i,j),f}^{(m,n),w,d_W} \\ & + C_F \sum_{w\in W} F_w + C_{WR} \sum_{(m,n)\in P_W, d_W\in D_W} R_{(m,n),d_W}. \end{aligned} \tag{4.4}$$

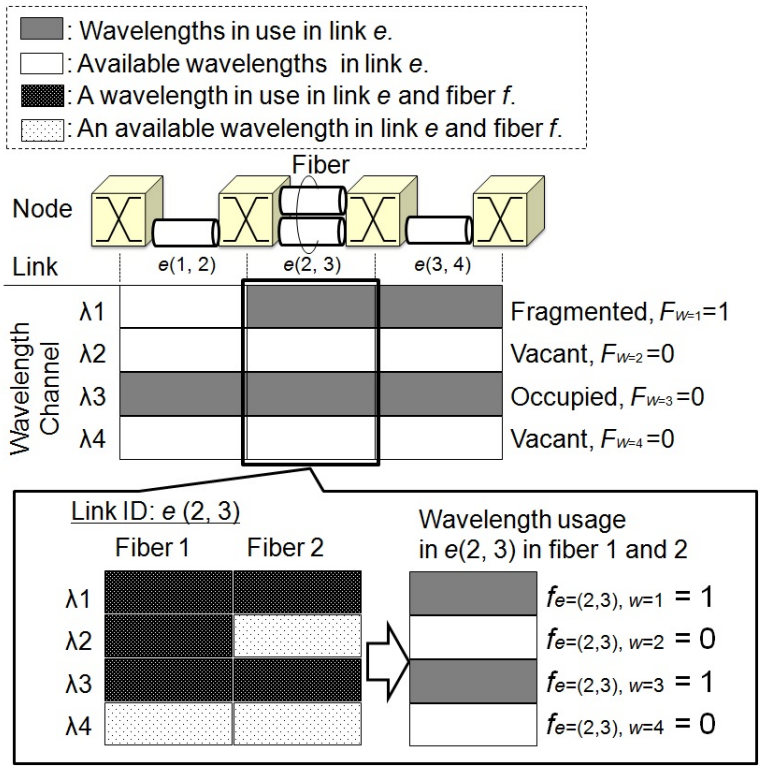

Figure 4.2. Explanation of wavelength fragmentation

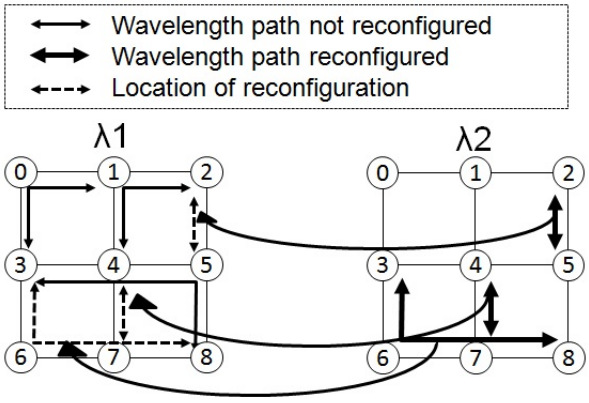

(a) Case1: Reconfiguration from $\lambda 2$ to $\lambda 1$.

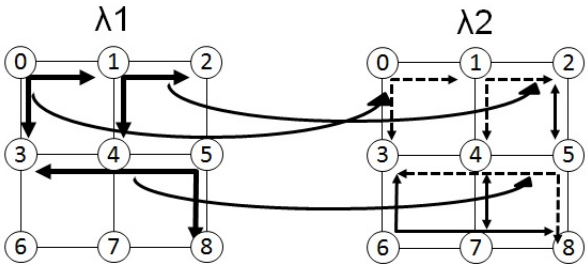

(b) Case2: Reconfiguration from $\lambda 1$ to $\lambda 2$.

Figure 4.3. Explanation of reconfiguration cost function

The number of fragmented wavelength channels and changed wavelength paths are decided by the value of C_F and C_{WR}, respectively. When C_{WR} is equal to 0, if the second term, $C_F \sum_w F_w$, is equal to 0 in the case of a detour route longer than the shortest one in a wavelength channel, the paths are allowed to detour less than or equal to the sum of C_F and the number of shortest hops. When the physical topology is a grid, for instance the 4×4 grid , there are no detour routes one hop longer than the shortest route. Then, for example, if C_F is equal to 1, it can be designed for the shortest route in the topology. This dissertation assumes that C_F is equal to 1 for defragemntation design. When C_F is equal to 0, this design does not consider defragmentation. The third term, $C_{WR} \sum_{(m,n),d_W} R_{(m,n),d_W}$, is determined by the number of wavelengths that can be reused in the new path set. This dissertation assumes that C_{WR} is expressed as a function of the number of fibers in the networks as follows:

$$C_{WR} = k \cdot \frac{1}{\sum_{(i,j)\in E} f_{(i,j)}}, \tag{4.5}$$

where k is constant number. The number of changed wavelengths is analyzed while varying k.

□ Inequality constraints for fragmentation cost:

Equations (4.1) and (4.2) are decided using the characteristics of the floor and ceiling functions given by

$$\frac{y}{x} - 1 \;<\; \left\lfloor \frac{y}{x} \right\rfloor < \frac{y}{x} + \frac{1}{x} : x > 0, 0 \le y \le x, \{x, y\} \in \mathbb{Z}, \tag{4.6}$$

$$\frac{y}{x} - \frac{1}{x} \;<\; \left\lceil \frac{y}{x} \right\rceil < \frac{y}{x} + 1 : x > 0, 0 \le y \le x, \{x, y\} \in \mathbb{Z}. \tag{4.7}$$

The inequality constraint of (4.6) or (4.7) sets the floor or ceiling function of y/x to 0 or 1. Equation (4.1) describes the use of the inequality constraint of (4.6) as

$$\frac{\sum_{f\in F,(m,n)\in P_W,d_W\in D_W} p_{(i,j),f}^{(m,n),w,d_W}}{f_{(i,j)}} - 1 < f_{(i,j),w} < \frac{\sum_{f\in F,(m,n)\in P_W,d_W\in D_W} p_{(i,j),f}^{(m,n),w,d_W}}{f_{(i,j)}} + \frac{1}{f_{(i,j)}}. \tag{4.8}$$

The first term and second term in Equation (4.2) describes the use of the inequality constraint of (4.7) and (4.6), respectively, as follows:

$$\frac{\sum_{(i,j)\in E} f_{(i,j),w}}{|E|} - \frac{1}{|E|} \;<\; \left\lceil \frac{\sum_{(i,j)\in E} f_{(i,j),w}}{|E|} \right\rceil \;<\; \frac{\sum_{(i,j)\in E} f_{(i,j),w}}{|E|} + 1. \tag{4.9}$$

$$\frac{\sum_{(i,j)\in E} f_{(i,j),w}}{|E|} - 1 \;<\; \left\lfloor \frac{\sum_{(i,j)\in E} f_{(i,j),w}}{|E|} \right\rfloor \;<\; \frac{\sum_{(i,j)\in E} f_{(i,j),w}}{|E|} + \frac{1}{|E|}. \tag{4.10}$$

□ On wavelength route constraints:

$$\sum_{i\in V, f\in F} p_{(i,k),f}^{(m,n),w,d_W} = \sum_{j\in V, f\in F} p_{(k,j),f}^{(m,n),w,d_W} \quad \text{if } k \neq m,n \ \forall (m,n) \in P_W, w \in W, d_W \in D_W. \tag{4.11}$$

$$\sum_{i\in V, f\in F} p_{(i,m),f}^{(m,n),w,d_W} = 0 \ \forall (m,n) \in P_W, w \in W, d_W \in D_W. \tag{4.12}$$

$$\sum_{j\in V, f\in F} p_{(n,j),f}^{(m,n),w,d_W} = 0 \ \forall (m,n) \in P_W, w \in W, d_W \in D_W. \tag{4.13}$$

$$\sum_{j\in V, f\in F} p_{(m,j),f}^{(m,n),w,d_W} = \lambda_{(m,n)}^{w,d_W} \ \forall (m,n) \in P_W, w \in W, d_W \in D_W. \tag{4.14}$$

$$\sum_{i\in V, f\in F} p_{(i,n),f}^{(m,n),w,d_W} = \lambda_{(m,n)}^{w,d_W} \ \forall (m,n) \in P_W, w \in W, d_W \in D_W. \tag{4.15}$$

$$\sum_{w\in W} \lambda_{(m,n)}^{w,d_W} = 1 \ \forall (m,n) \in P_W, d_W \in D_W. \tag{4.16}$$

The routing of the wavelength path and wavelength continuity constraints follow the principles of multi-commodity flow equations (or flow conservation) [42]. The explanations of Equations (4.11-4.16) are as follows:

- Equation (4.11) ensures that, for an intermediate node of a wavelength path, the number of incoming wavelength paths is equal to the number of outgoing wavelength paths.
- Equation (4.12) ensures that, for the source node of a wavelength path, the number of incoming wavelength paths is 0.
- Equation (4.13) ensures that, for the destination node of a wavelength path, the number of outgoing wavelength paths is 0.
- Equation (4.14) ensures that, for the source node of a wavelength path, the number of outgoing wavelength paths is equal to the number of wavelength paths between the node pair.
- Equation (4.15) ensures that, for the destination node of a wavelength path, the number of incoming wavelength paths is equal to the number of wavelength paths between the node pair.
- Equation (4.16) ensures that the wavelength can be present in one wavelength path.

□ Link capacity constraint:

$$\sum_{(m,n)\in P_W, w\in W, d_W\in D_W} p_{(i,j),f}^{(m,n),w,d_W} \leq N_{WM} \ \forall (i,j) \in E, f \in F. \tag{4.17}$$

The number of wavelengths is equal or less than the number of wavelengths multiplexed in a fiber.

□ Multi-fiber constraint:

$$\sum_{(i,j)\in E, n\in V, w\in W} p_{(i,j),f}^{(m,n),w,d_W} \leq N_{WM} \cdot M_{m,f} \ \forall m \in V, f \in F. \tag{4.18}$$

The wavelength paths are passed through the multiplexer/demultiplexer capability connecting the fiber in the node. Here, $\sum_{m,f} M_{m,f}/2$ is the sum of fibers in the network.

4.4 Migrating Sequence without Service Disruption

In this section, a migrating sequence algorithm is introduced that prevents service disruption. Effective migration requires that the issue of dependency cycles between the paths before reconfiguration and after reconfiguration be addressed. For instance, the route and wavelength of path p_i selected to complete reconfiguration, may be blocked by existing path p_j which in turn may need to be reconfigured. Here p_i can only be reconfigured after p_j, i.e., p_i depends on p_j which is represented as $p_i \mapsto p_j$. This dependence existing between reconfiguration requests can be represented as a graph, the "resource dependency graph" [63]. Furthermore, request p_i might depend on request p_j, which might depend on p_k, which in turn might again depend on p_i. so $p_i \mapsto p_j \mapsto p_k \mapsto p_i$ which yields a dependency cycle. Such dependency cycles in a resource dependency graph need to be resolved to determine effective migrating sequences for the network. Here, a migrating sequence algorithm is introduced that uses spare wavelengths to break the dependency cycle (called decyclization).

Algorithm 1 Migrating Sequence Algorithm without Service Disruption

Input: Set of wavelength paths before and after reconfiguration and physical topology $G(V, E)$.
Output: Migrating sequence

1: For all changed paths, generate dependency graphs.
2: Select a dependency graph.
3: Find the wavelength path at the tail endpoint of the dependency graph.
4: If the dependency graph has a cycle, go to Step 5, otherwise go to Step 6.
5: Perform decyclization to establish a wavelength path using spare wavelength, and go to Step 7.
6: Establish the wavelength path at the route and wavelength based on the reconfiguration design, and go to Step 7.
7: Delete old wavelength path before reconfiguration.
8: If the migration of all wavelength paths in the dependency graph is finished, go to Step 9, otherwise reenter Step 4 for the next wavelength path in the dependency graph.
9: Iterate Step 2 until all changed paths are migrated.

First, dependency graphs from the old path set to the new one are generated using, for example, Johnson's algorithm [71]. Next, one of the dependency graphs is selected, and a wavelength path at the tail end point of the dependency graph is identified. If a wavelength path that can be reconfigured without blocking is

found, i.e. not cyclic, reconfiguration begins sequentially from the tail endpoint of the dependency graph. If the dependency graph indicates a cycle, which means the graph returns to some wavelength path, the cycle is broken by migrating to a spare wavelength. The above-mentioned sequence is applied to all wavelength paths that are to be reconfigured. In Step 5 and Step 6, the reconfiguration can be performed without service disruption by setting 1+1 protection.

The migrating algorithm is explained using the simple example of Fig. 4.4; it shows reconfiguration design for a 3×3 grid. Before reconfiguration, three paths are accommodated, a is 1-4-3 route with $\lambda 1$, b is 3-0-1-2-5-8 route with $\lambda 2$, c is 2-5-4 route with $\lambda 1$, as shown in Fig. 4.4 (a); for reconfiguration, three paths are changed, a becomes 1-0-3 route with $\lambda 1$, b is 3-4-5-8 route with $\lambda 1$, c is 2-1-4 route with $\lambda 1$, as shown in Fig. 4.4 (b). Figure 4.5 shows the dependency graph for reconfiguration considered here. Figure 4.5 (a) shows the image of a dependency cycle, and Figure 4.5 (b) shows the image of using a spare wavelength to establish decyclization. From Figure 4.4, the dependency relation before and after reconfiguration is $a \mapsto b$, $c \mapsto b$, $b \mapsto a$, and $b \mapsto c$, so path a, b, and c form a dependency cycle as shown in Fig. 4.5 (a). In this example, first of all, wavelength path b is migrated to establish decyclization using a spare wavelength, after that a or c is migrated, sequentially.

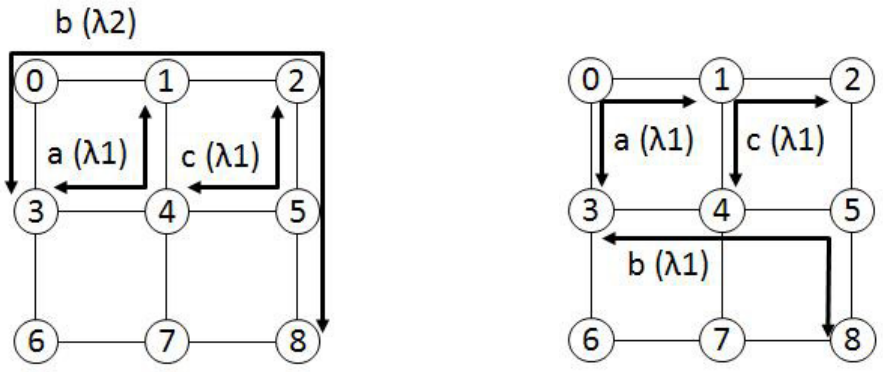

(a) Before reconfiguration. (b) After reconfiguration.

Figure 4.4. Example of reconfiguration design in a 3 × 3 grid topology

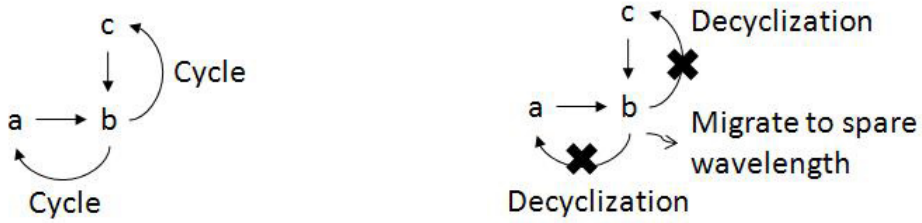

(a) Dependency cycle. (b) Decyclization.

Figure 4.5. Dependency cycle and decyclization image

4.5 Wavelength Defragmentation Based on Wavelength Resource Management

An adaptive reconfiguration scheme based on wavelength path resource management is proposed. The scheme comprises three phases. First, wavelength path resources are managed such that the number of wavelength paths that can be accommodated between all node pairs is calculated for each accommodated path. Second, if that number is less than the threshold value set by the network carrier for some node pair, reconfiguration is designed. Third, the number of wavelength path resources calculated is increased after redesigning the paths. Wavelength paths are reconfigured; otherwise, reconfiguration is not triggered until fiber links are added between the pair of target nodes.

4.5.1 Wavelength Path Resource Management

The wavelength path resource algorithm calculates the number of wavelength paths that can be accommodated for all node pairs. First, k routes for all node pairs are calculated. Next, for a wavelength channel, routes are deleted that have a link where the wavelength is used. Subsequently, disjoint route pairs are found and the number of disjoint routes is calculated for each pair. The maximum number of disjoint routes is decided and the sum of the disjoint routes for all wavelength channels between each node pair is calculated. The algorithm flow is shown in Algorithm 2.

Figures 4.6 (a) and (b) show an example of the algorithm for the number of wavelength path resources. First, k routes are calculated between node 0 and node 6. Next, the route in which a wavelength, λ 1, is used between node 3 and node 6 is deleted. In this example, there are two link disjoint route pairs which are pair 1 having 2 routes, 0-1-4-6 and 0-2-5-6, and pair 2 having 1 route, 0-2-5-6. Then, the maximum number of disjoint routes in link disjoint pair 1 is found in Step 3. Figure 4.7 shows a management table for the wavelength path resources indicating the number of wavelength paths that can be accommodated. The rows indicate the wavelength channel and the columns represent the pairs between the source and destination. The table is updated for each path accommodated and the bottom line shows the sum of the number of wavelength paths that can be accommodated for each node pair. When the number in the bottom line is less than the number predetermined by the operator, reconfiguration is performed.

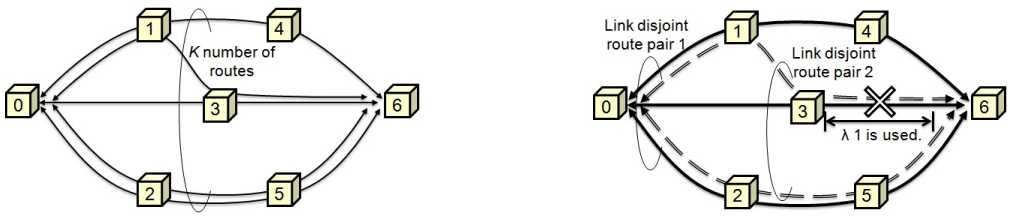

(a) Step 1. (b) Steps 2 and 3.

Figure 4.6. Image of wavelength path resource management algorithm.

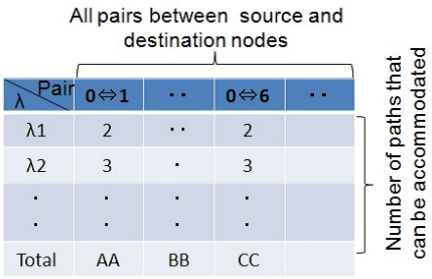

Figure 4.7. Management table.

Algorithm 2 Wavelength path resource management

INPUT: Set of wavelengths used on each physical link.
OUTPUT: Number of wavelength paths between each node pair that can be accommodated on the fiber.

1: Calculate k routes for all node pairs.
2: For a wavelength channel, delete routes that have a link carrying a used wavelength.
3: Find disjoint route pairs for each route and calculate the number of disjoint routes.
4: Decide the maximum number of disjoint routes from Step 3 considering the wavelength continuity constraint.
5: Repeat Steps 2 to 4 for all wavelength channels
6: Calculate the sum of the number of disjoint routes for all wavelength channels between each node pair.

4.5.2 Heuristic Algorithms for Wavelength Defragmentation

Two wavelength defragmentation algorithms according to the accommodation rate are proposed, which are Fixed Route Defragmentation - according to the Accommodation Rate (FRD-AR) and Alternative Route Defragmentation - according to Accommodation Rate (ARD-AR). Here, The accommodation rate of the wavelength channel is defined as the ratio of the number of used links to the total number of links including multiple fibers for a wavelength as shown in Algorithm 3. The features of the proposed algorithm are given below.

1. Adaptive selection for reconfiguring a wavelength channel according to the accommodation rate.
2. Reduction in the number of migration sequences due to the reconfiguration from a low to high accommodation rate for one wavelength channel compared to reconfiguration not considering the accommodation rate.

The FRD-AR algorithm reconfigures wavelength paths from the lowest wavelength accommodation rate of the wavelength channel to the highest rate. The ARD-AR

Algorithm 3 FRD-AR/ARD-AR

INPUT: Set of wavelength paths before reconfiguration and physical topology.
OUTPUT: Reconfiguration design and migrating sequence.

1: Calculate wavelength accommodation rate for each wavelength channel.
2: Sort wavelength channels in descending order from the highest accommodation rate, and generate a search table.
3: Delete the wavelength channels with accommodation rates of 1 or 0 from the table.
4: Find a vacant wavelength in the fixed route/alternate shortest route that includes multiple fibers per link from the top line until one line from the bottom for the wavelength path in the bottom line.
5: If there is a vacant wavelength, then reconfigure the wavelength path. Otherwise, the wavelength path is not reconfigured.
6: If the search for all wavelength paths in the bottom line is completed, delete this line (wavelength channel) from the search table and go to Step 7. Otherwise, repeat Step 4 and Step 5.
7: Repeat Steps 4 to 6 until all wavelength paths are searched in all lines.

algorithm extends the FRD-AR algorithm from fixed route search to shortest alternative route search in Step 4 in the FRD-AR algorithm. Figure 4.8 shows an example of the proposed algorithm. Figure 4.8 (a) is a simple example of the physical topology, which consists of 4 nodes, 3 links, and 2 fibers in each link. The wavelength accommodation rate for each wavelength channel is calculated. When wavelength paths are accommodated such as in Fig. 4.8 (b), the wavelength accommodation rate is calculated as shown in the column to the far right. Next, the wavelength channels are sorted in descending order from the highest accommodation rate, and a search table is generated as shown in Fig. 4.8 (c). The wavelength channels for the accommodation rates of 1 and 0 are deleted from the table. For the wavelength path indicated in the bottom line, a search is performed for a vacant wavelength in the fixed route among the multiple fibers per link from the top line (λ 5) until one line from the bottom (λ 6). If there is a vacant wavelength, the wavelength path migrates to that path; otherwise, the wavelength path does not change. This step is repeated until all wavelength paths are searched in all lines. Figure 4.8 (d) shows an image of the migration sequence. In this case, a search of wavelength channel λ 5 indicates no appropriate vacant wavelengths to accommodate the wavelength paths in wavelength channel λ 3. Since there are no appropriate reconfigurable locations, a searched is performed on the next line. In this example, the wavelength paths can be reconfigured in wavelength channel λ 3 into the wavelength path in λ 7. In the same way, the two wavelength paths are reconfigured in λ 6 into λ 4, and reconfigure the wavelength path in λ 4 into λ 5.

The other heuristic algorithm is proposed that extends the FRD-AR/ARD-AR algorithms. The algorithm performs pre-adjustment by rerouting existing paths in the reconfigured wavelength channel. The proposed Pre-adjustment by Rerouting Existing paths (PRE) algorithm is shown in Algorithm 4. The PRE algorithm extends Step 5 of the FRD-AR/ARD-AR algorithms. Figure 4.9 shows Step 5 in

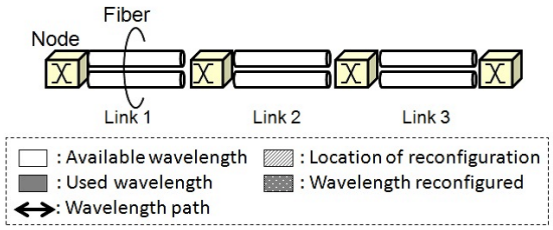

(a) Example topology.

STEP 1

	Fiber 1			Fiber 2			Accommodation Rate
	Link 1	Link 2	Link 3	Link 1	Link 2	Link 3	
λ1							0
λ2							1
λ3							2/6
λ4							3/6
λ5							5/6
λ6							3/6
λ7							4/6

(b) Wavelength path accommodation status .

	Fiber 1			Fiber 2			Accommodation Rate
	Link 1	Link 2	Link 3	Link 1	Link 2	Link 3	
λ2							1
λ5							5/6
λ7							4/6
λ4						↔	3/6
λ6	↔			↔			3/6
λ3					↔	↔	2/6
λ1							0

(c) Search table.

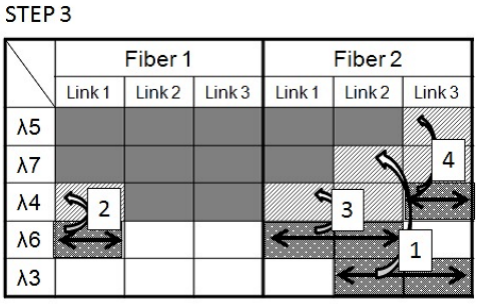

(d) Migration sequence.

Figure 4.8. Explanation of FRD-AR.

the PRE algorithm. When a target wavelength path cannot be reconfigured in alternate routes, it searches for a reconfigurable wavelength channel by combining routes between the target path and existing path in the reconfigured wavelength channel. In Step 8, migrating sequences are decided by using Algorithm 1.

The computational complexity for each of these algorithms from Step 4 to Step 7 is obtained. In regard to the FRD-AR algorithm, the computational complexity in Step 4 and 5 is $O(w-1)$ and then, that form Step 4 to 6 is $O(n_w(w-1))$, where n_w is the number of wavelength paths in the wavelength channel w. Therefor, the computational complexity in the FRD-AR algorithm when the repeat time is $(w-1)$ in Step 7 can be obtained as follows:

$$O_{\mathrm{FRD}} = n_w(w-1)^2. \tag{4.19}$$

In regard to the ARD-AR algorithm, an alternate route in Step 4 is assumed the use of Depth First Search (DFS) or Breadth First Search (BFS) algorithm, and then the computational complexity of the alternate route search is $O(|E|+|V|)$ [72]. Therefore, in the same way as that of FRD-AR algorithm, the computational complexity in the ARD-AR algorithm can be obtained approximately as follows.

$$O_{\mathrm{ARD}} = n_w(w-1)^2(|E|+|V|). \tag{4.20}$$

The PRE algorithm in Step 5 searches for a reconfigurable wavelength channel by combining routes between the target path and existing paths in the reconfigured

Algorithm 4 PRE

INPUT: Set of wavelength paths before reconfiguration and physical topology.
OUTPUT: Reconfiguration design and migrating sequence.

1: Calculate the wavelength accommodation rate for each wavelength channel.
2: Sort wavelength channels in descending order from the highest accommodation rate, and generate a search table.
3: Delete the wavelength channels with accommodation rates of 1 or 0 from the table.
4: Find a vacant wavelength in the shortest alternate route that includes multiple fibers per link from the top line until one line from the bottom for the wavelength path in the bottom line.
5: If there is a vacant wavelength, then reconfigure the wavelength path. Otherwise, find a location that can be reconfigured from the top line until one line from the bottom by combining routes searched between the target reconfigured path and the wavelength paths of the reconfigured channel.
6: If the search for all wavelength paths in the bottom line is completed, delete this line (wavelength channel) from the search table and go to Step 7. Otherwise, repeat Step 4 and Step 5.
7: Repeat Steps 4 to 6 until all wavelength paths are searched in all lines.
8: For all changed paths, dependency graphs are generated and migrating sequences are decided.

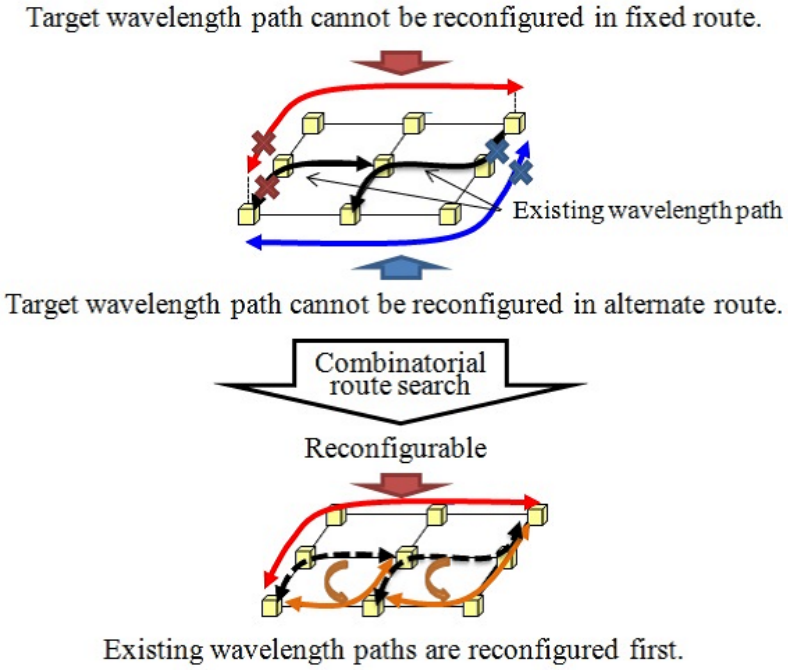

Figure 4.9. Image of Step 5 in the PRE algorithm.

wavelength channel. The computational complexity of combinatorial search by k number route for a wavelength path is $O(k^{n_w+1})$. Then, the computational complexity in worst case is approximately obtained as

$$O_{\mathrm{PRE}} \simeq n_w(w-1)^2 k^{n_w+1}. \tag{4.21}$$

4.6 Numerical Evaluation for ILP-based Wavelength Defragmenation

The proposed reconfiguration design based on ILP is evaluated. The effect of employing wavelength fragmentation and reconfiguration costs are analyzed in view of the number of fibers as shown in Figs. 4.11-4.12, the number of fragmented wavelength channels as shown in Fig. 4.13, the number of changed wavelengths as shown in Fig. 4.14, and computation time for the calculations as shown in Fig. 4.15. The objectives for evaluation are No Reconfiguration (NR), Reconfiguration without Defragmentation (Rw/oD), and Reconfiguration with Defragmentation (RD) with k values of 0, 1/2, 1, 2, 3, and 4, where k is a constant that determines the relative reconfiguration cost parameter C_{WR} in Equation (4.5).

4.6.1 Simulation Conditions

The physical topologies examined are a 12-node simplified Japan core (JPN) network , shown in Fig. 4.10 (a) [25], a 14-node National science foundation (NSF) network, shown in Fig. 4.10 (b) [73], a 16-node European core (EUR) network , shown in Fig. 4.10 (c) [74] and a 4×4 grid, shown in Fig. 4.10 (d). The number of wavelengths multiplexed in a fiber (N_{WM}) is 10 to evaluate the effectiveness of the proposed design quickly. Making N_{WM} bigger than 10, will yield the same tendency. Wavelength paths are accommodated randomly one-by-one from their source to destination nodes using the shortest routes with random wavelength assignment. Reconfiguration is performed upon the receipt of every 10th path demand. The accommodated patterns are changed 10 times and the average of the results is calculated. Initially, all links are equipped with one fiber. When a new path cannot be accommodated, fibers are added on the shortest route link. As the ILP solver, CPLEX [75] is used running on a workstation with a Xeon 3.3GHz processor and 48GB of RAM.

4.6.2 Results and Discussion

Figure 4.11 compares RD and Rw/oD to No reconfiguration in terms of the maximum reduction rate of the number of fibers. The effectiveness of the defragmentation in the JPN network, NSF network, EUR network, and 4×4 grid is as much as 5%, 4%, 12%, and 15%, respectively, compared to Rw/oD. The effectiveness of reconfiguration with defragmentation compared to No reconfiguration is from 8% to 19%.

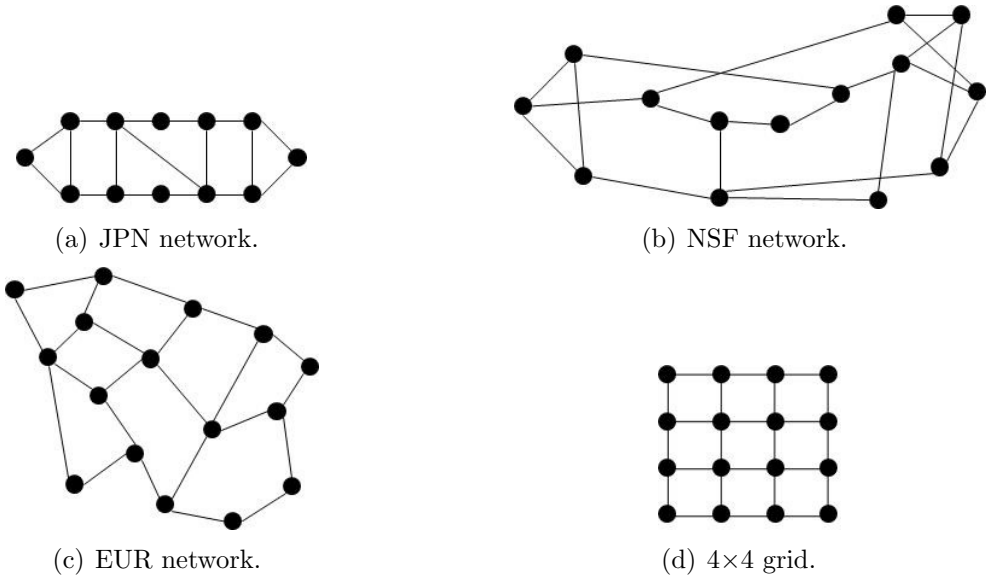

(a) JPN network. (b) NSF network.

(c) EUR network. (d) 4×4 grid.

Figure 4.10. Physical topologies examined in the simulation

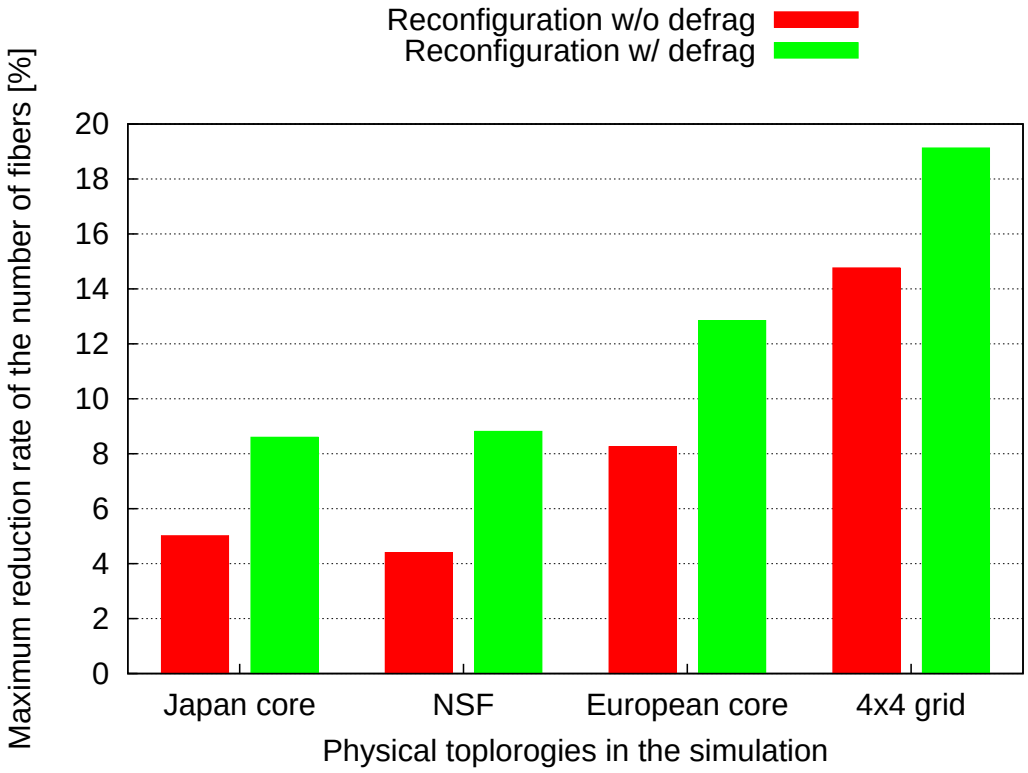

Figure 4.11. Comparison of RD and Rw/oD to No reconfiguration with regard to maximimum reduction rate of the number of fibers.

Figure 4.12 shows the relative number of fibers for Rw/oD, RD ($k = 1/2$, 1, 2, 3, and 4) normalized by NR. There is almost no difference between the results for $k = 0$, $1/2$, and 1. Additionally, the effectiveness of defragmentation increases with the wavelength path demands.

Figure 4.13 shows the number of fragmented wavelength channels in which the wavelength channels are not completely occupied or vacant through all physical links, normalized by the number of wavelengths multiplexed in a fiber, 10. There is only a slight difference between the number of fragmented wavelength channels for RD ($k = 0$) and that for RD ($k = 1/2$). The fragmentation can be also suppressed 30%-50%. From Figures. 4.12 and 4.13, the effectiveness of our reconfigure design proposal increases with the number of nodes.

Figure 4.14 shows that the number of changed wavelengths is reduced approximately 50%-90% employing reduction cost. When the reduction cost has k values of $1/2$ or 1, the effectiveness of defragmentation for number of fibers used is the same as that when the reduction cost is not considered ($k = 0$) as shown in Fig. 4.12.

Figure 4.15 shows the computation time for the calculation. If not employing the reconfiguration cost, the computation time is drastically increasing with increasing the number of wavelength path demands. On the other hand, the computation time can be decreased by employing the reconfiguration cost.

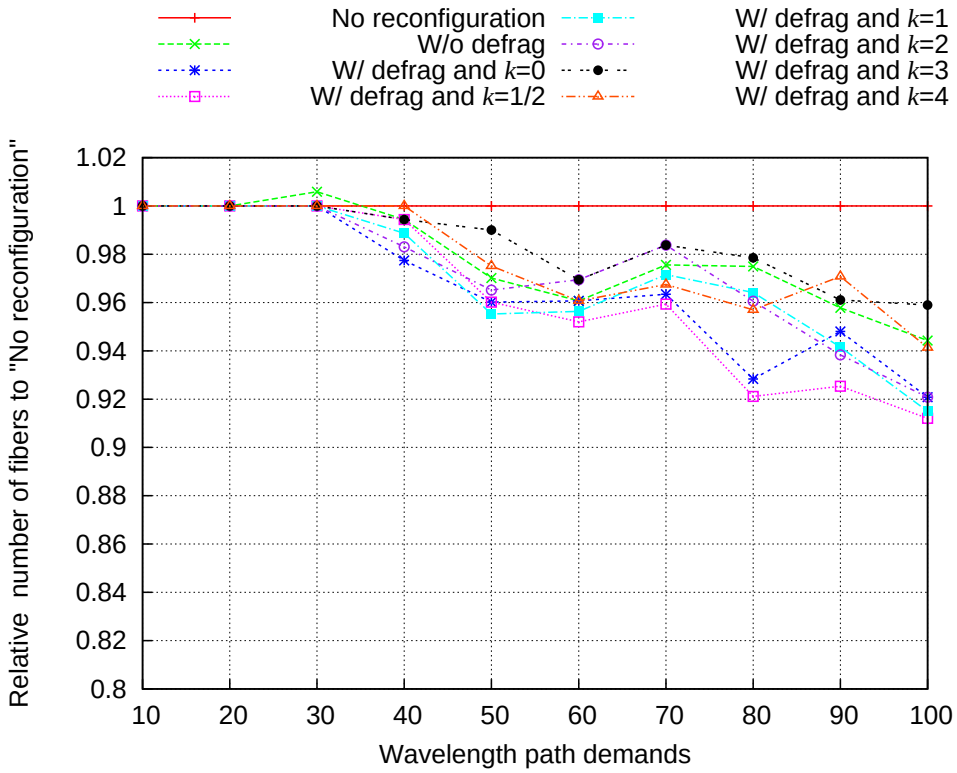

(a) JPN network.

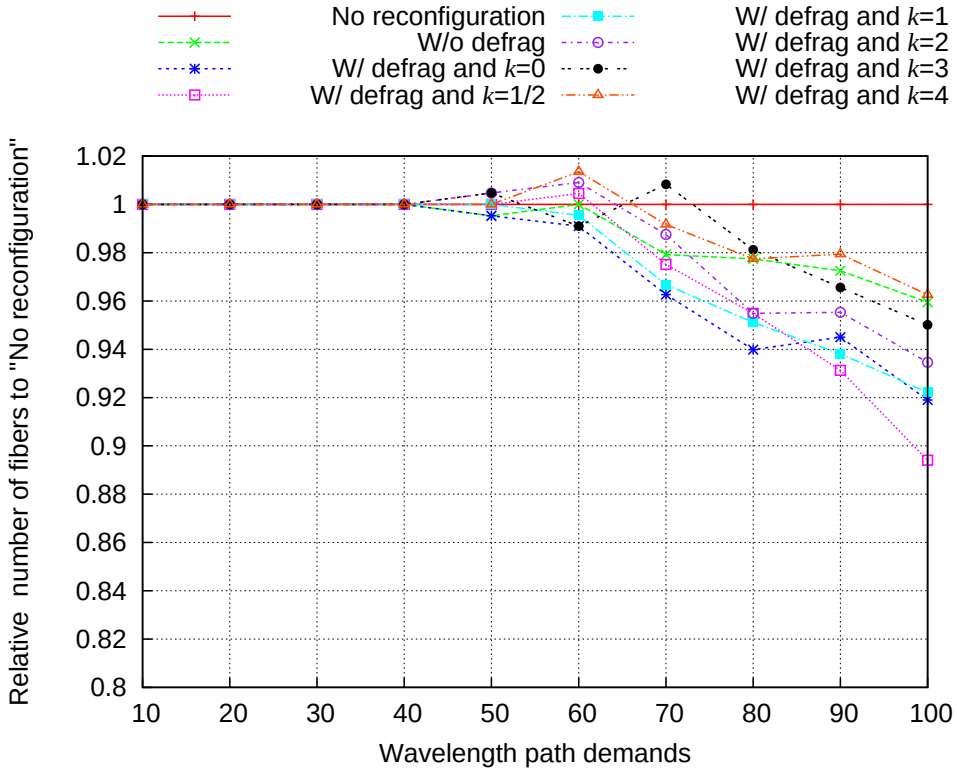

(b) NSF network.

Figure 4.12. Comparison of the relative number of fibers for ILP-based wavelength defragmenation in JPN and NSF.

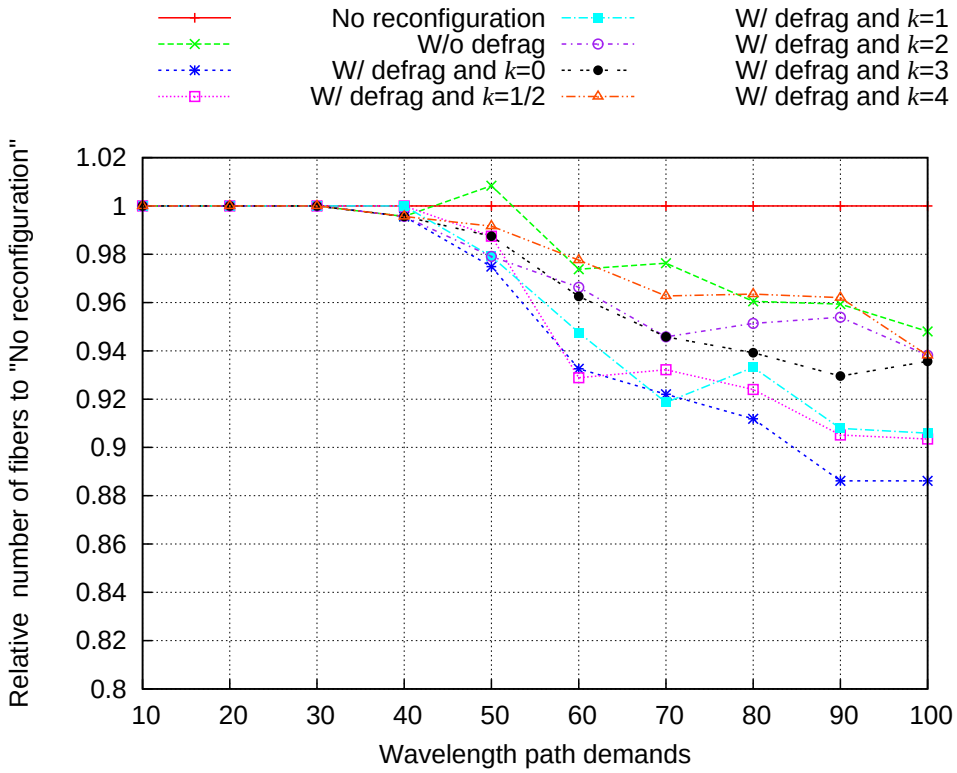

(c) EUR network.

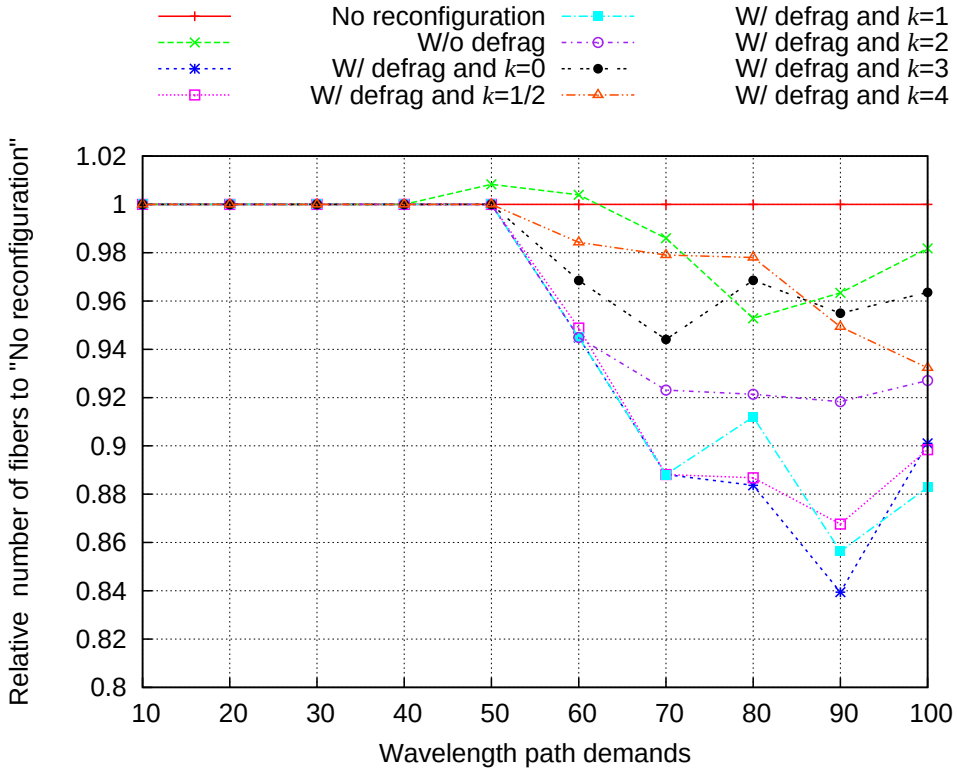

(d) 4×4 grid.

Figure 4.12. Comparison of the relative number of fibers for ILP-based wavelength defragmenation in EUR and 4×4 grid.

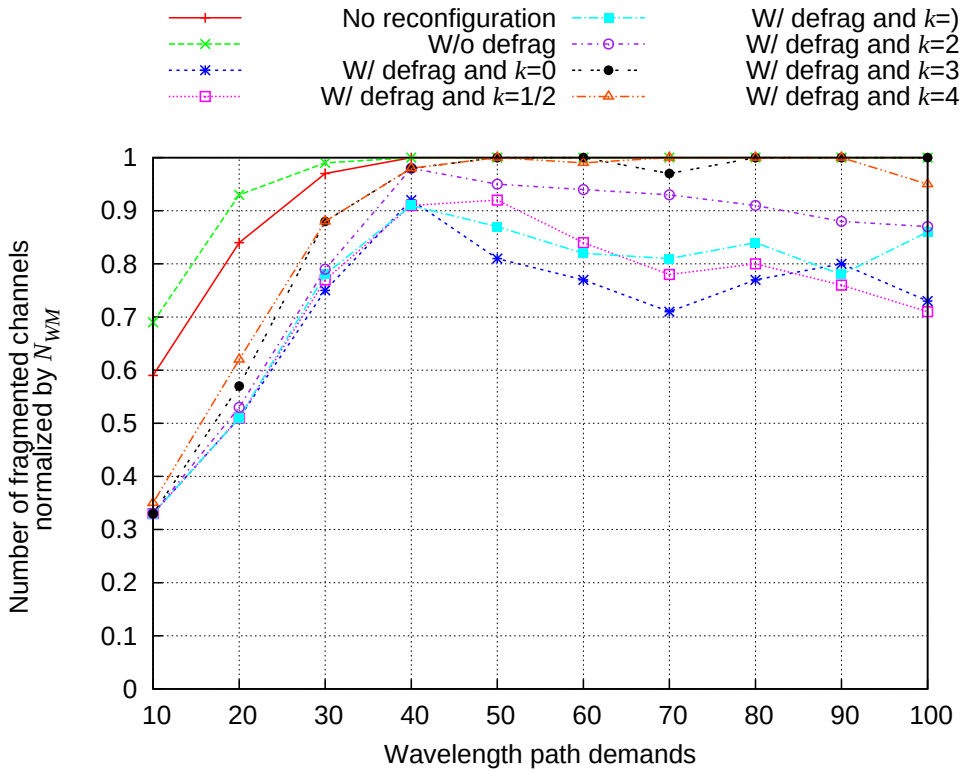

(a) JPN network.

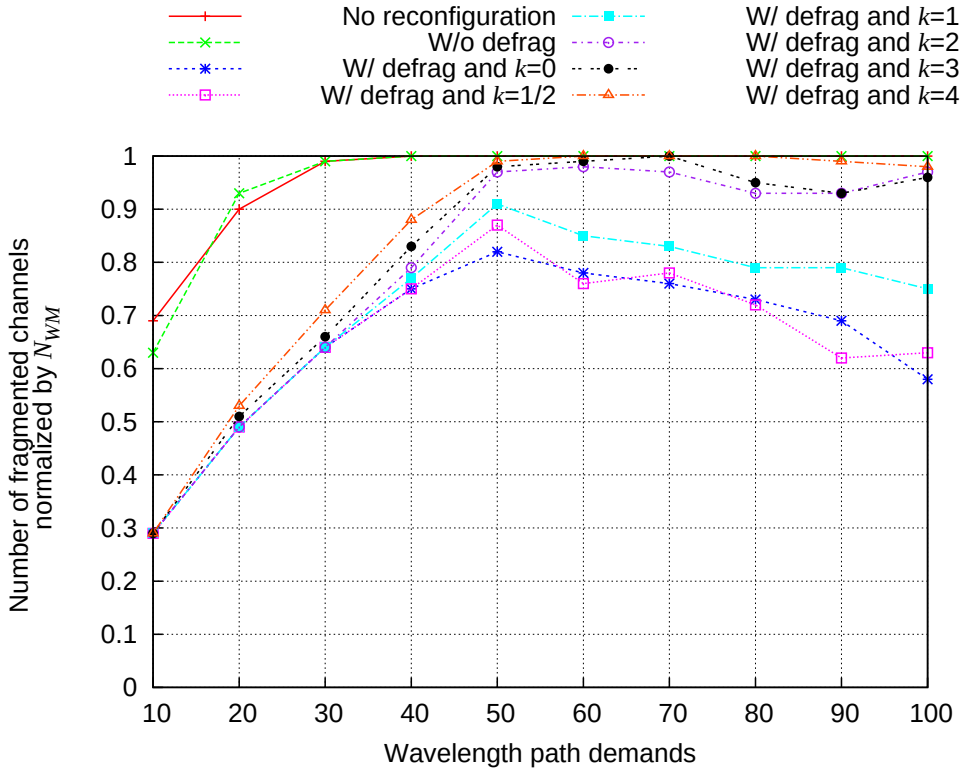

(b) NSF network.

Figure 4.13. Comparison of the number of fragmented wavelength channels for ILP-based wavelength defragmenation in JPN and NSF.

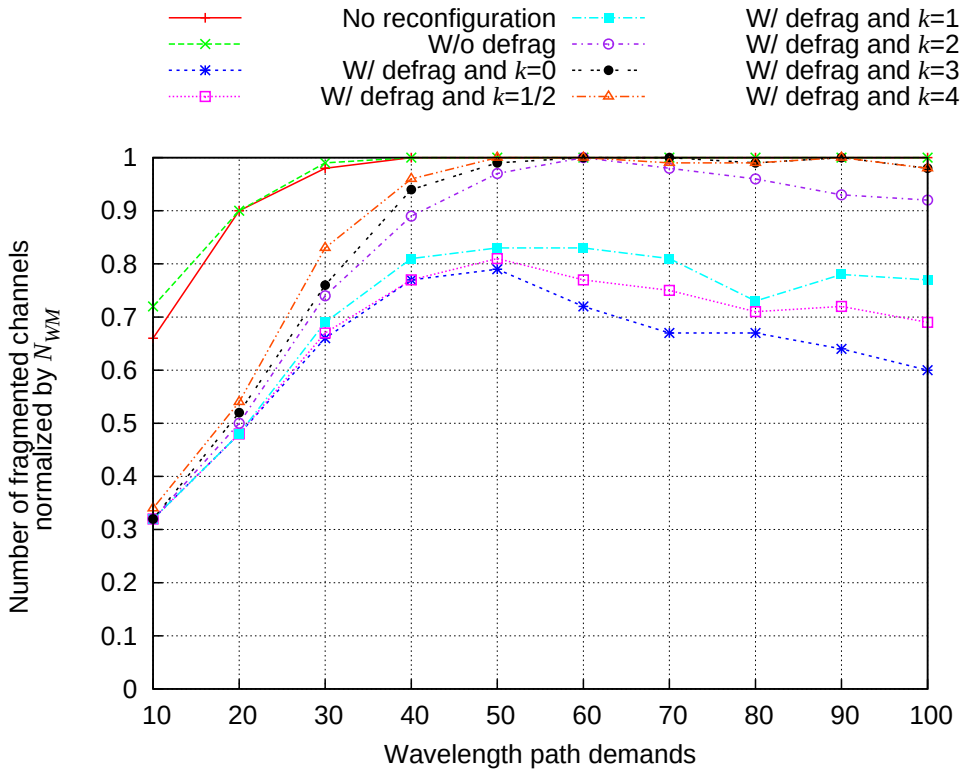

(c) EUR network.

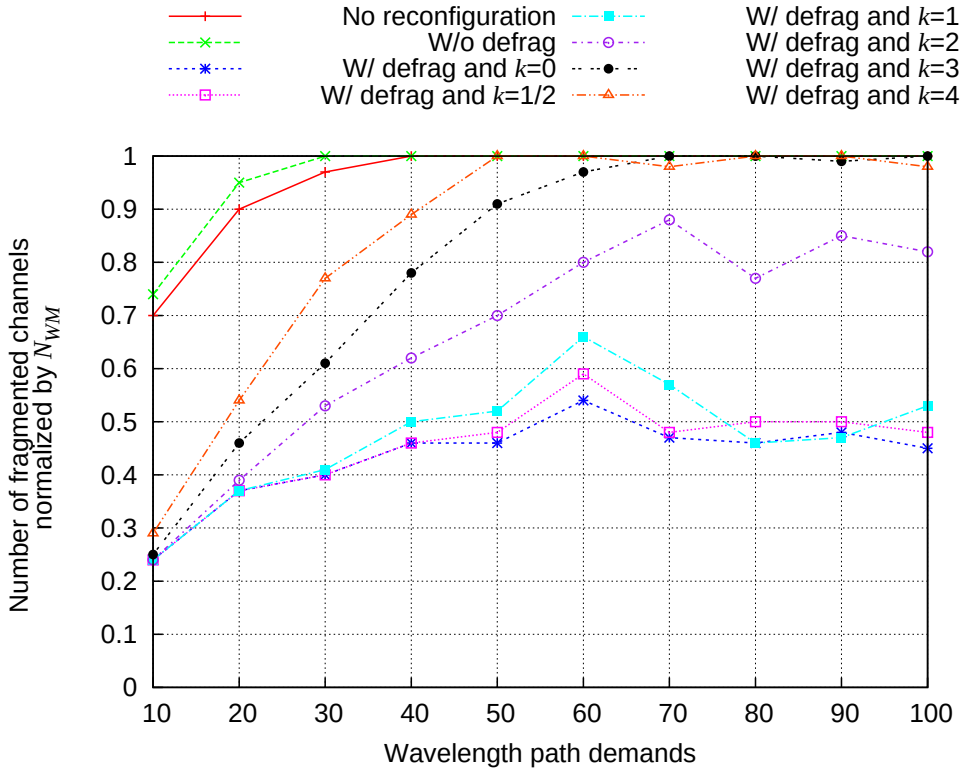

(d) 4×4 grid.

Figure 4.13. Comparison of the number of fragmented wavelength channels for ILP-based wavelength defragmenation in EUR and 4×4 grid.

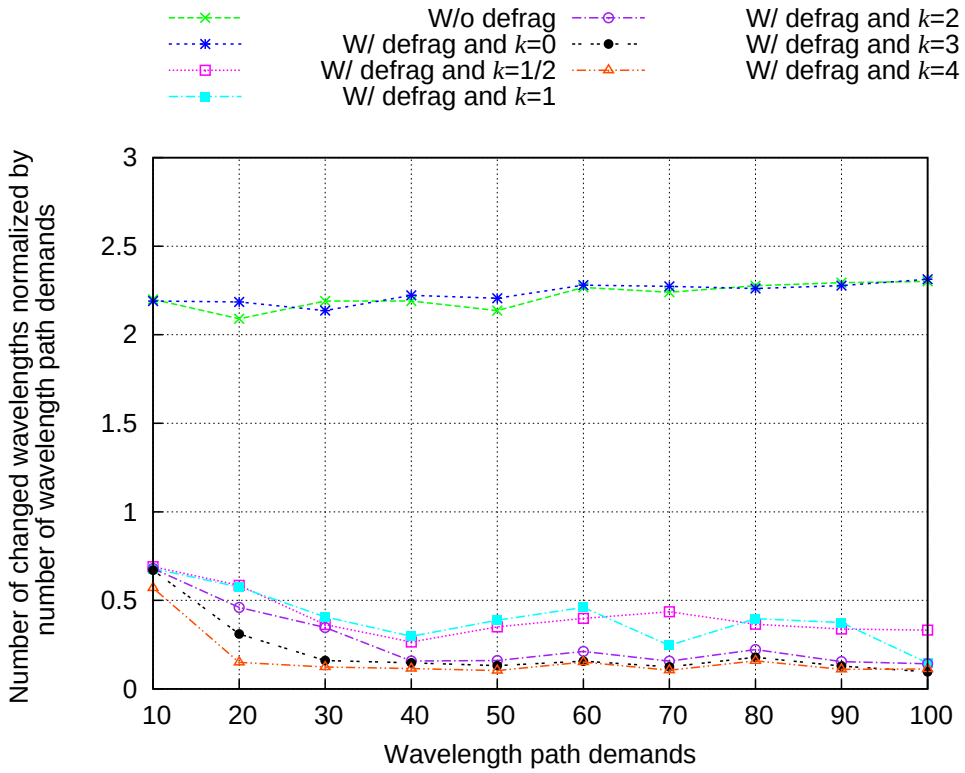

(a) JPN network.

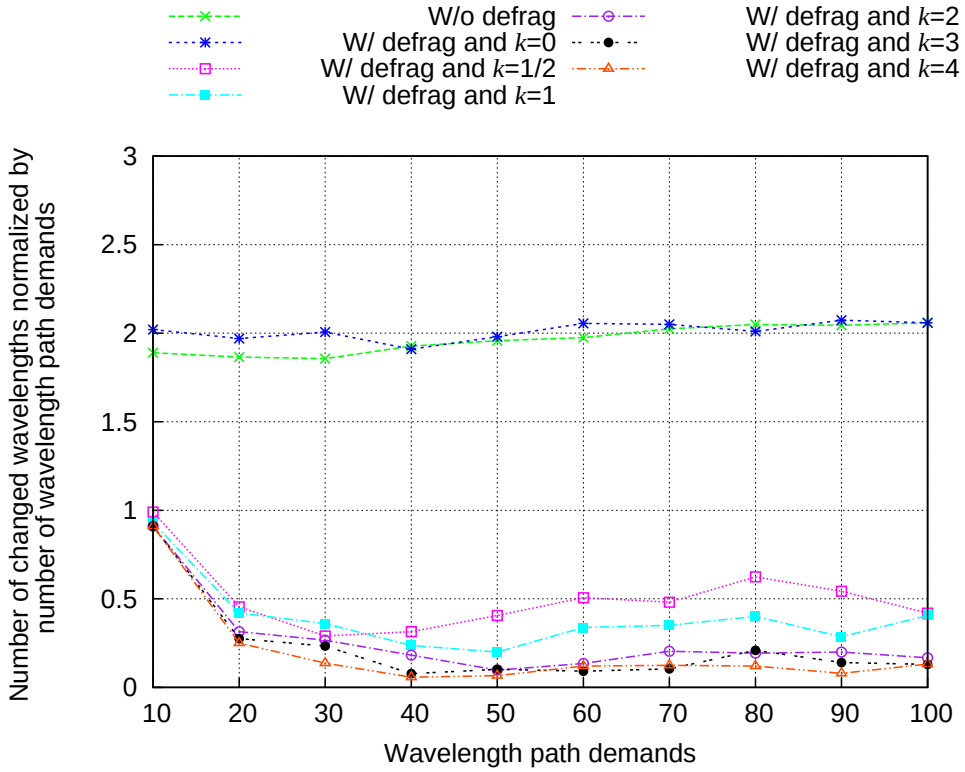

(b) NSF network.

Figure 4.14. Comparison of the number of changed wavelengths for ILP-based wavelength defragmenation in JPN and NSF.

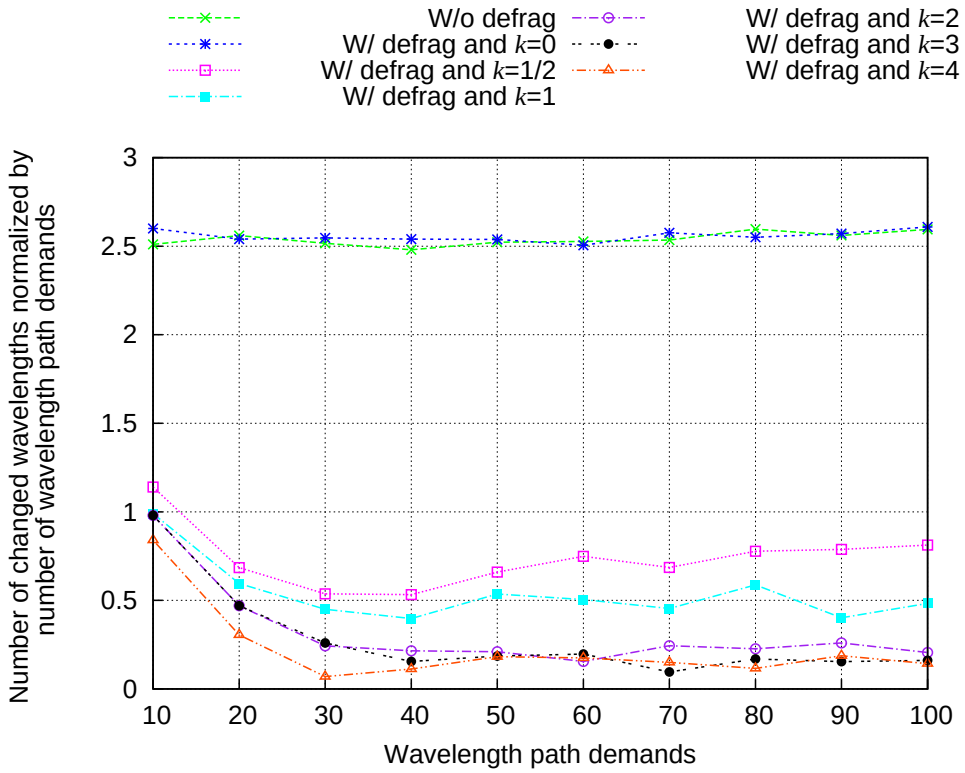

(c) EUR network.

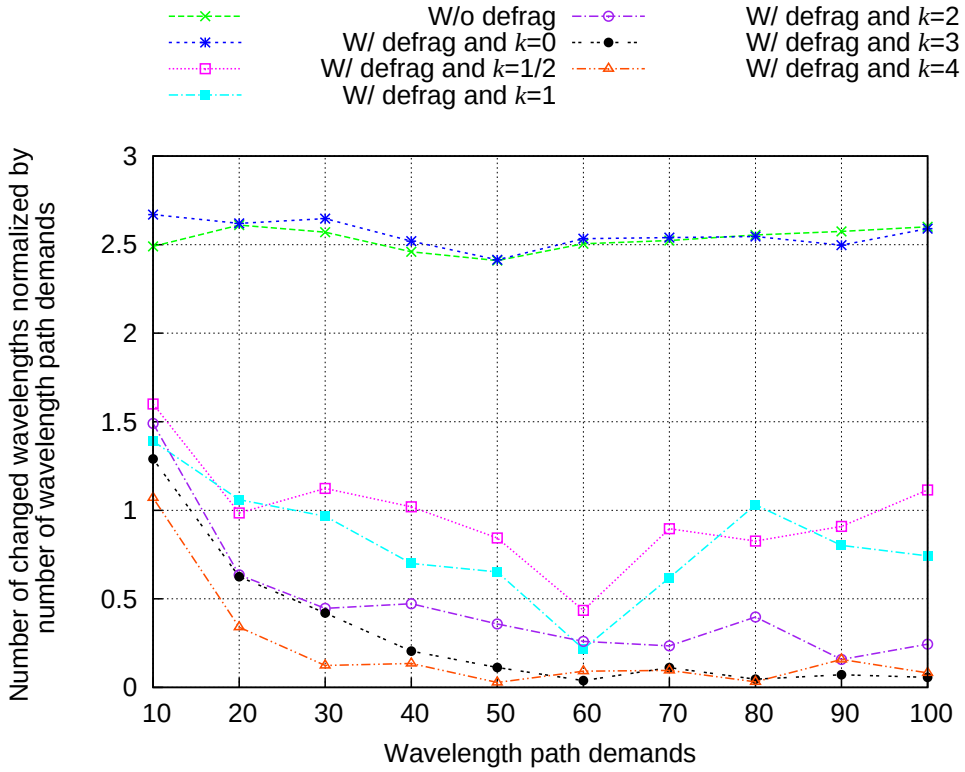

(d) 4×4 grid.

Figure 4.14. Comparison of the number of changed wavelengths for ILP-based wavelength defragmenation in EUR and 4×4 grid.

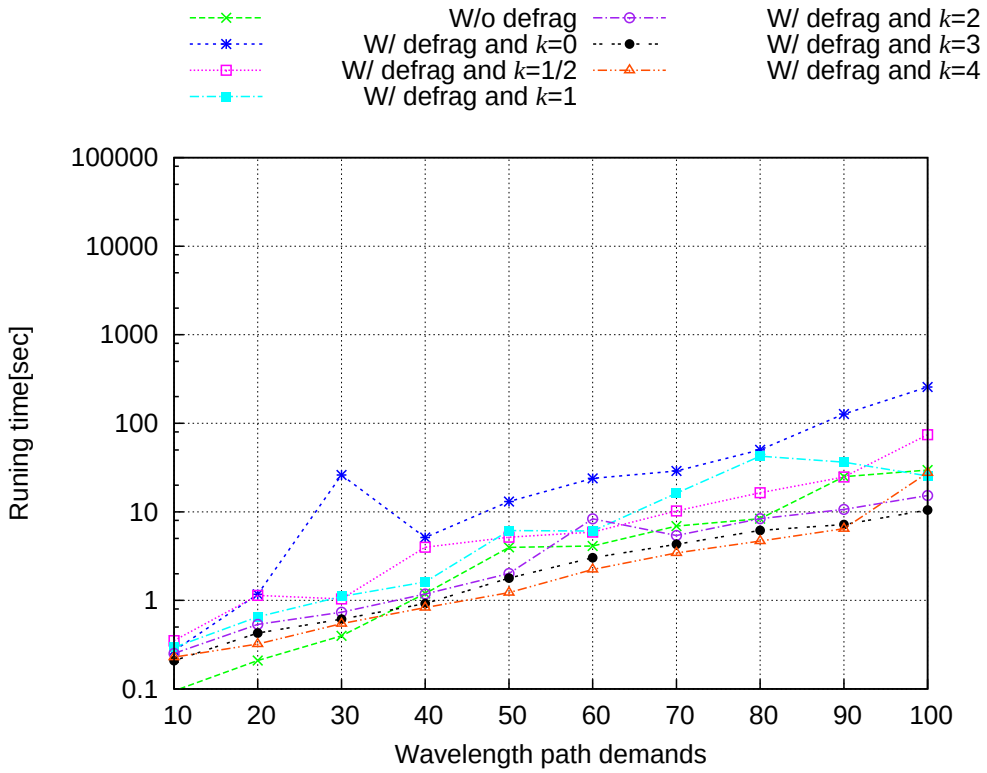

(a) JPN network.

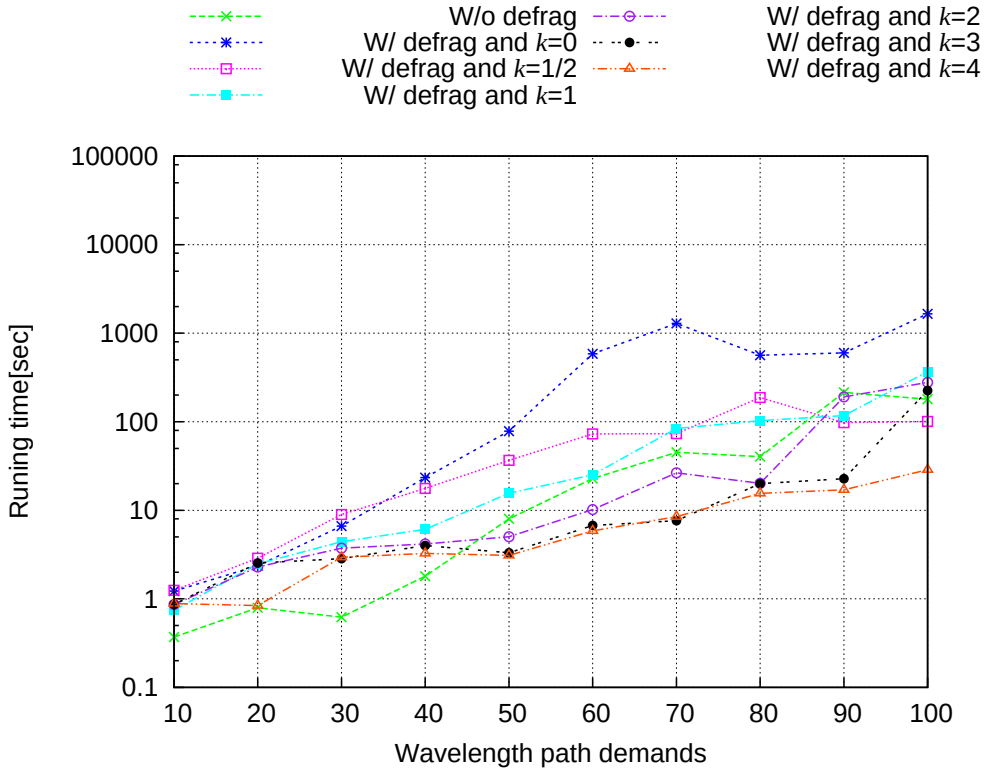

(b) NSF network.

Figure 4.15. Comparison of running time for ILP-based wavelength defragmenation in JPN and NSF.

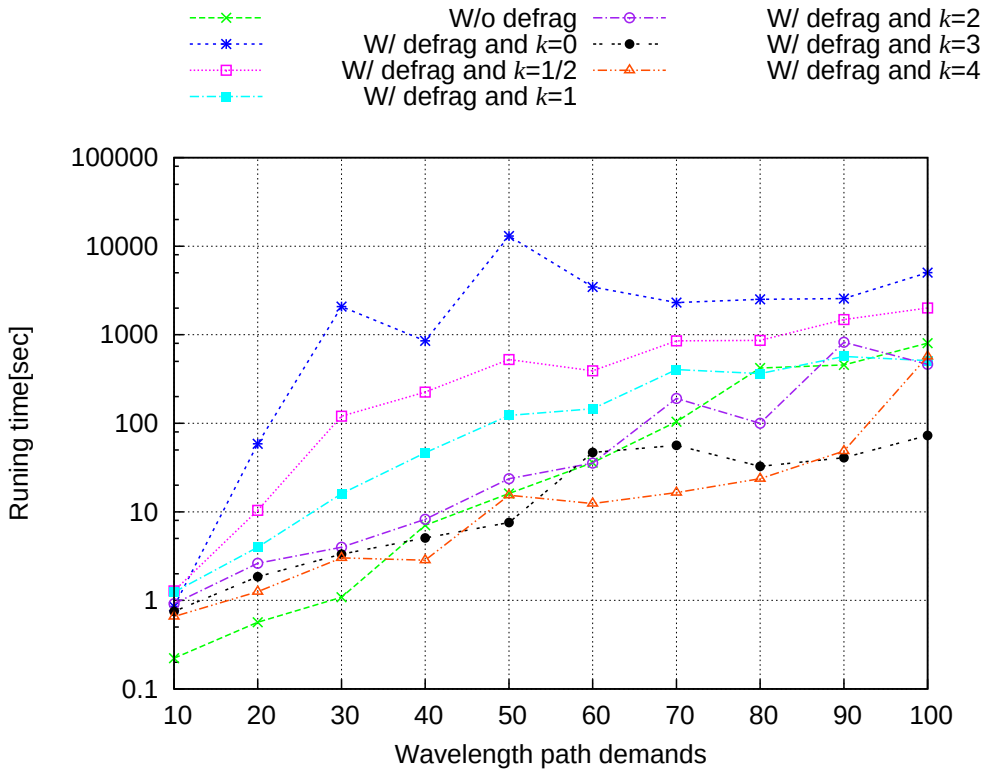

(c) EUR network.

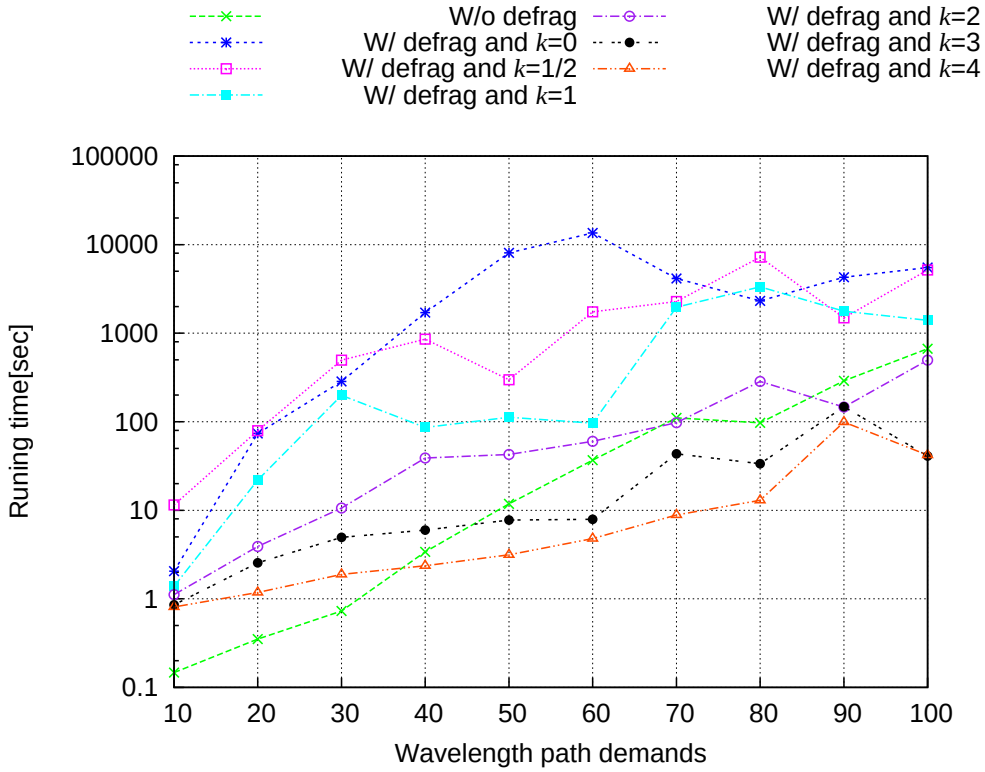

(d) 4×4 grid.

Figure 4.15. Comparison of running time for ILP-based wavelength defragmenation in EUR and 4×4 grid.

4.7 Numerical Evaluation for Heuristic Wavelength Defragmentation Algorithms

Following algorithms are evaluated: No reconfiguration, Push-pull, FRD-AR, ARD-AR, and PRE. To simulate the Push-pull algorithm proposed by [57], the fixed route defragmentation (FRD) algorithm is used in which defragmentation is performed in fixed routes in ascending order of the number of wavelength channels. Evaluation items for comparison are the number of fibers, wavelength accommodation rate, number of wavelength resources, and number of migration sequences.

4.7.1 Simulation Conditions

The employed physical topology is the NSF network with 14 nodes and 21 links as shown in Fig. 4.16 (a) and COST266 with 26 nodes and 43 links as shown in Fig. 4.16 (b). Wavelength paths are accommodated randomly one-by-one from the source to the destination node. Wavelength paths are accommodated in order of the shortest route and FF wavelength assignment. Reconfiguration is performed when the wavelength path resources, i.e., the number of wavelength paths that can be accommodated at some source and destination nodes, is less than 4. The fiber extension policy states that when it becomes impossible to store a path, the shortest path search is performed and the fewest links are selected based on the number of extensions. The number of wavelengths multiplexed in a fiber is 40.

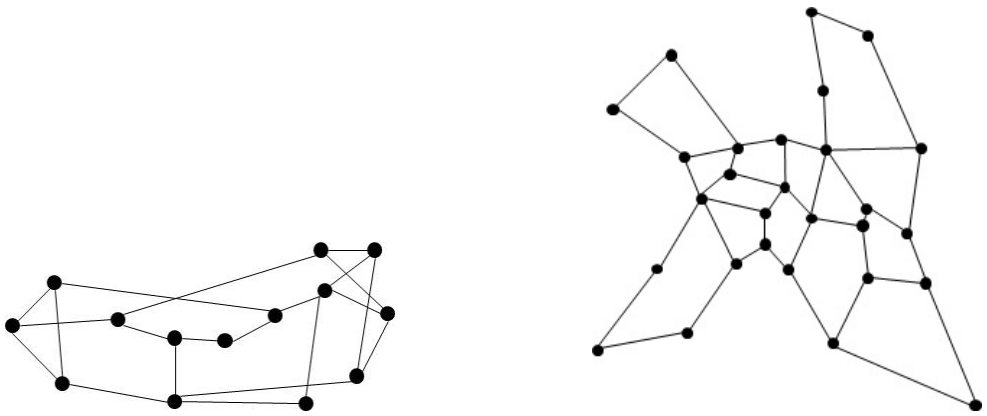

(a) NSF. (b) COST266.

Figure 4.16. Physical topology in the simulation.

4.7.2 Results and Discussion

Comparative results based on the number of fibers are shown in Fig. 4.17 and (a) shows the results of the number of fibers in the NSF network and 4.17 (b) shows the results of that for COST266. The numbers of fibers for the Puhs-pull, FRD-AR, ARD-AR, and PRE algorithms are reduced by 5%, 6%, 7%, and 8% at maximum, respectively, compared to that for no reconfiguration in the NSF

network and COST266. The effectiveness of the wavelength defragmentation, i.e., the PRE algorithm, is approximately 2% at maximum compared to that for ARD-AR in the NSF and COST266.

Comparative results for the accommodation rate are shown in Fig. 4.18. Wavelength accommodation rate A is the number of wavelength per number of used fibers per $N_{WM} = 40$ described in Equation (3.8). From the results among wavelength defragmentation, Push-pull, FRD-AR, and ARD-AR, the effectiveness of the wavelength defragmentation is approximately 5%-8% compared to no wavelength defragmentation. The difference in the accommodation rate between each defragmentation algorithm is slight.

The normalized number of migrating sequences for Push-pull, FRD-AR, and PRE to that for ARD-AR, is shown in Fig. 4.19. The number of migrating sequences in both networks decreases according to Push-pull, FRD-AR, and ARD-AR in that order and the number of migrating sequences for Push-pull is 1.9 times that for ARD-AR. On the other hand, that for PRE is 4.0 times that for ARD-AR in COST266 and is almost same of that for Push-pull in NSF. The reason that the number of the migrating sequences for PRE is large is that all resources are searched including the target reconfigured wavelength path in the wavelength channel and that some dependency cycles emerge and migrating sequences are increased to delete dependency cycles.

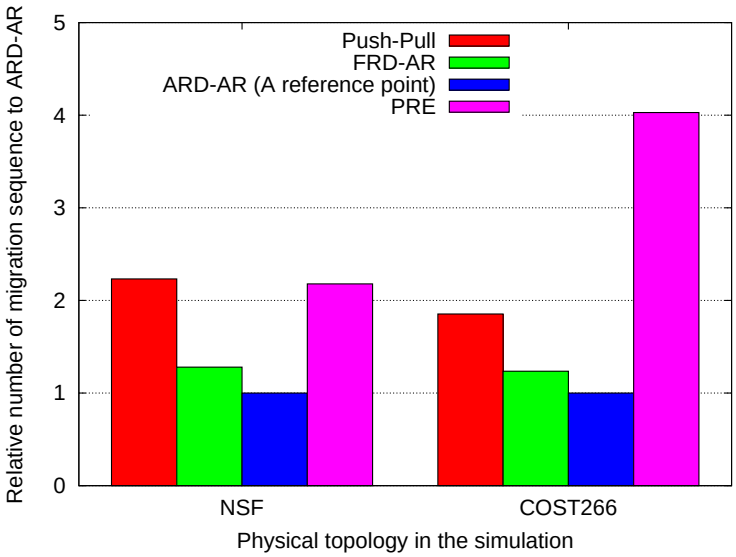

Figure 4.19. Comparison of reduction rate in number of migration sequences to Push-pull algorithm.

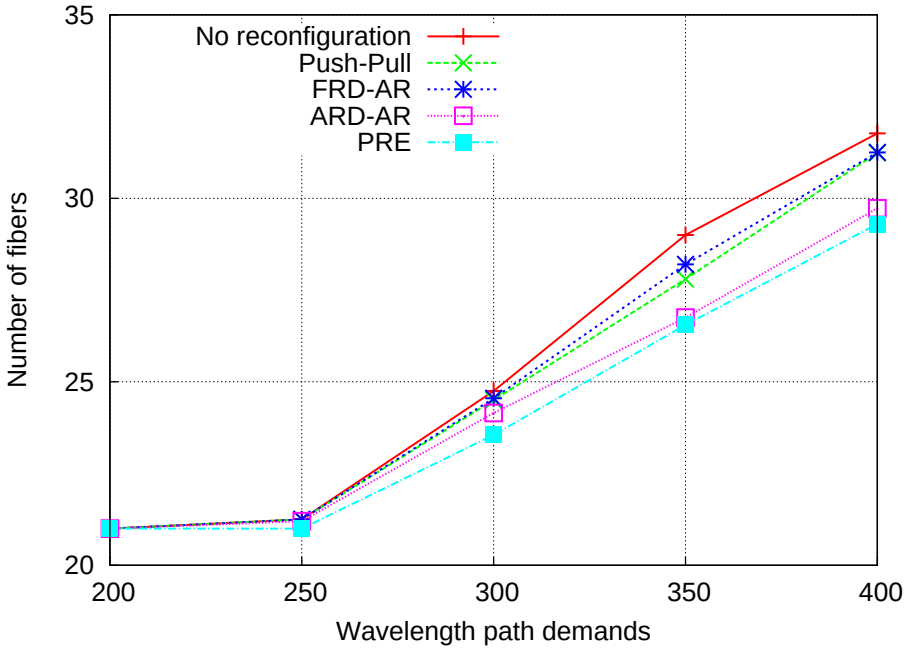

(a) Results of NSF.

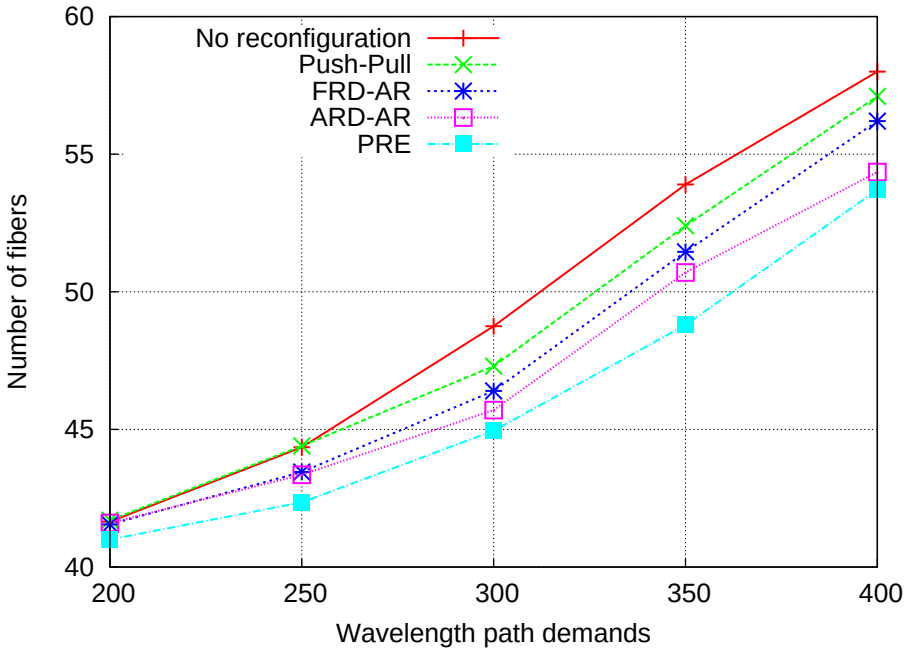

(b) Results of COST266.

Figure 4.17. Comparison of number of fibers for heuristic algorithms.

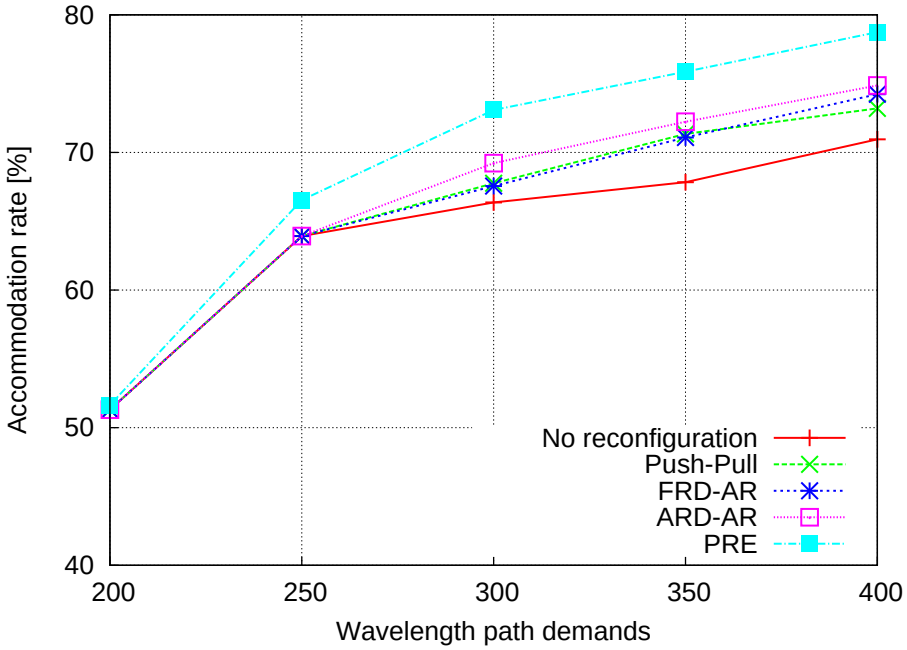

(a) Results of NSF.

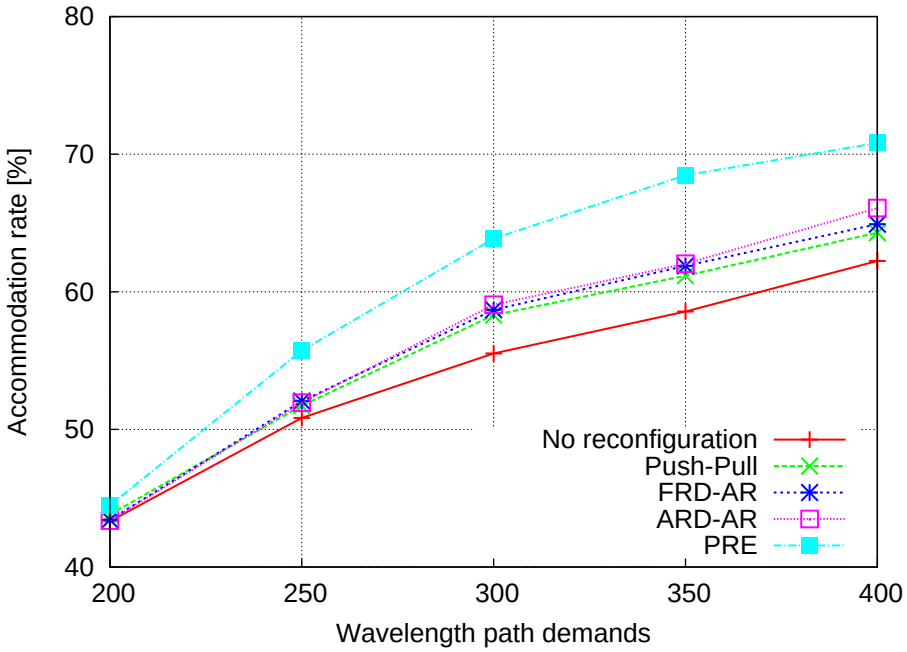

(b) Results of COST266.

Figure 4.18. Comparison of accommodation rate for heuristic algorithms.

4.8 Summary

This chapter presented a wavelength path reconfiguration scheme that reduces wavelength fragmentation in three phases: i) reconfiguration trigger phase; ii) reconfiguration design phase; and iii) migrating sequence phase from old path set to new path set. Two cost models were introduced: wavelength fragmentation cost and reconfiguration cost, and a reconfiguration design was introduced that reduces the number of changed wavelengths while retaining the effectiveness of wavelength defragmentation using ILP. For the migration phase, a migrating sequence algorithm was proposed that prevents service disruption by using spare wavelengths to break the dependency cycles that may be formed in moving to the new path set. Numerical evaluations showed that the number of fibers is suppressed by 4%-15% by employing the fragmentation cost, and that the number of changed wavelengths was reduced approximately 50%-90% while retailing the effectiveness of defragmentation. Additionally, the computation time can be decreased.

A wavelength defragmentation scheme based on wavelength resource management was proposed. Three heuristic algorithms were also introduced. The proposed and conventional algorithms were analyzed from the viewpoints of the number of fibers, accommodation rate, and number of migrating sequences needed. Numerical evaluations showed that the number of fibers can be reduced by up to 9% and that the accommodation efficiency is increased by approximately 5%-8% compared to the case when reconfiguration is not performed. The numbers of fibers for the Puhs-pull, FRD-AR, ARD-AR, and PRE algorithms are reduced by 5%, 6%, 7%, and 8% at maximum, respectively, compared to that for no reconfiguration. The number of migrating sequences decreases in the order Push-pull, FRD-AR, and ARD-AR, with Push-pull needing is 1.9 times more sequences than ARD-AR. On the other hand, PRE needs more migrating sequences since it must delete dependency cycles.

This chapter showed that reconfiguration for wavelength defragmentation can reduce the capital expenditure cost. On the other hand, there are some risks in terms of service disruption and a delay difference before and after reconfiguration. Therefore, it is important to use the algorithms appropriately. For instance, when there are many migrating sequences, the PRE algorithm can be used for some services in which reconfiguration risks do not need to be considered heavily. The path accommodation design and the reconfiguration scheme for using these algorithms appropriately for different services are described in Chapter 7.

Chapter 5

Sub-lambda Path Regrooming with Wavelength Defragmentation

This chapter presents sub-lambda path regrooming with wavelength defragmentation. This chapter proposes two steps reconfiguration scheme using ILP which performs sub-lambda path regrooming after wavelength defragmentation. An adaptive reconfiguration scheme based on wavelength path resource management is also presented including a heuristic sub-lambda path regrooming algorithm. Employing the proposed scheme, network can be designed to reduce not only the number of fiber but also the number of network devices.

5.1 Introduction

As described in Chapter 4, wavelength path reconfiguration to minimize fragmentation is a promising solution to reduce the resource requirements on core and metro networks. On the other hand, in the sub-lambda (or electrical) transport layer, the optimal virtual topology is adjusted according to traffic fluctuations [30]. When the volume of traffic is small and traffic emerges from different locations, accommodating traffic in multiple wavelength paths, i.e., a multi-hop sub-lambda path, can effectively reduce the resource requirements. When the traffic volume increases at the same source and destination nodes, accommodating the traffic in a single wavelength path, i.e., a single-hop sub-lambda path, is better. For effective accommodation of traffic, it is necessary to reconfigure wavelength paths cooperatively with sub-lambda paths. Figure 5.1 shows an image of sub-lambda path regrooming and wavelength path reconfiguration. At the reconfiguration stage, first sub-lambda paths are regroomed (reconfigured) into wavelength paths to minimize the equipment resource used, such as transponders. Wavelength paths not accommodating sub-lambda paths are deleted. Subsequently, wavelength paths are reconfigured to minimize the number of wavelengths used or spectrum fragmentation for future incoming traffic. Thereby, the number of equipment can be reduced and fiber resources can be used more effectively.

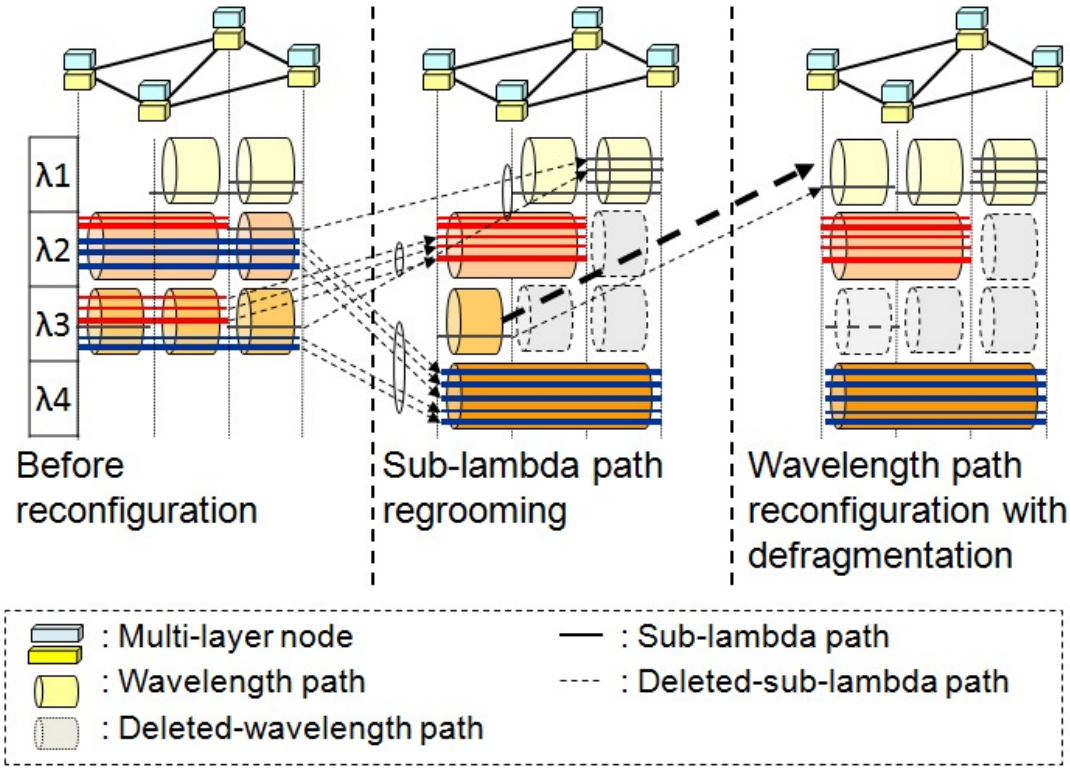

Figure 5.1. Image of sub-lambda path regrooming and wavelength path reconfiguration.

This chapter presents sub-lambda path regrooming with wavelength defragmentation. Two steps reconfiguration scheme using ILP is proposed. An adaptive reconfiguration scheme based on wavelength path resource management is also presented including a heuristic sub-lambda path regrooming algorithm. Numerical evaluations show that employing the proposed scheme, network can be designed to reduce not only the number of fiber but also the number of network devices.

5.2 Problem Statements and Assumptions for Multi-layer Path Reconfiguration Design

A multi-layer node architecture is also assumed such that each node is equipped with a WXC without a wavelength-conversion capability and an ODU-XC so that a wavelength path must be set up with the same wavelength between ODU-XC nodes. The node comprises an OTM-IF with a WDM function, an OCh-IF, an ODU-IF and WDM transponders. The ODU-XC is assumed to be added to WXC in parallel when all ports in ODU-XC are used.

The ODU-XC provides routing for multi-hop or single-hop sub-lambda paths. In this chapter, multi-layer path accommodation is assumed; i.e wavelength paths are accommodated in fibers. After that sub-lambda paths are accommodated in the wavelength paths as multi-hop sub-lambda paths. The reconfiguration problem is stated as follows.

Given:

- Physical network topology graph $G(V, E)$.
- Number of wavelengths multiplexed in a fiber.
- Number of fibers on a link.
- Number of multi-granular sub-lambda paths between each node pair.
- Set of wavelength paths and sub-lambda paths before reconfiguration.

Determine:

- Regrooming of sub-lambda paths that reduces the equipment cost.
- Reconfiguration of wavelength paths that reduces wavelength blocking for subsequent incoming traffic.
- Reduction of the number of migration sequences.

5.3 Greenfield Regrooming with Wavelength Defragmentation

Since high-bandwidth wavelength paths are filled up by many low-speed traffic streams, it is necessity to accommodate low-speed traffic efficiently as described in Section 2.4. Additionally, wavelength path reconfiguration to reduce fragmentation can be reduced number of using fiber as shown in Chapter 4. To address those issues, the Greenfield regrooming with wavelength defragmentation (GRWD) scheme is proposed. The "Greenfield" is defined as all of the network resources including existing paths. Periodically, e.g., every day or every weekend, GRWD is triggered and performed in two steps: re-grooming and wavelength defragmentation.

First, the virtual topology is reoptimized to minimize the total network cost. When the traffic between the same node pair increases, it is cost effective to reconfigure a direct wavelength path between the pair of nodes to groom. Additionally, since the efficiency of accommodating sub-lambada paths into the wavelength path decreases with the number of times the paths are deleted or established, it is also cost effective to regroom the sub-lambda paths into fewer wavelength paths and to delete the spare wavelength paths. Second, wavelength allocation is reoptimized to minimize the employed range of wavelength channels in the network. The second step has no direct relation to the network cost, but it can reduce the potential cost by minimizing wavelength blocking for further incoming traffic demand. It is expected that it will be effective especially for multiple-hop demands under high-traffic accommodation conditions. After these two calculation steps, wavelength paths and sub-lambda paths are reconfigured based on the results. From the viewpoint of a carrier network, the disruption of services is not assumed. Hence, when the operation for reconfiguration is applied to all targeted wavelength paths, the network can be reconfigured without service disruption by setting 1+1 protections. The values of cost for network equipments are described in [76]. The cost of the OCh-IF is calculated as C_{MI} divided by N_{WM}. The ODU type is considered ODU-1, ODU-2 and ODU-3. Given parameters and variables in the problem are following.

- Given: C_S, C_W, D_S, N_{DP}, N_{DPM}, N_{WM}, $p_{0(i,j)}^{(m,n),w}$, $s_{0(m,n)}^{(s,d),c_S,d_S}$ and $\sigma_{(s,d)}^{c_S,d_S}$.
- Equipment costs: C_{CI}, C_{DI,c_S}, C_{DX}, C_{MI}, C_T and C_{WX}.
- Variables: $CI_{(i,j)}^{w}$, $DI_{(m,n),c_S}$, DX_m, $MI_{(i,j)}$, $p_{(i,j)}^{(m,n),w}$, $s_{(m,n)}^{(s,d),c_S,d_S}$, T_m, $v_{(m,n)}$ and $v_{(m,n)}^{w}$.

The $MI_{(i,j)}$ is equal to the $f_{(i,j)}$ which is the number of fibers. The objective function for the first calculation step is to minimize the total network cost and is formulated as follows.

$$\begin{aligned}\text{Minimize :} C_{WX}|V| + C_{MI}\sum_{(i,j)\in E} MI_{(i,j)} + C_{CI}\sum_{(i,j)\in E, w\in W} CI_{(i,j)}^{w} + C_T\sum_{m\in V} T_m \\ + C_{DX}\sum_{m\in V} DX_m + \sum_{(i,j)\in E, c_S\in C_S} C_{DI,c_S}\cdot DI_{(i,j),c_S} \quad (5.1)\end{aligned}$$

The objective function for the second calculation step minimizes the employed range of the wavelength channels in the network. Wavelength channels are numbered from 1 to N_{WM} and wavelength paths are reconfigured to smaller number wavelength channel. It is formulated as follows.

$$\text{Minimize :} \sum_{w\in W} w\cdot\left(\sum_{(i,j)\in E,(m,n)\in P_W} p_{(i,j)}^{(m,n),w}\right) \quad (5.2)$$

In the objective function, wavelength path are reconfigured from smaller number wavelength channel and total number of used wavelength channel is minimized. The constraints of multi-hop grooming use the principles from multi-commodity flow for physical routing of wavelength paths and for routing of ODU paths on a virtual topology described in Section 2.4. The Equations (2.7) and (2.8) are replaced with Equation (5.3). The Equations (2.9) - (2.21) are also added. Another constraints for those devices are given below.

$$\sum_{n\in V}\left(v_{(m,n)} + v_{(n,m)}\right) = T_m \forall m \in V. \quad (5.3)$$

$$\sum_{w\in W} CI_{(i,j)}^{w} \leq N_{WM}\cdot MI_{(i,j)} \forall (i,j)\in E. \quad (5.4)$$

$$\sum_{(m,n)\in P_W}\left(p_{(i,j)}^{(m,n),w} + p_{(i,j)}^{(n,m),w}\right) = CI_{(i,j)}^{w} \forall (i,j)\in E, w\in W. \quad (5.5)$$

$$\sum_{n\in V, c_S\in C_S} N_{DP,c_S}\cdot DI_{(m,n),c_S} \leq N_{DPM}\cdot DX_m \forall m\in V. \quad (5.6)$$

$$\sum_{(s,d)\in P_S}\left(s_{(m,n)}^{(s,d),c_S,d_S} + s_{(n,m)}^{(s,d),c_S,d_S}\right) = DI_{(m,n),c_S} \forall (m,n)\in P_W, c_S\in C_S, d_S\in D_S. \quad (5.7)$$

Explanation of equations:

- Equation (5.3) ensures that number of wavelength paths in node m is equal to the number of transponders.
- Equation (5.4) ensures that the number of OCh-IFs is equal to or less than the number of OTM-IFs multiplied by the number of wavelengths multiplexed in a fiber.
- Equation (5.5) ensures that the numbers of wavelength paths, w, between (m, n) in the link (i, j) and fibers, f, are equal to the number of OCh-IFs.
- Equation (5.6) ensures that the number of ODU-IFs in node m is equal to or less than the number of ODU-XCs multiplied by the maximum number of ODU-IF ports.
- Equation (5.7) ensures that the number of ODU paths of ODU type c_S between (s, d) in virtual topology (m, n) is equal to the number of ODU-IFs.

All wavelengths are numbered, and wavelength paths are reconfigured to a lower numbered wavelength. As additional constraints, the route of the wavelength paths is unchanged, and variables for the equipment, ODU-XC, OTM-IF, ODU-IF, and transponder are fixed based on the results of first calculation step.

5.4 Adaptive Reconfiguration Based on Wavelength Path Resource Management

In this section, an adaptive reconfiguration based on wavelength path resource management is presented. This scheme is based on the scheme described in Section 4.5. The adaptive reconfiguration scheme comprises the three steps below. The flow is shown in Figure 5.2.

1. Wavelength path resource management: The number of wavelength paths that can be accommodated between all node pairs is calculated for each path accommodated.
2. Reconfiguration trigger: If that number is less than the threshold value set by the network carrier for some node pair, reconfiguration is performed.
3. Reconfiguration: Sub-lambda path is regroomed and wavelength path are reconfigured.

In Step 3, if the number of wavelength path resources is increased after redesigning the paths, reconfiguration is performed; otherwise, reconfiguration is not triggered until fiber links are added between the pair of target nodes. The wavelength path resource algorithm is used in Algorithm 2.

5.4.1 Heuristic Algorithm for Sub-lambda Path Regrooming

The MST algorithm described in Section 2.4 is extended to reconfigure sub-lambda paths without service disruption. Sub-lambda path regrooming, i.e., the Multi-

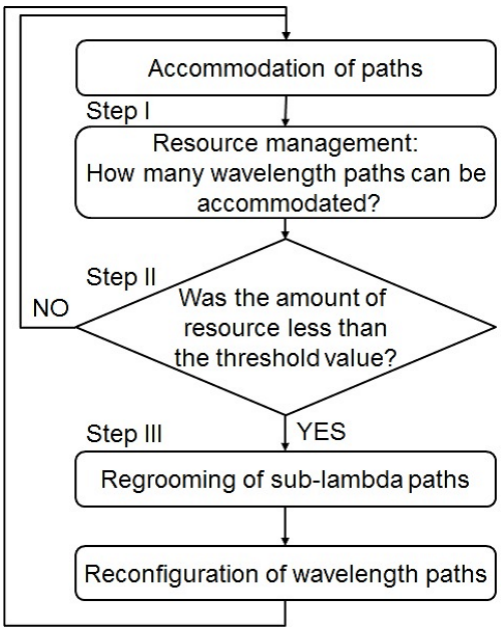

Figure 5.2. Adaptive sub-lambda path regrooming and wavelength path reconfiguration scheme.

hop to Single-hop First (MSF) algorithm, is described in Algorithm 5. There are three main phases. In Phase I (Steps 1-3), multi-hop sub-lambda paths are regroomed in descending order of virtual hops in the virtual topology to an existing single-wavelength path. In Phase II (Steps 4-5), the combination that consumes the wavelength bandwidth through regrooming is determined. Then, single-wavelength paths are established as the shortest route and wavelength assignment using FF algorithm and those sub-lambda paths are regroomed. In Phase III (Step 6), the multi-hop sub-lambda paths not yet regroomed are regroomed to existing multiple-wavelength paths. Figure 5.3 shows an image of the MSF algorithm. Capacity of wavelength path and sub-lambda path is assumed to 40 Gbit/s and 10 Gbit/s, respectively. In Phase I, multi-hop sub-lambda paths, M-S 1 and M-S 2, in the $\lambda 1$ are regroomed to the single-wavelength path, in the $\lambda 4$ and M-S 4, in the $\lambda 1$ are regroomed to the single-wavelength path, in the $\lambda 2$. In Phase II, summation of capacity of M-S 3, M-S 5, M-S 6 and M-S 7 consumes the capacity of wavelength path. Single-wavelength path that source and destination nodes are same as target sub-lambda path, (M-S 3, M-S 5, M-S 6 and M-S 7), is established newly in the $\lambda 5$, and their sub-lambda paths are regroomed to the wavelength path. In Phase III, M-S 8 is regroomed to multiple-wavelength paths in the $\lambda 2$.

The past study was shown that the rate at which the multi-hop sub-lambda paths are changed before and after reoptimization is decreased by 45%-88% in an environment with incremental traffic [36]. Therefore, in Phases I and II (Steps 1-5), the number of transponders can be reduced effectively for incremental traffic by regrooming based on the descending order of the number of virtual hops.

Algorithm 5 MSF

INPUT: Set of sub-lambda and wavelength paths before reconfiguration and physical topology.

OUTPUT: Sub-lambda path regrooming design and migration sequence.

1: Find sub-lambda paths in descending order of the number of physical route hops.
2: Regrooming in descending order of the number of virtual hops in the virtual topology to an existing single-wavelength path. If sub-lambda paths in the wavelength path are vacant, delete the wavelength paths.
3: Repeat Step 2 until all sub-lambda paths selected in Step 1 are processed.
4: Search for a combination that consumes the wavelength bandwidth by regrooming some sub-lambda paths. If there is such a combination and the wavelength paths that can accommodate those sub-lambda paths are vacant, establish single-wavelength paths as the shortest route and FF wavelength assignment. Reconfigure those sub-lambda paths and delete the vacant multiple-wavelength paths.
5: Repeat Steps 1 to 5 until all node pairs have been processed.
6: For multi-hop sub-lambda paths that have yet to be regroomed, regrooming multi-hop sub-lambda paths to existing multiple-wavelength paths in descending order of the number of virtual hops.

5.5 Numerical Evaluation for Greenfield Regrooming with Wavelength Defragmentation

5.5.1 Simulation Conditions

In this simulation, the statistical distribution of the ODU path type (ODU-1: ODU-2: ODU-3) is assumed to 5: 2: 3 using the same ratio as (STM-1: STM-4: STM-16) [73], and the physical topology is a 2×3 grid or 3×3 grid as shown in Fig. 5.4. Multi-granularity bidirectional ODU path demands is assumed in a full mesh topology. These demands are accommodated randomly one-by-one from the source to the destination node using object function 5.2. The patterns are changed 10 times and the average of the results is calculated. A workstation with a Xeon 3.3 GHz processor and 48 GB RAM is used for the simulation. The ILP formulation for SG comprises the added constraints of not changing the route and wavelength of the existing wavelength paths or the route of the existing ODU paths as given below:

$$p_{(i,j)}^{(m,n),w} \geq p_{0(i,j)}^{(m,n),w} \forall (i,j) \in E, w \in W, (m,n)\ P_W. \tag{5.8}$$

$$s_{(m,n)}^{(s,d),t,d_S} \geq s_{0(m,n)}^{(s,d),t,d_S} \forall (s,d) \in P_S, (m,n) \in P_W, t \in \{1,2,3\}, d_S \in D_S. \tag{5.9}$$

Therefore, SG can provide the optimal design for sequential path provisioning in the meaning that it satisfies the objective function for a sequential path. The proposed scheme performs re-optimization every 50 ODU path demands.

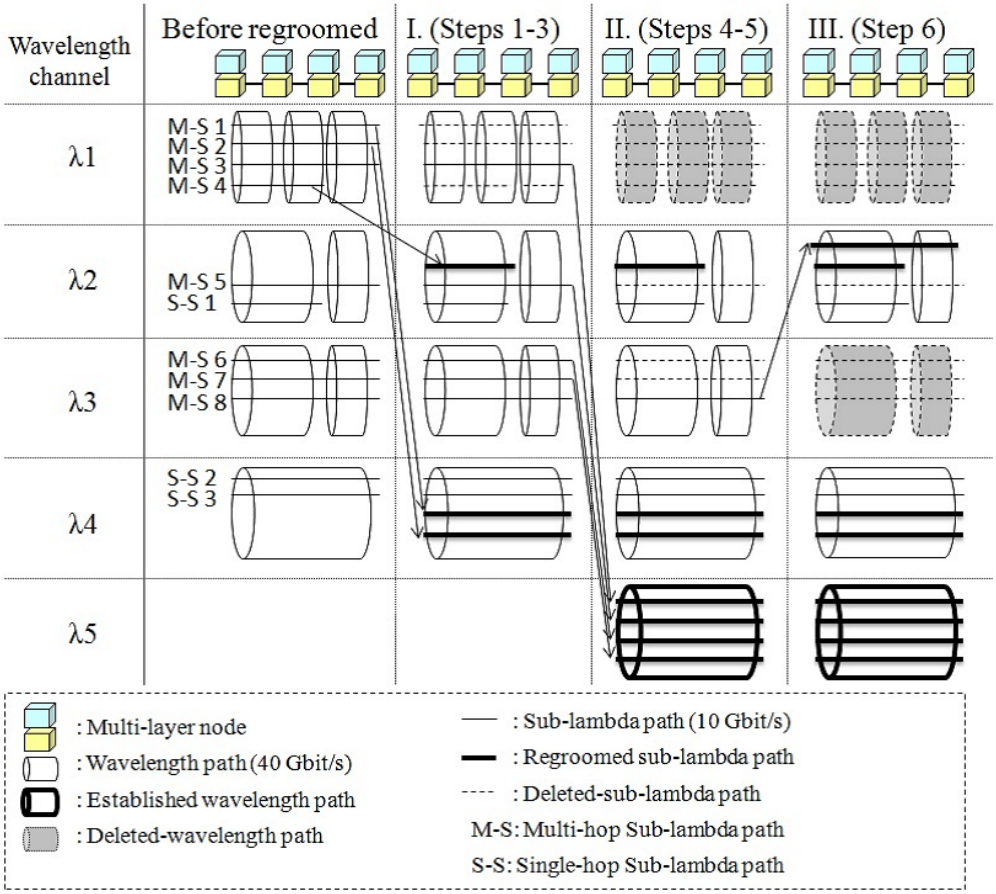

Figure 5.3. Image of the MSF algorithm.

5.5.2 Results and Discussion

The average running time for a SG calculation is approximately 0.8 sec and 5.0 sec in the 2×3 grid and 3×3 grid, respectively. The average running time for the first step calculation is approximately 2.1 sec and 39 sec, and that for the second step calculation is approximately 1.2 sec and 14 sec for the 2×3 grid and 3×3 grid, respectively.

The results of the simulation are shown in Figs. 5.5, 5.6, and 5.7. Figure 5.5 shows the number of OTM-Ifs in the 3×3 grid. The number of OTM-IFs corresponds to the number of fiber-links needed. As shown in Fig. 5.5, the expansion timing of the node transport equipment in the proposed scheme can be slow according to the increase in traffic demand. When the traffic demand is 3[Tbps], 4[Tbps], and 5[Tbps], the number of OTM-IFs for GRWD compared to not employing the second step is 5%, 7%, and 7% respectively. Figure 5.6 shows the number of ODU paths for single-hop grooming paths and multi-hop grooming paths except for single hops in the 3×3 grid. When the amount of traffic is small, i.e., less than approximately 1[Tbps], the average rate at which of the number of transponder is decreased before and after performing GRWD is 17%. At that time, the rate at which the multi-hop paths are changed is increased by 65%. On the

(a) 2×3 grid. (b) 3×3 grid.

Figure 5.4. Physical topology in the simulation.

other hand, the average rate at which of the number of transponder is decreased before and after performing GRWD is 5%-12%. At that time, the rate at which the multi-hop paths are changed before and after performing GRWD is decreased by 45%-88%. Figure 5.7 shows active network equipment cost reduction of up to 12% in the 2×3 grid and 16% in the 3×3 grid for GRWD compared to SG.

Numerical simulations show that the proposed GRWD scheme can design a network to minimize the number of sets of transport equipment such as ODU-switches. Under high-traffic accommodation conditions, wavelength defragmentation becomes effective. Additionally, the specific feature is shown that the rate at which the multi-hop sub-lambda paths are changed before and after re-optimization is decreased deeply in an environment with incremental traffic.

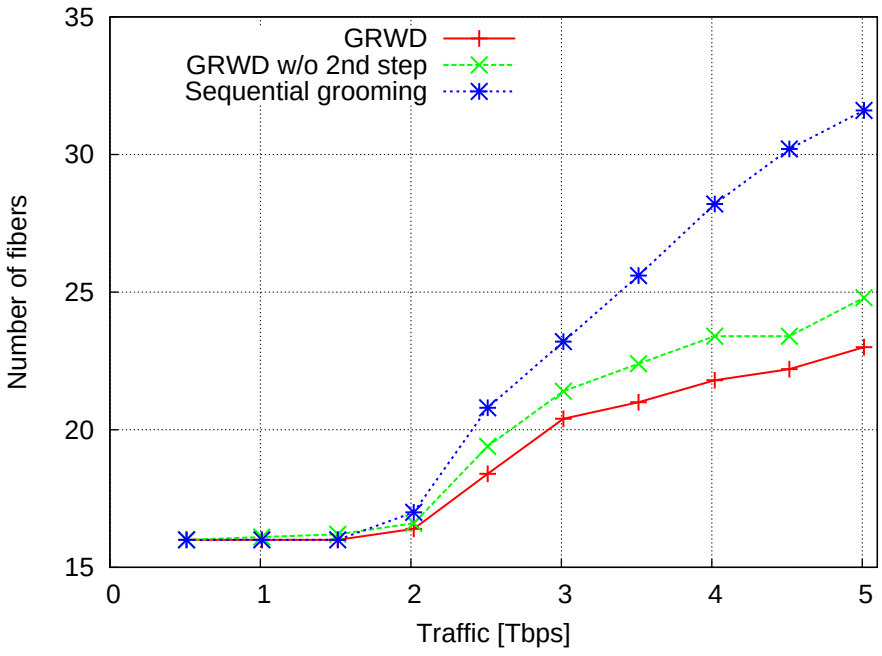

Figure 5.5. Comparison of number of OTM-IFs for GRWD and SG.

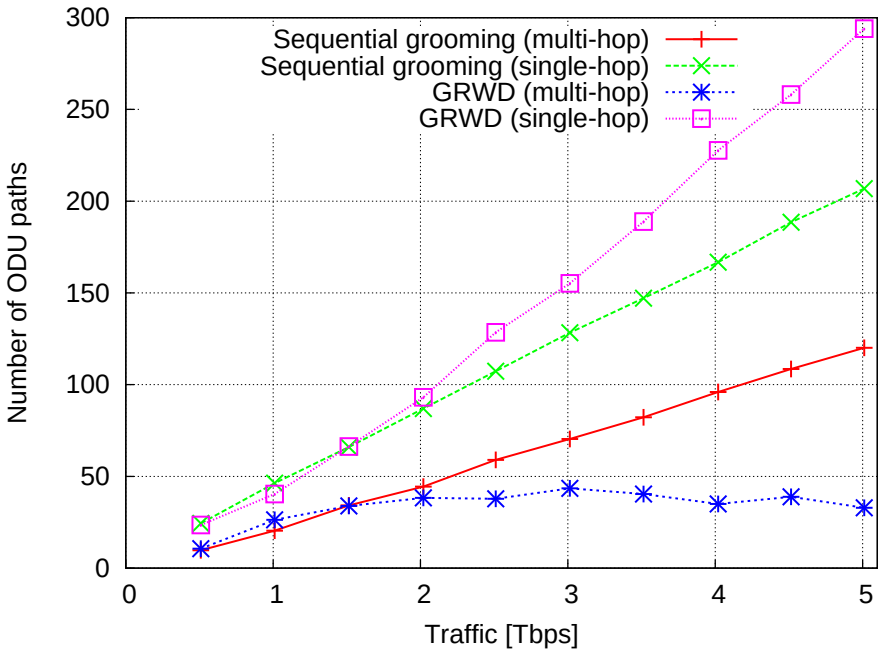

Figure 5.6. Comparison of number of ODU paths for GRWD and SG.

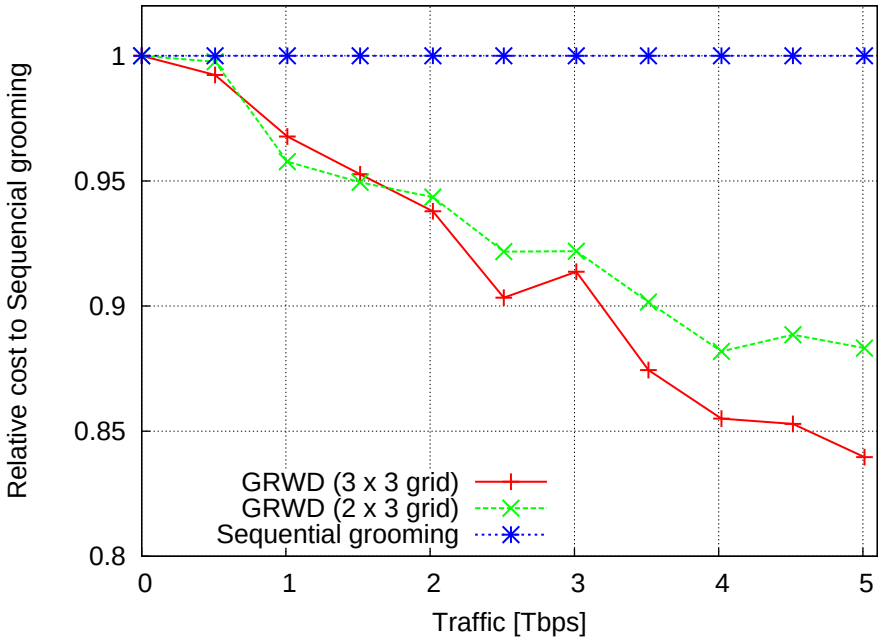

Figure 5.7. Comparison of relative cost for GRWD and SG.

5.6 Numerical Evaluation for Adaptive Reconfiguration Based on Wavelength Path Resource Management

This section evaluates for the adaptive reconfiguration based on wavelength path resource management. The following algorithms/combinations are evaluated: no reconfiguration, only sub-lambda path regrooming MSF, MSF and Push-pull, MSF and FRD-AR, and MSF and ARD-AR. Here, the conventional wavelength defragmentation algorithm is the Push-pull algorithm, in which defragmentation is performed in fixed routes in ascending order of the number of wavelength channels. Evaluation items for comparison are the number of fibers, equipment cost, wavelength accommodation rate, number of wavelength resources, and number of migration sequences.

5.6.1 Simulation Conditions

The employed physical topology is a NSF network with 14 nodes and 21 links and COST266 network with 26 nodes and 43 links as shown in Fig. 4.16 in Section 4.6.2. Multi-granular ODU path demands in a full mesh topology are assumed. These demands are accommodated randomly one-by-one from the source to the destination node. The patterns are changed 10 times and the average of the results is calculated. Wavelength paths are accommodated as the shortest route and wavelength assignment using FF algorithm. Sub-lambda paths are configured in multiple-wavelength paths within three hops [77]. Reconfiguration is performed when the wavelength path resources, i.e., the number of wavelength paths that can be accommodated at some source and destination nodes, is less than 4. The statistical ratio of the traffic demand for each sub-lambda path (2.5 G : 10 G : 40 G) is 5 : 2 : 3 [73]. The number of wavelengths multiplexed in a fiber is 40. The fiber extension policy states that when it becomes impossible to store a path, the shortest path search is performed and the fewest links are selected based on the number of extensions. The number of ODU ports is 32. When all ODU ports are used, ODU-XC is added to the WXC.

5.6.2 Results and Discussion

Comparative results based on the number of fibers are shown in Fig. 5.8. Figure (a) and (b) is the result of NSF and COST266, respectively. The numbers of fibers for "MSF and ARD-AR" is reduced by 14% in NSF and 7% in COST266 compared to that for no reconfiguration. The numbers of fibers for "MSF and FRD-AR" is reduced by 12% in NSF and 5% in COST266 at maximum compared to that for no reconfiguration. The effectiveness of wavelength defragmentation, i.e., the ARD-AR algorithm, is approximately 5% at maximum compared to that for only sub-lambda path regrooming, i.e., the MSF algorithm.

The comparative results for the relative equipment cost for no reconfiguration is shown in Fig. 5.9. Total cost C_{Total} is the sum of the node device cost described

in Equation 5.1 in Section 5.3. The total cost for "MSF and ARD-AR" can be reduced by up to 9% in NSF and 8% in COST266 compared to that for no reconfiguration. The total cost for MSF can be reduced by up to 8% in NSF and 7% in COST266 compared to that for no reconfiguration.These results show that the proposed multi-layer reconfiguration scheme uses the wavelength resources of the fibers more effectively and reduces the network equipment cost.

The comparative results for the accommodation rate are shown in Fig. 5.10. The wavelength accommodation rate A is the number of wavelength per the number of used fiber per $N_{WM} = 40$ described in Equation (3.8). From the results among wavelength defragmentation Push-pull, FRD-AR, and ARD-AR, the effectiveness of wavelength defragmentation is approximately 4%-5% in both NSF and COST266 compared to no reconfiguration. However, the accommodation rate of only sub-lambda path regrooming MSF is lowest compared with others. Enhancing the accommodation rate is necessary for wavelength defragmentation. The comparative results of normalized number of wavelength path resources, which is the number of wavelength path resources normalized by the number of used fiber times $N_{WM} = 40$, are shown in Fig. 5.11. The tendency of the results is opposite to that for the results of the accommodation rate.

The number of migration sequences is calculated as the sum of the number of migration wavelength and sub-lambda paths including decyclization dependency cycles described in Section 4.3. Comparative results for the reduction rate for the number of migration sequences for "MSF and FRD-AR", and "MSF and ARD-AR" to that for MSF and conventional Push-pull, is shown in Fig. 5.12. The proposed FRD-AR and ARD-AR are reduced approximately 23%- 35% in both NSF and COST266. Based on these results, the proposed algorithm considering the accommodation rate can suppress the number of migration sequences.

It is expected a reduction in the capital expenditure while reducing the operational cost and an enhancement to the network scalability by reducing the number of required node degrees. The proposed scheme will be applied to high-capacity and highly mobile traffic and to some services that allow instantaneous disruption.

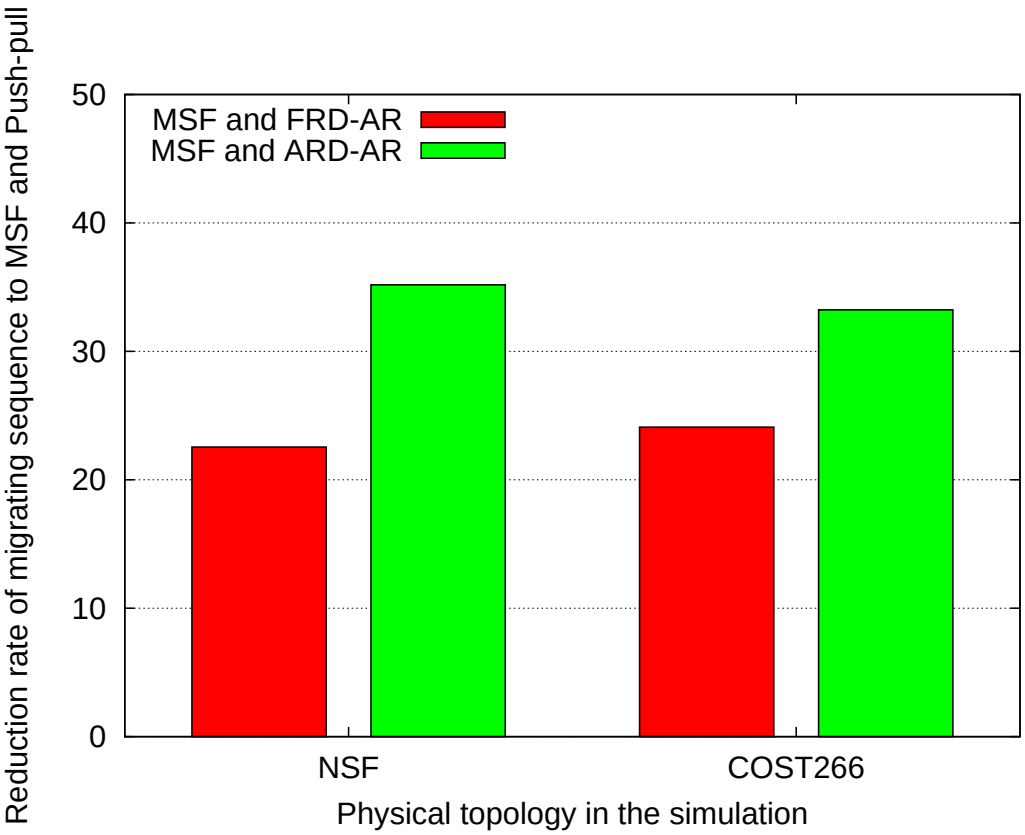

Figure 5.12. Comparison of reduction rate for number of migration sequences.

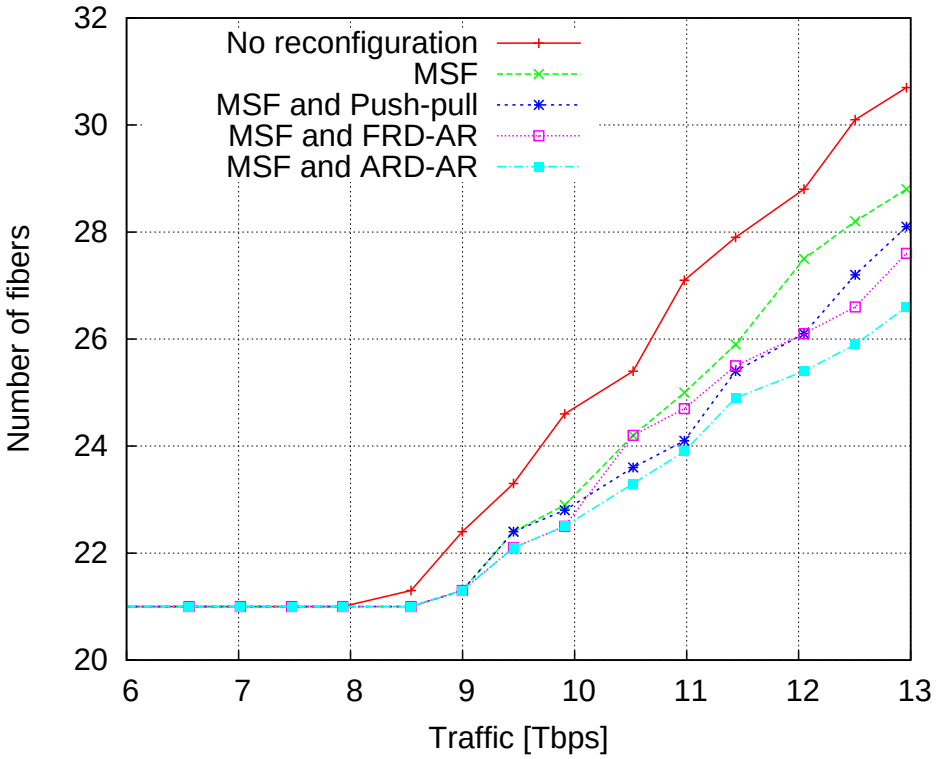

(a) Results of NSF.

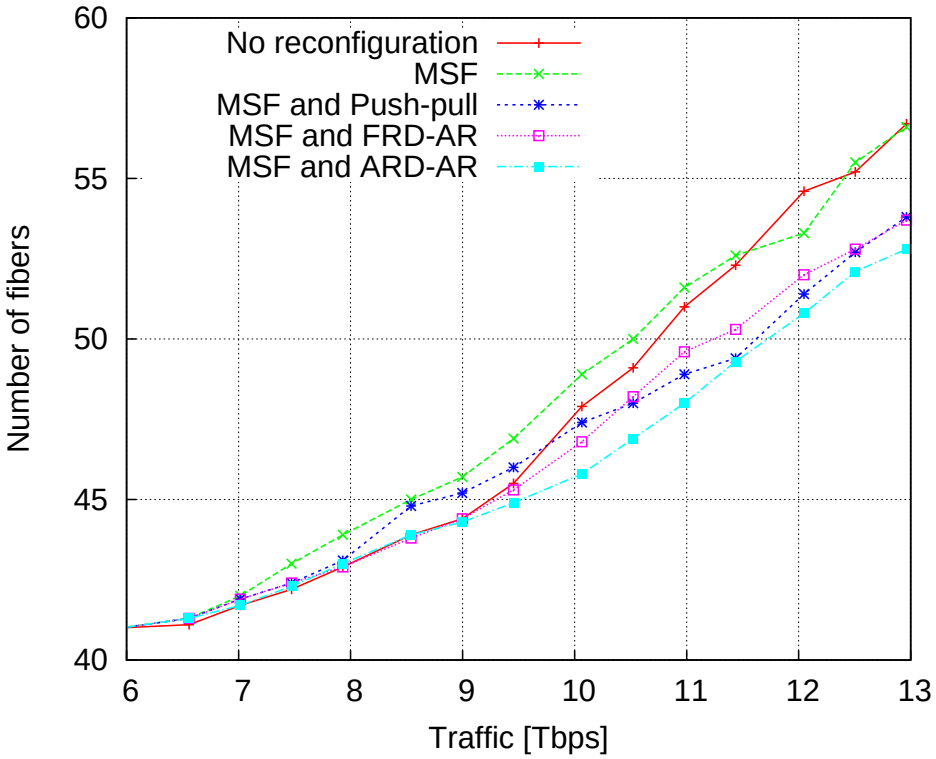

(b) Results of COST266.

Figure 5.8. Comparison of number of fibers for heuristic multi-layer reconfiguration algorithms.

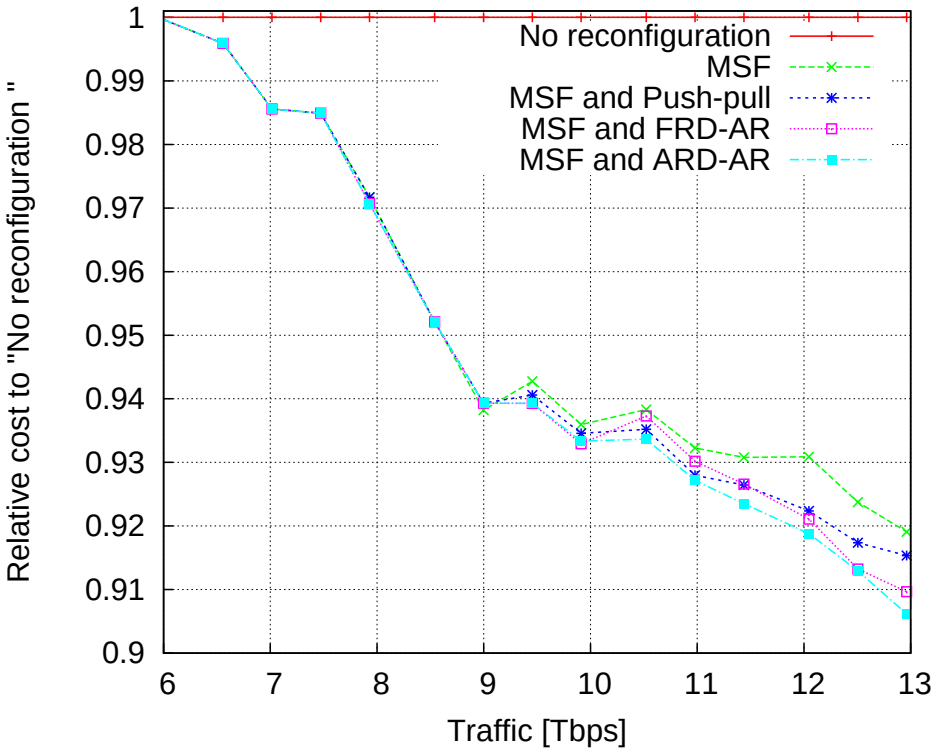

(a) Results of NSF.

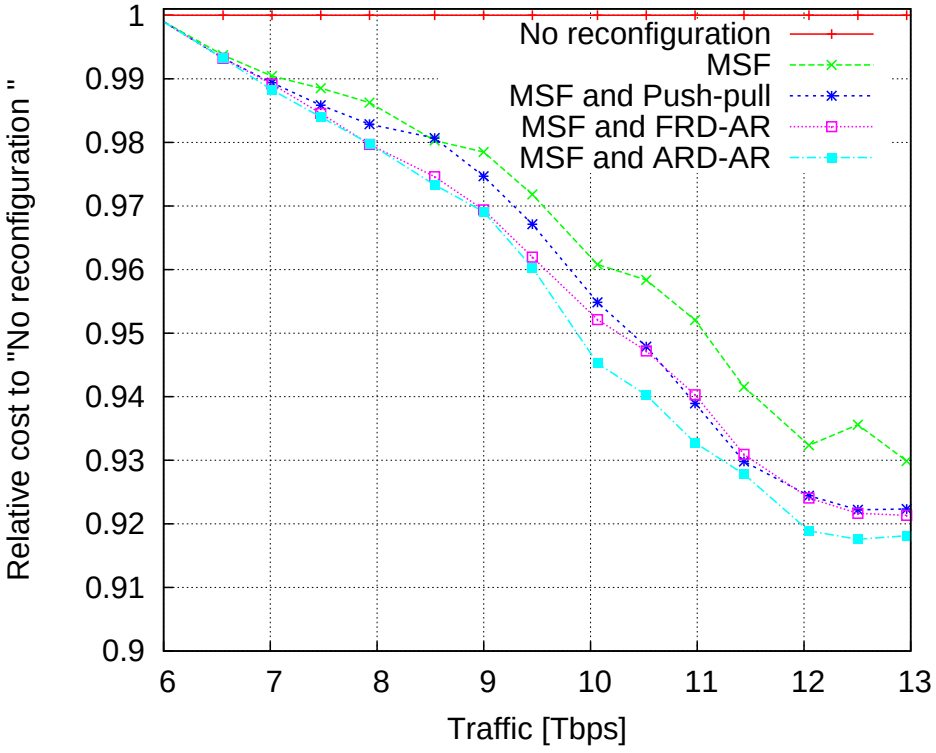

(b) Results of COST266.

Figure 5.9. Comparison of relative cost for heuristic multi-layer reconfiguration algorithms to No reconfiguration.

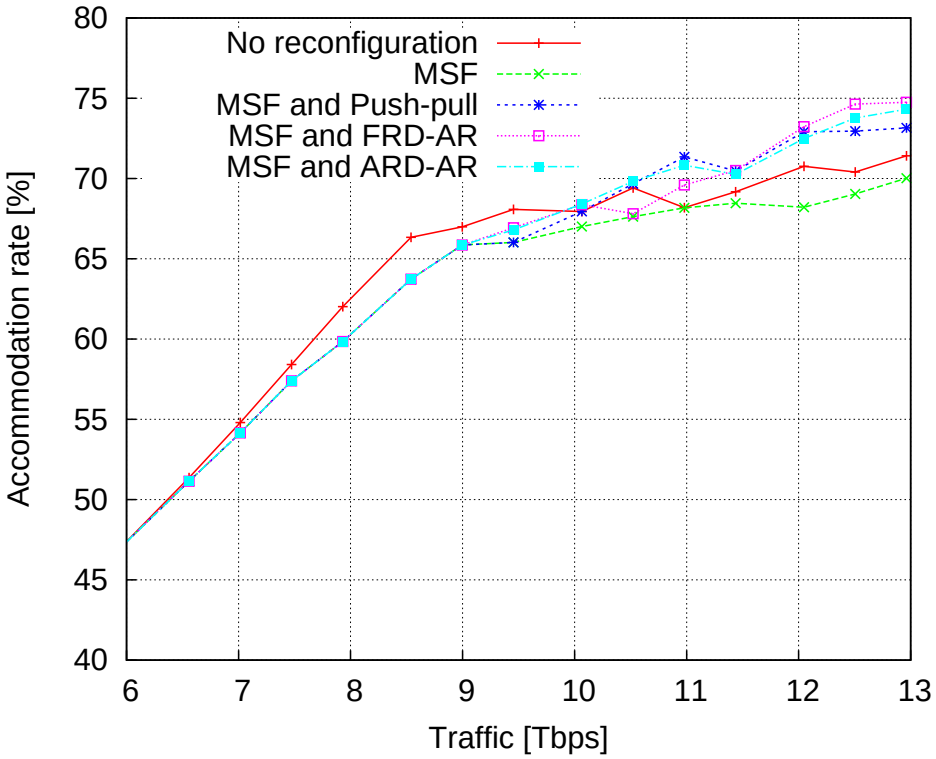

(a) Results of NSF.

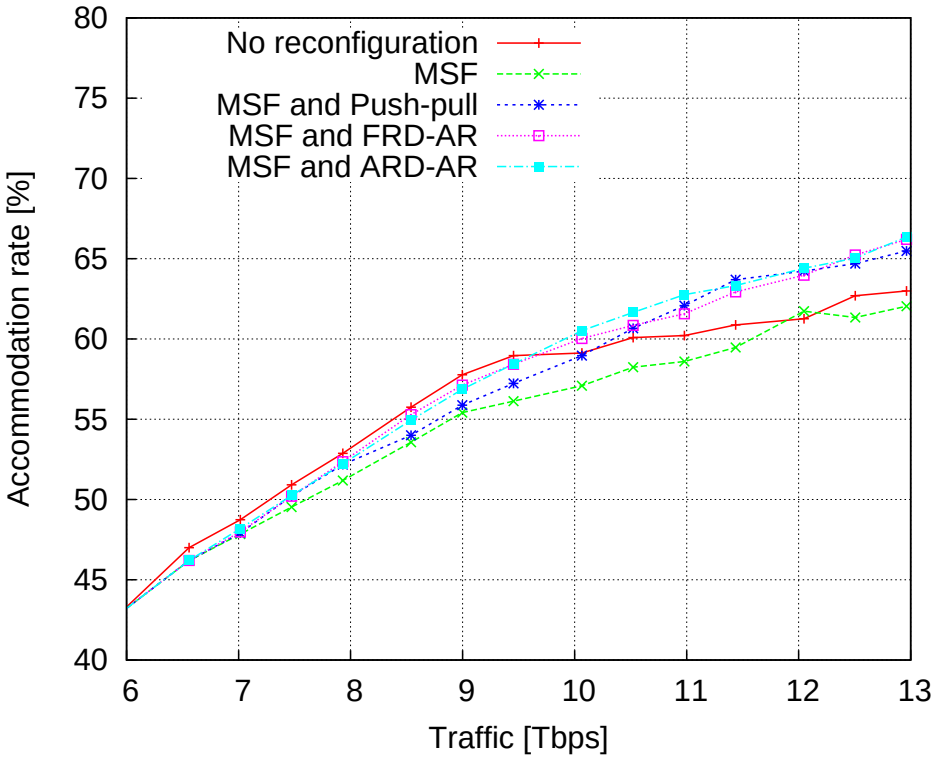

(b) Results of COST266.

Figure 5.10. Comparison of accommodation rate for heuristic multi-layer reconfiguration algorithms .

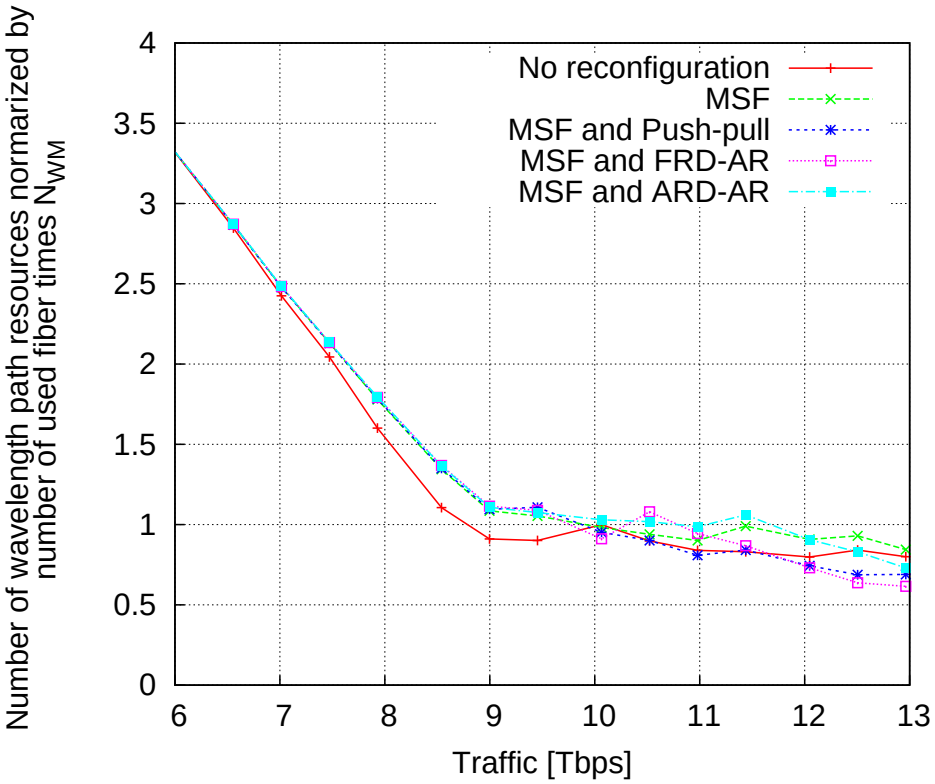

(a) Results of NSF.

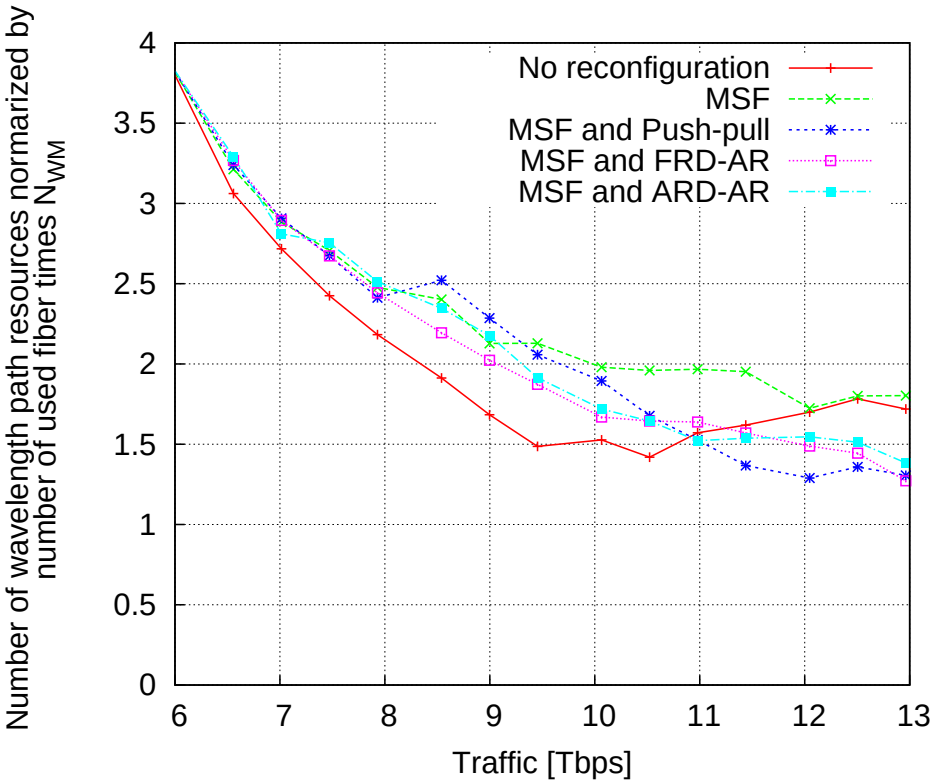

(b) Results of COST266.

Figure 5.11. Comparison of normalized number of wavelength path resources for heuristic multi-layer reconfiguration algorithms .

5.7 Summary

This chapter presented sub-lambda path regrooming with wavelength defragmentation. First, the GRWD scheme was proposed. Periodically, e.g., every day or every weekend, is triggered and performed in two steps: re-grooming and wavelength defragmentation. Numerical evaluations showed as follows. The number of OTM-IFs for GRWD compared to not employing the second step is 5%, 7%, and 7% respectively. The number of transponder is decreased before and after performing GRWD about 5%-12%. Active network equipment cost reduction of up to 12% in the 2×3 grid and 16% in the 3×3 grid for GRWD compared to SG. Additionally, the specific feature is shown that the rate at which the multi-hop sub-lambda paths are changed before and after re-optimization is decreased by 45%-88% in an environment with incremental traffic.

An adaptive reconfiguration based on wavelength path resource management was presented. A sub-lambda path regrooming algorithm was also proposed which regrooms multi-hop sub-lambda path to single-hop sub-lambda path first and two wavelength path reconfiguration algorithms that reduce wavelength fragmentation and the number of migration sequences considering the accommodation rate in wavelength channels without service disruption. Numerical evaluations showed that the number of fibers is suppressed by 12%-14% and the equipment cost is reduced by approximately 8%-9% compared to when no reconfiguration is used. The results also show that the accommodation rate increases as the degree of effectiveness of the wavelength defragmentation increases. The proposed multi-layer reconfiguration scheme is shown to use the wavelength resources of the fibers more effectively. The number of migration sequences for the proposed wavelength defragmentation algorithms is reduced by approximately 23%-35% compared to that for the conventional algorithm.

This chapter showed that sub-lambda path regrooming with wavelength defragmentation can be reduced capital expenditure cost more than only wavelength path reconfiguration and can be an enhancement to the network scalability by reducing the number of required node degrees.

Chapter 6

Differential Reliability Classes Based Path Accommodation Design and Reconfiguration

This Chapter presents differentiated reconfiguration to address the trade-off relationship between accommodation efficiency and disruption risks in virtualized multi-layer transport networks that considers reliability classes defined as a combination of including or excluding a secondary path and allowing or not allowing reconfiguration. A multi-layer redundant path accommodation design scheme and a reconfiguration algorithm are proposed. An evaluation algorithm for reliability is also introduced. The proposed reconfigurable networks are shown to be a cost effective solution that maintains reliability.

6.1 Introduction

Various Internet services and applications have emerged that require not only a wide bandwidth but also high levels of quality and reliability [78]. For example, financial services require short delays and a high reliability level [79], and service providers must pay a penalty if a contract is violated due to delay or loss. On the other hand, Internet browsing and some services may allow instantaneous disruption and do not need a high reliability level from networks. Therefore, the paths in the transport layer should accommodate these traffic demands with various levels of granularity according to different reliable requirements. Multi-layer transport networks, in which network operation is based on collaboration between sublambda and wavelength paths, has been shown to be effective in accommodating traffic with various levels of granularity [80,81]. For different service requirements, a virtualized network was proposed in which the infrastructure is virtually sliced to accommodate different reliability classes [82]. Provisioning according to a service level agreement (SLA), which represents the contract of availability between a service provider and its client, was also proposed in [83]. In IP over WDM networks that considering both differentiated survivability services and transmission quality, four reliability classes were defined: optical layer dedicated protection, optical layer

shared protection, IP/MPLS layer shared protection, and no-protection [84]. On the other hand, to accommodate paths more efficiently, network reconfiguration and reoptimization represent promising candidates for quasi-dynamic and multi-granular traffic [38]. Reconfiguration however incurs some risks such as service disruption and fluctuations in delay. These are factors in a trade-off relationship between accommodation efficiency and disruption risks.

To address this trade-off relationship, this chapter proposes a virtualized multi-layer transport network design and reconfiguration for different reliability classes using combinations involving the inclusion or exclusion of a secondary path, and allowing or not allowing reconfiguration. Numerical evaluations show effective suppression of the number of fibers and network equipment costs while retaining reliability according to the reliability class.

6.2 Virtualization for Differential Reliability Path Accommodation Design and Reconfiguration

Figure 6.1 shows a virtualized transport network for different reliability classes. The left hand side of Fig. 6.1 shows the conventional virtualized single layer, sub-lambda layer, and network design that are segmented and virtualized in an infrastructure network [82]. The right hand side of Fig. 6.1 shows the proposed virtualized multi-layer, sub-lambda layer over wavelength layer, network design, and reconfiguration that have different reliability classes using combinations involving the inclusion or exclusion of a secondary path, and allowing or not allowing reconfiguration.

Table 6.1 gives the definitions of the reliability classes. The higher reliability class (H^+RC) has a secondary path and does not allow reconfiguration, the high reliability class (HRC) has a secondary path and allows reconfiguration, the low reliability class (LRC) does not have a secondary path and does not allow reconfiguration, and the lower reliability class (L^-RC) does not have a secondary path and allows reconfiguration. Wavelength and sub-lambda paths are designed for each class. The wavelength and sub-lambda paths have a reliability class identifier and a primary or secondary path. Thereby, each path can be virtually accommodated in the same physical network similar to a separate network. In network operation, multi-layer paths are established in the multi-layer transport network based on the network design results. Subsequently, the paths in some reliability classes allowing reconfiguration are triggered to begin reconfiguration from the network management plane.

6.3 Multi-layer Redundant Path Accommodation Design

The proposed heuristic algorithm is proposed for multi-layer redundant path accommodation design considering different reliability classes. The proposed algorithm has two features:

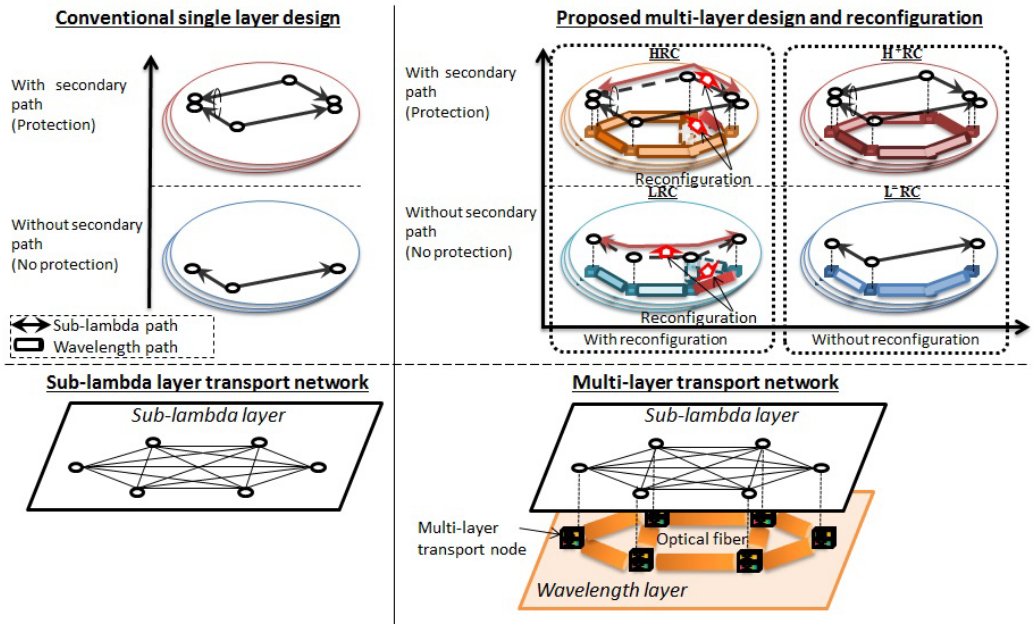

Figure 6.1. Virtualized transport network for different reliability classes.

Table 6.1. Reliability Class Definitions in Terms of Resiliency and Reconfiguration.

Reliability Class	W/ or W/o Secondary Path	W/ or W/o Reconfiguration
$H^{+}RC$	W/ secondary path (Protection)	W/o reconfiguration
HRC	W/ secondary path (Protection)	W/ reconfiguration
LRC	W/o secondary path (No-protection)	W/o reconfiguration
$L^{-}RC$	W/o secondary path (No-protection)	W/ reconfiguration

1. Reliable path design: Combinations of redundant paths are designed as routes that satisfy the reliability requirement.
2. Cost minimized design: Sub-lambda paths are groomed at intermediate nodes based on the combinations of redundant paths that satisfy the reliability requirement.

The steps in the proposed algorithm are described in Algorithm 6. A set of sub-lambda path demands as input information includes source and destination nodes, bandwidth, reliability class, and reliability and quality requirements. The SLA determines the reliability requirement for each class, and whether or not node and link disjoints are needed. The quality is represented by the difference in delay. In Steps 5-7, the sub-lambda path has identifier for different reliability classes and the primary or secondary path. Thereby, primary or secondary sub-lambda paths in the same reliability class are groomed at intermediate nodes in different wavelength paths. Paths in different reliability classes can also be accommodated virtually in the same physical network, and they are distributing to different virtual networks. In LRC and $L^{-}RC$, paths are designed without considering the combination of redundant routes in Algorithm 6.

Algorithm 6 Multi-layer redundant path accommodation design considering different reliability classes

INPUT: Topologies in the wavelength layer and sub-lambda layer, and a set of sub-lambda path demand.

OUTPUT: Routes in the wavelength and sub-lambda layer, and the wavelength.

1: Search for combinations of redundant routes between source and destination nodes in the sub-lambda layer.
2: Filter combinations of redundant routes based on the reliability and quality requirements.
3: Search for combinations of redundant routes in the wavelength layer from the results of Step 2.
4: Filter in the same manner as in Step 2.
5: Search for the shortest hop route in the sub-lambda layer that has the available bandwidth that exceeds that required by the sub-lambda path in the same reliability class.
6: If routes are not found, search for the least number of newly established wavelength paths and go to Step 7. Otherwise, search for the shortest hop route among the existing wavelength paths and go to END.
7: Search for the shortest hop route in the wavelength and sub-lambda layers, respectively.
8: Wavelength paths are newly designed based on a FF wavelength assignment.

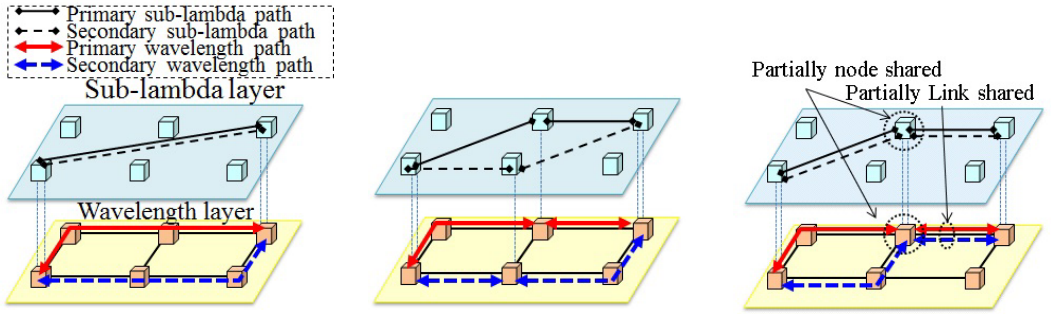

(a) Single-hop with node and link disjoint.

(b) Multi-hop with node and link disjoint.

(c) Multi-hop with partially node or link shared.

Figure 6.2. Multi-layer redundant path accommodation design.

Figure 6.2 shows three kinds of redundant path pairs. In Step 1, route candidate pairs in these paths, i.e. (a), (b), and (c) in Fig 6.2 are searched. Subsequently, if the reliability requirement includes node-and-link disjointness, (c) with no disjoint route is filtered out. In Steps 3 and 4, for two remaining combinations, (a) and (b), routes that satisfy the reliability requirement are searched. If there are no existing wavelength paths, (a) with a single-hop path is selected based on Steps 5 to 8. If there are existing multiple wavelength paths that have more than the required vacant bandwidth, (b) with the multi-hop path is selected.

6.4 Reconfiguration for Multi-layer Redundant Paths

To actualize the proposed network, an adaptive multi-layer reconfiguration scheme was introduced in Chapter 5 [38]. There are two objective functions: to minimize the total equipment cost and to minimize the wavelength fragmentation. The reconfiguration algorithms for redundant paths, rerouting both primary and secondary paths, and rerouting only secondary paths were introduced in [54]. New reconfiguration algorithms for both primary and secondary paths are proposed while maintaining the same reliability and quality levels. The proposed reconfiguration algorithms are the Reconfiguration Secondary path First (RSF) algorithm is shown as Algorithm 7 and the Reconfiguration Mixed Primary and Secondary path (RMPS) algorithm is shown as Algorithm 8. The RSF algorithm is as follows. First, reconfiguration design for a secondary path is searched. Second, the reconfiguration designs are filtered and those that do not satisfy the reliability and quality requirements are discarded. Next, as the same way from Step 1 to 3, reconfiguration design for primary path is decided. The RMPS algorithm is a reconfiguration design that does not distinguishing the primary path from the secondary path in the first step in the RSF algorithm.

In this chapter, in Steps 1 and 4 of Algorithm 7, the MSF algorithm is used as the sub-lambda path reconfiguration algorithm described in Chapter 5. Additionally, the ARD-AR is used as the wavelength path reconfiguration algorithm described in Chapter 4 [35]. In the proposed algorithms, since path protection is employed, there is no service disruption except in the case that a primary path or secondary path is cut due to a violent disaster, network equipment failure, or fiber cut when reconfiguring. Using the above-mentioned scheme, the sub-lambda and wavelength paths are reconfigured. The sub-lambda and wavelength paths in the lower reliability class are established as backup paths and reconfigured. After reconfiguration is successfully completed, the backup paths in the lower reliability class are deleted.

Algorithm 7 RSF

INPUT: Topologies in the wavelength layer and sub-lambda layer, and a set of sub-lambda and wavelength paths before reconfiguration.
OUTPUT: Sub-lambda and wavelength path reconfiguration design and migration sequence.

1: Search for a reconfiguration design for a secondary path using the sub-lambda path and wavelength path reconfiguration algorithm, respectively.
2: Filter out routes that do not satisfy the reliability and quality requirements.
3: Reconfiguration design for secondary path is selected.
4: Search for a reconfiguration design for the primary path in the same manner as in Step 1.
5: Filter routes that do not satisfy the reliability and quality requirements.
6: Reconfiguration design for primary path is selected.

Algorithm 8 RMPS

INPUT: Topologies in the wavelength layer and sub-lambda layer, and a set of sub-lambda and wavelength paths before reconfiguration.
OUTPUT: Sub-lambda and wavelength path reconfiguration design and migration sequence.

1: Search for reconfiguration design for both primary and secondary paths using sub-lambda path and wavelength path reconfiguration algorithms, respectively.
2: Filter out routes that do not satisfy the reliability and quality requirements.
3: Reconfiguration design is selected.

6.5 Analysis of Communication Reliability

There have been studies on evaluation techniques for reliability. Simplified calculation for reliability is a method used in truth tables [85]. First, a truth table is created in which the status, $\phi(c)$, for all $x(\in X)$ is calculated where $x(\in X)$ is a link and node in graph $G(V, E)$, $c(\in C)$ is a combination of failure status, normal (1) or failure (0), for all x, $\phi(c)$ is the communication status of c between source and destination. Second, reliability of $\phi(c)$, $p(\phi(c))$, is calculated for all combinations of status c. Third, the sum of $p(\phi(c))$ is calculated and communication reliability R is evaluated. The order of the calculation time is $O(2^{|X|})$ and as the network scale increased, the calculation time increases exponentially. Therefore, an approximation technique using the truth table was proposed. When a truth table is created, a combination of status c is ignored for failure of x over some numbers. Approximated reliability R' is evaluated from upper limit R^+ and lower limit R^-. Term R^+ is evaluated from where $\phi(c)$ is only failure status and R^- is evaluated from where $\phi(c)$ is only normal status. Term R^+ and R^- are formulated as follows.

$$R^+(G) = 1 - \sum_{c \in C} p(\phi(c) = 0), \tag{6.1}$$

$$R^-(G) = \sum_{c \in C} p(\phi(c) = 1). \tag{6.2}$$

Then, the approximated reliability, R', is evaluated as follows.

$$R'(G) = \frac{R^+(G) + R^-(G)}{2}. \tag{6.3}$$

Other techniques to reduce the calculation time such as factoring and reduction techniques have been proposed [86, 87]. The factoring technique is defined such that communication reliability is given by

$$R(G) = pR(G * x) + (1 - p)R(G - x), \tag{6.4}$$

where p is the reliability of x, and $G * x$ and $G - x$ are the new networks obtained by contracting and deleting the given link or node x. The reduction technique can reduce the size of a graph while preserving its reliability. For analyzing path reliability, removal reduction and series reduction are introduced. In the removal

reduction links and nodes that the route does not pass through are removed. When The graph G' constructed newly is formulated as follows.

$$\text{If } \forall y \in Y, \exists x \notin \psi(Y), \text{then } G' = G - x, \tag{6.5}$$

where $y \in Y$ is a route, $\psi(y)$ is a set comprising link and node through which route y passes. The series reduction can resolve new reliability issues between nodes belonging in route y. Newly constructed reliability $p'(x_i)$ is formulated as follows.

$$\text{If } \forall x_i \in X, \forall x_j \in X, \{y | y \in Y, x_i \in \psi(Y)\} = \{y | y \in Y, x_j \in \psi(Y)\}, \text{then } p'(x_i) = p(x_i)p(x_j), \tag{6.6}$$

where $\{x_i, x_j\} \in X$. To effectively and accurately analyze the reliability, an approximation reliability evaluation algorithm is introduced incorporating N time - floating and reduction techniques using truth table that ignores over M number failures as shown in Algorithm 9.

Algorithm 9 N time - floating and reduction techniques using truth table that ignores over M number failures

INPUT: Topology in the wavelength layer, physical routes, and reliability of x.
OUTPUT: Communication reliability R.

1: Apply removal reduction in G as described in Equation (6.5).
2: Decide target link or node, x, at random for floating technique.
3: For x, apply floating technique and create two statuses of normal and failure. Reliability of normal is p_x and that of failure is $1 - p_x$.
4: For graph $G - x$, if communication is disconnected, reliability in $G - x$ is 0, finish the floating technique at this time, and go to Step 6. Otherwise, go to next Step.
5: Apply series reduction as described in Equation (6.6).
6: Repeat recursively from Step 2 to 5 N times.
7: For all x in graphs $G * x$ and $G - x$ to which the floating technique can be applied, create a truth table that ignores over M number failures. The approximated reliability is evaluated.
8: Sum the reliability in all G' branches and reliability evaluated in Step 7.

Figure 6.3 shows the explanation for evaluating reliability. In this example, the floating technique is assumed to be applied at one time ($N = 1$) and when the truth table is created, failures over 3 ($M = 3$) are ignored. Only the link reliability is considered. In I, link A-B is the target to which the floating technique is to be applied. Next, graph G is branched as status of normal link A-B in II in graph G_1 and status of failure link A-B in III in graph G_2. Each reliability is evaluated to $p_{e(a,b)}$ and $1 - p_{e(a,b)}$ respectively, where $p_{e(i,j)}$ is reliability in link $i(\in V)$ and $j(\in V)$. In IV, reduction technique is applied between A and D, and the reliability in this graph is evaluated as follows.

$$R(G_2) = (1 - p_{e(a,b)})(p_{e(a,c)}p_{e(c,d)}). \tag{6.7}$$

On the other hand, in V, a truth table that does not consider simultaneous failure over three links is created and then $R^{+}(G_1)$ and $R^{-}(G_1)$ are calculated as follows.

$$R'^{+}(G_1) = 1 - \big\{(1 - p_{e(b,d)})p_{e(a,c)}(1 - p_{e(c,d)})\big\}, \tag{6.8}$$

$$R'^{-}(G_1) = p_{e(b,d)}p_{e(a,c)}p_{e(c,d)} + p_{e(b,d)}p_{e(a,c)}(1 - p_{e(c,d)}) + p_{e(b,d)}(1 - p_{e(a,c)})p_{e(c,d)} + \cdots. \tag{6.9}$$

Finally, from Equations (6.7) - (6.9), the communication reliability can be evaluated as follows.

$$R(G_1 + G_2) = p_{e(b,d)}\frac{R^{+}(G_1) + R^{-}(G_1)}{2} + R(G_2). \tag{6.10}$$

6.6 Numerical Evaluation

6.6.1 Simulation conditions

The simulation conditions are described hereafter. Routes comprising redundant paths are assumed to be node and link disjoints and the quality level, i.e., difference in delay does not consider. Multi-granular sub-lambda path demands in a full mesh topology are assumed. These demands are accommodated randomly one-by-one from the source to the destination node. The patterns are changed 10 times and the average of the results is calculated. The statistical ratios assumed for the reliability classes are 1 : 1 : 1 : 1 for H^{+}RC : HRC : LRC : L^{-}RC and all classes are divided based on an equal ratio. Reconfiguration is performed when the wavelength path resources, i.e., the number of wavelength paths that can be accommodated at some source and destination node, is less than four. The threshold number for reconfiguration is assumed to be 10 % of the number of wavelengths multiplexed in a fiber (=40). The fiber extension policy is defined such that when it becomes impossible to store a path, the shortest path search is performed and the fewest links are selected based on the number of extensions. The number of ports in the ODU-XC is 32 and that is extended when all ports are used. The statistical ratio of the traffic demand for each sub-lambda path (2.5 G : 10 G : 40 G) is 5 : 2 : 3. The wavelength bandwidth is 40 G. The employed physical topology is the NSF network (14 nodes and 21 links) as shown in Fig. 4.16 (a) in Section 4.6.2.

6.6.2 Results and Discussion

Comparative results for the number of fibers, the number of transponders and the number of ODU-XCs are shown in Figs. 6.4, 6.5 and 6.6 respectively. As shown in Fig. 6.4, the number of fibers for the proposed design with reconfiguration using RSF or RMPS can be reduced by a few fibers compared to that for No reconfiguration. As shown in Fig. 6.5, the number of transponders can be reduced by approximately 29 for RSF and 25 for RMPS at 9 [Tbps] representing reduction

I. Applied floating technique at one time.

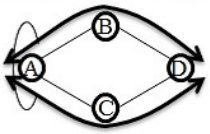

II. Link A-B is assumed not to fail.
⇒Reliability: $p_{e(a,b)}$

III. Link A-B is assumed to fail.
⇒ Reliability: $1 - p_{e(a,b)}$

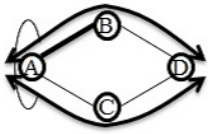

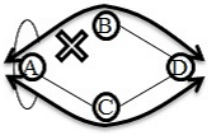

V. Create truth table not considering simultaneous failure over three links.
⇒Approximated reliability:
$p_{e(a,b)}(R^{+}+R^{-})/2$

IV. Reduction technique is applied between A and D.
⇒Reliability:
$(1 - p_{e(b,d)})\,(p_{e(a,c)}p_{e(c,d)})$

Link / Status	BD	AC	CD	Φ(c)	
c1	1	1	1	1	Normal
c2	1	1	0	1	
c3	1	0	1	1	
c4	0	1	1	1	
c5	1	0	0	1	
c6	0	1	0	0	Failure
c7	0	0	1	1	Normal

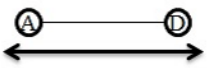

VI. Total reliability = $p_{e(a,b)}(R^{+}+R^{-})/2 + (1 - p_{e(b,d)})(p_{e(a,c)}p_{e(c,d)})$

Figure 6.3. Explanation of reliability evaluation.

is rates of 6 % for RSF and 5.3 % for RMPS, respectively. As shown in Fig. 6.6, there is no significant difference between proposed design with reconfiguration and no reconfiguration.

The comparative results for the relative equipment cost for no reconfiguration is shown in Fig. 6.7. Total cost C_{Total} is the sum of the node device cost described in Equation 5.1 in Section 5.3. As shown in Fig. 6.7, compared to no reconfiguration the reduction in the equipment cost for the proposed design with reconfiguration can be increased gradually by approximately 6 % for RSF and 5.5% for RMPS. Based on these results, the cost effectiveness of the proposed design is shown. There is hardly any difference between the effectiveness for RSF and that for RMPS. The reason is that there are no constraints to accommodate the primary path in this simulation. For instance, when the primary path route must be accommodated under constraints of the shortest route, the results for RSF and RMPS may be different. Those analyses are left for further study.

In this simulation, the reliability of each link is assumed to be 0.9999 ($= 1 - 10^{-4}$) and the node reliability is not considered. The evaluation algorithm for reliability is described in Section 6.5. The floating technique is assumed to be applied ten times ($N = 10$) and when a truth table is created, failure over 2 ($M = 2$) is ignored. Table 6.2 gives the average reliability, which is defined as the sum of all path reliabilities divided by the number of paths, for "No reconfiguration" , "Reconfiguration (RSF)" and "Reconfiguration (RMPS)". When the volume of traffic is increased, the reliability of the proposed design with RSF or RMPS to that for no reconfiguration is $(1 - 10^{-6})$ times. The difference in reliability occurs because when reconfiguring, a low granularity sub-lambda path is reconfigured to vacant existing wavelength paths including a detour route. The numbers of paths accommodated in the detour route for RSF and RMPS exceed that for no reconfiguration. The proposed design with reconfiguration is considered to retain the link disjoint based on the results where there are no large fluctuations in reliability according to increasing traffic.

Table 6.2. Comparison of Reliability

Traffic [Tbps]	No reconfiguration	RSF	RMPS
1.5	0.9998801	0.9998801	0.9998801
3.0	0.9998773	0.9998772	0.9998772
4.5	0.9998764	0.9998743	0.9998741
6.0	0.9998772	0.9998752	0.9998750
7.5	0.9998777	0.9998749	0.9998750
9.0	0.9998766	0.9998745	0.9998747

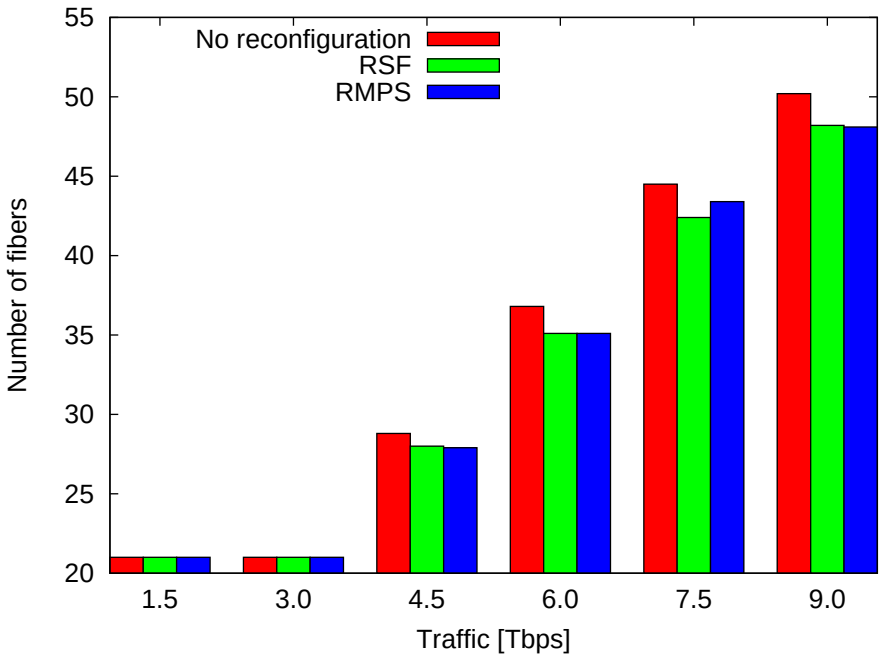

Figure 6.4. Comparison of number of fibers for differential reliability path.

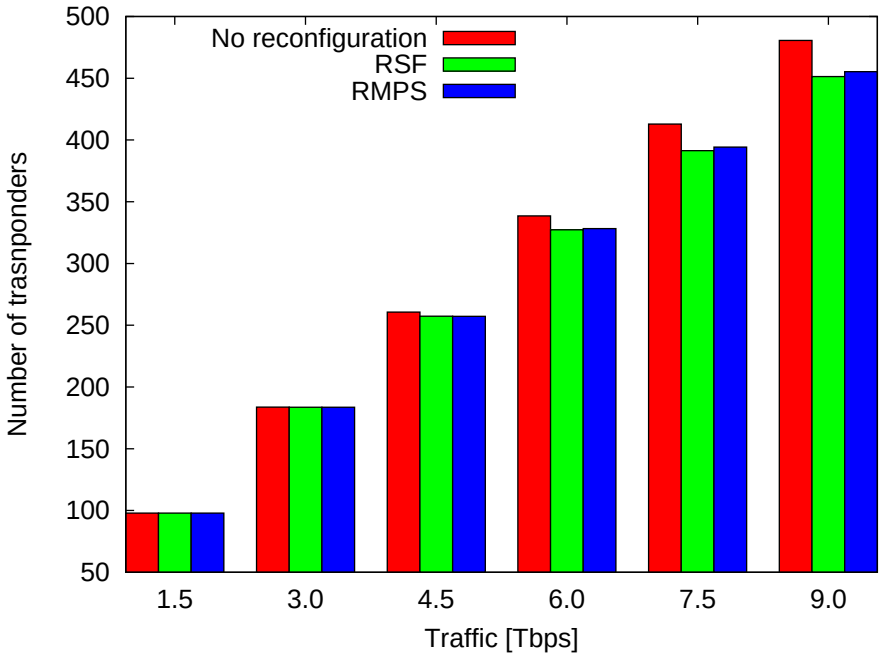

Figure 6.5. Comparison of number of transponders for differential reliability path.

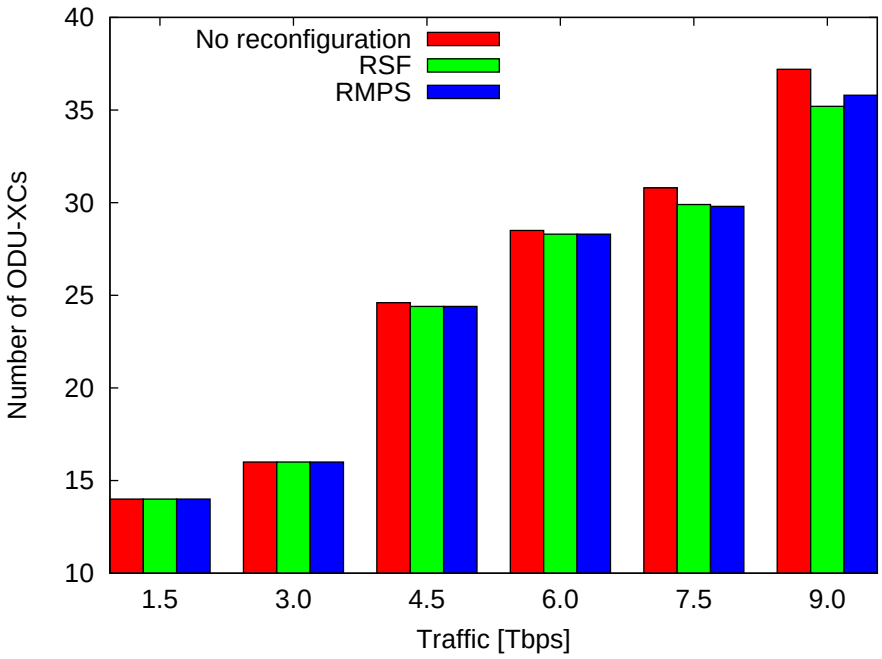

Figure 6.6. Comparison of number of ODU-XCs for differential reliability path.

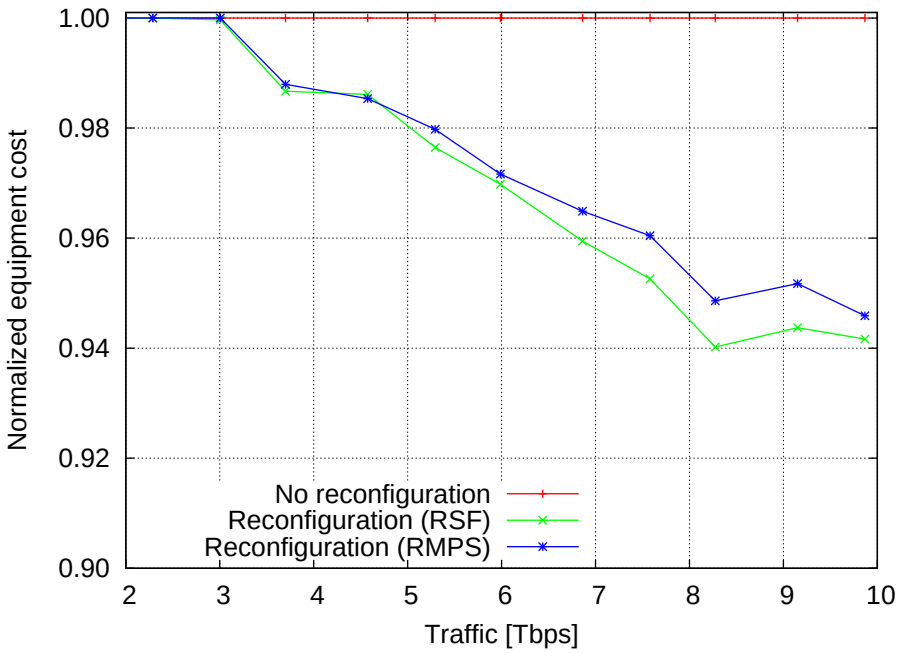

Figure 6.7. Comparison of equipment cost for differential reliability path.

6.7 Summary

This chapter presented differentiated reconfiguration to address the trade-off relationship between accommodation efficiency and disruption risks in virtualized multi-layer transport networks that considers reliability classes defined as a combination of including or excluding a secondary path and allowing or not allowing reconfiguration. To actualize the proposed design, a multi-layer redundant path accommodation design scheme and a reconfiguration algorithm were proposed. An evaluation algorithm for reliability was also introduced. Numerical evaluations assuming all classes were equally represented, showed that the proposed design scheme with reconfiguration reduces the required number of fibers slightly compared to that without consideration of reliability classes and that the equipment cost can be reduced by approximately 6 %. To analyze the availability, it was introduced that N time - floating and reduction techniques using truth table that ignores over M number failures. Reliability comparisons showed that the proposed design scheme with reconfiguration is considered to retain link disjointness. The proposed reconfigurable networks were shown to be a cost effective solution while maintaining reliability.

Chapter 7

Conclusions

7.1 Research Summary

This dissertation presented innovative research on reconfigurable multi-layer and multi-granular photonic transport network design. Chapter 1 presented the introductory background. Quasi-dynamic and multi-granular traffic will certainly increase in the future. Therefore, in the wavelength layer, wavelength fragmentation will increase and wavelength accommodation efficiency will degrade. In the sub-lambda layer, the optimum virtual topology is also changing according to the amount of traffic and sources and sinks of the traffic. Chapter 2 presented a comprehensive review of related work. For effective accommodation of traffic, it is necessary to reconfigure wavelength paths in cooperation with sub-lambda paths. The contributions of this dissertation are summarized below.

Chapter 3 presented optical path accommodation design and resource management schemes for optical transparent WDM networks. The pre-planning based wavelength path reconfiguration scheme was proposed. In the pre-planning stage, optical path is designed in advance based on demand prediction and reserved on calculated routes as path group. In the operation stage, optical path is accommodated and virtually reconfigured routes and wavelengths in the logical end-to-end link if demand prediction is different from the actual demand. The proposed PRW scheme achieves fast provisioning and flexibility in dealing with changes in the prediction of optical path demand.

Chapter 4 presented a wavelength path reconfiguration scheme that reduces wavelength fragmentation in three phases: i) reconfiguration trigger phase; ii) reconfiguration design phase; and iii) migrating sequence phase from old path set to new path set. Two cost models were introduced: wavelength fragmentation cost and reconfiguration cost, and a reconfiguration design was introduced that reduces the number of changed wavelengths while retaining the effectiveness of wavelength defragmentation using ILP. For the migration phase, a migrating sequence algorithm was proposed that prevents service disruption by using spare wavelengths to break the dependency cycles that may be formed in moving to the new path set. A wavelength defragmentation scheme based on wavelength resource management and three heuristic algorithms based on it were proposed. The proposed schemes were shown that the number of fibers and the number of migrating sequences can

be reduced, and that the accommodation efficiency is increased compared to the case when reconfiguration is not performed.

Chapter 5 presented sub-lambda path regrooming with wavelength defragmentation. The ILP-based GRWD scheme was proposed that reconfiguration is performed in two steps: first step of sub-lambda path re-grooming and second step of wavelength defragmentation. For the heuristic approach, an adaptive reconfiguration scheme based on wavelength path resource management was presented. A sub-lambda path regrooming algorithm, MSF, was also proposed which regrooming multi-hop sub-lambda paths to single-hop sub-lambda paths first. The proposed sub-lambda path regrooming with wavelength defragmentation schemes were shown that the rate at which the multi-hop sub-lambda paths are changed before and after re-optimization is also decreased deeply in an environment with incremental traffic, and that the CAPEX, not only the number of fiber but also the number of transponders, can be reduced compared to conventional schemes and no reconfiguration.

Chapter 6 presented differentiated reconfiguration to address the trade-off in virtualized multi-layer transport networks that considers reliability classes defined as a combination of including or excluding a secondary path and allowing or not allowing reconfiguration. To actualize the proposed design, a multi-layer redundant path accommodation design scheme and a reconfiguration algorithm were proposed. An evaluation algorithm for reliability was also introduced. The proposed reconfigurable networks were shown to be a cost effective solution while maintaining reliability.

7.2 Future Prospects

This dissertation introduced proposals for reconfiguration that are highly effective as they resolve the following four study challenges: 1. Wavelength path accommodation design and reconfiguration, 2. Sub-lambda path regrooming, 3. Reduction in migrating sequence and 4. Path accommodation design and reconfiguration for different reliability classes. When high capacity and dynamic traffic streams will emerge in the near future, for instance, with the deployment of LTE-Advanced, these proposals could be used to reduce not only CAPEX but also OPEX.

On the other hand, a recent proposal is the spectrum-efficient and scalable optical network architecture called the spectrum-sliced elastic optical path network [88]. The necessary spectral resources on a given route are sliced off from the available pool and adaptively allocated to the end-to-end optical path according to the client data rate and the available spectral resources. In the elastic optical network, reconfiguration can be also a promising way of reducing the capital expenditure cost. In distance adaptive operation [89], the route distance constraint should be addressed at reconfiguration where the performances of various modulation formats, i.e. QPSK, 16QAM and 64QAM must be considered. In addition, the spectrum continuity constraint is also critical. Reconfiguration design with these two constraints that targets fragmentation and reconfiguration costs is left for further study.

References

[1] K.-I. Sato and H. Hasegawa, "Optical networking technologies that will create future bandwidth-abundant networks," *Journal of Optical Communications and Networking*, vol. 1, no. 2, pp. A81–A93, 2009.

[2] Cisco Global Cloud Index: Forecast and Methodology, 2013-2018,White paper,2014.

[3] Cisco Visual Networking Index: Forecast and Methodology, 2014-2019,White paper,2015.

[4] A. Ghosh, R. Ratasuk, B. Mondal, N. Mangalvedhe, and T. Thomas, "LTE-advanced: next-generation wireless broadband technology," *IEEE Wireless Communications*, vol. 17, no. 3, pp. 10–22, 2010.

[5] Y. Miyamoto and H. Takenouchi, "Dense space-division-multiplexing optical communications technology for petabit-per-second class transmission," *NTT Technical Review*, vol. 12, no. 12, pp. 1–7, Dec. 2014.

[6] E. Yamazaki, M. Tomizawa, and Y. Miyamoto, "100-Gb/s optical transport network and beyond employing digital signal processing," *IEEE Communications Magazine*, vol. 50, no. 2, pp. s43–s49, 2012.

[7] T. Kobayashi, A. Sano, A. Matsuura, M. Yoshida, T. Sakano, H. Kubota, Y. Miyamoto, K. Ishihara, M. Mizoguchi, and M. Nagatani, "45.2 Tb/s C-band WDM transmission over 240km using 538Gb/s PDM-64QAM single carrier FDM signal with digital pilot tone," in *Proceedings of European Conference and Exposition on Optical Communications (ECOC)*, pp. Th–13, 2011.

[8] K.-I. Sato and M. Koga, *Broadband optical networking technologies: Photonic networks (in Japanese)*. IEICE, 2003.

[9] A. H Reeves, French Patent, No. 49 159/833 929,1937.

[10] M. R. Aaron, "PCM transmission in the exchange plant," *Bell System Technical Journal*, vol. 41, no. 1, pp. 99–141, 1962.

[11] K. Kao and G. A. Hockham, "Dielectric-fibre surface waveguides for optical frequencies," in *Proceedings of the Institution of Electrical Engineers (IEE)*, vol. 113, pp. 1151–1158, 1966.

[12] T. Miya, Y. Terunuma, T. Hosaka, and T. Miyashita, "Ultimate low-loss single-mode fibre at 1.55 μm," *Electronics Letters*, vol. 15, no. 4, pp. 106–108, 1979.

[13] S. Shimada and N. Uchida, "Field trial of medium small capacity optical fiber transmission-systems," *Review of The Electrical Communications Laboratories*, vol. 29, no. 11-1, pp. 1087–1093, 1981.

[14] H. Ishio, "Japanese field trails and applications in telephony," *IEEE Journal on Selected Areas in Communications*, vol. 1, no. 3, pp. 404–412, 1983.

[15] S. Matsuoka, "Ultrahigh-speed ultrahigh-capacity transport network technology for cost-effective core and metro networks," *NTT Technical Review*, vol. 9, no. 8, 2011.

[16] T. Kawasaki, M. Inami, Y. Sasakura, D. Shimazaki, M. Horiguchi, and K. Koda, "Development of 100-Gbit/s packet transport system," *NTT Technical Review*, vol. 13, no. 3, 2015.

[17] "Network node interface for the synchronous digital hierarchy," ITU-T Recommendation, G. 707/Y.1322.

[18] "Interfaces for the optical transport network,"ITU-T Recommendation, G. 709/Y. 1331.

[19] "A framework for MPLS in transport networks,"IETF network working group, RFC. 5921.

[20] T. Ohara and O. Ishida, "Standardization activities for the optical transport network," *NTT Technical Review*, vol. 7, no. 3, 2009.

[21] "Architecture of optical transport networks," ITU-T Recommendation G. 872.

[22] M. Murakami and Y. Koike, "Overview of MPLS-TP standardization," *NTT Technical Review*, vol. 11, no. 5, May 2013.

[23] "Requirements for operations, administration, and maintenance (OAM) in MPLS Transport Networks," IETF network working group, RFC. 5860.

[24] "Operations, administration and maintenance mechanism for MPLS-TP in packet transport networks ," ITU-T Recommendation G. 8113.1.

[25] K.-I. Sato, S. Okamoto, and H. Hadama, "Network performance and integrity enhancement with optical path layer technologies," *IEEE Journal on Selected Areas in Communications*, vol. 12, no. 1, pp. 159–170, 1994.

[26] H. Zang, J. P. Jue, and B. Mukherjee, "A review of routing and wavelength assignment approaches for wavelength-routed optical WDM networks," *Optical Networks Magazine*, vol. 1, no. 1, pp. 47–60, 2000.

[27] A. Kadohata, A. Hirano, Y. Sone, and O. Ishida, "Wavelength path reconfiguration to reduce fragmentation and number of operations in WDM mesh networks," in *Proceedings of European Conference and Exposition on Optical Communications (ECOC)*, pp. Mo–2, 2011.

[28] K. Sone, X. Wang, S. Oda, G. Nakagawa, Y. Aoki, I. Kim, P. Palacharla, T. Hoshida, M. Sekiya, and J. C. Rasmussen, "First demonstration of hitless spectrum defragmentation using real-time coherent receivers in flexible grid optical networks," in *Proceedings of European Conference and Exhibition on Optical Communication (ECOC)*, pp. Th–3, 2012.

[29] F. Rambach, B. Konrad, L. Dembeck, U. Gebhard, M. Gunkel, M. Quagliotti, L. Serra, and V. López, "A multilayer cost model for metro/core networks," *Journal of Optical Communications and Networking*, vol. 5, no. 3, pp. 210–225, 2013.

[30] A. Gençata and B. Mukherjee, "Virtual-topology adaptation for WDM mesh networks under dynamic traffic," *IEEE/ACM Transactions on Networking*, vol. 11, no. 2, pp. 236–247, 2003.

[31] A. Kadohata, A. Watanabe, Y. Sone, T. Sakano, W. Imajuku, and M. Jinno, "Fast and flexible optical path accommodation design based on pre-planning and reconfiguration in transparent optical mesh networks," in *Proceedings of Optical Network Design and Modeling (ONDM), 2010 14th Conference on*, pp. 1–6, 2010.

[32] A. Kadohata, A. Hirano, F. Inuzuka, A. Watanabe, and O. Ishida, "Wavelength defragmentation design for multi-fiber WDM networks," in *Proceedings of The 10th International Conference on Optical Internet (COIN)*, 2012.

[33] A. Kadohata, A. Hirano, F. Inuzuka, A. Watanabe, and O. Ishida, "Wavelength path reconfiguration design in transparent optical WDM networks," *Journal of Optical Communications and Networking*, vol. 5, no. 7, pp. 751–761, 2013.

[34] A. Kadohata, T. Tanaka, A. Watanabe, F. Inuzuka, and A. Hirano, "Wavelength defragmentation algorithm for transparent multi-ring networks with multiple-fibers per link," in *Proceedings of Optical Fiber Communication Conference (OFC)*, pp. OW3A–7, 2013.

[35] A. Kadohata, A. Watanabe, A. Hirano, H. Hasegawa, and K.-I. Sato, "Pre-adjustment rerouting for wavelength defragmentation in optical transparent WDM networks," *IEICE Transactions on Communications*, vol. 98, no. 10, pp. 2014–2021, 2015.

[36] A. Kadohata, A. Hirano, M. Fukutoku, T. Ohara, Y. Sone, and O. Ishida, "Multi-layer greenfield re-grooming with wavelength defragmentation," *IEEE Communications Letters*, vol. 16, no. 4, pp. 530–532, 2012.

[37] A. Kadohata, "Adaptive reconfiguration of sub-lambda and wavelength paths for unpredictable traffic demands," in *Proceedings of Optical Fiber Communications Conference and Exhibition (OFC), 2014*, pp. 1–3, 2014.

[38] A. Kadohata, A. Watanabe, and A. Hirano, "Sub-lambda and wavelength path reconfiguration in multi-layer transport networks," *Journal of Optical Communications and Networking*, vol. 7, no. 3, pp. A432–A439, 2015.

[39] A. Kadohata, T. Tanaka, A. Watanabe, A. Hirano, H. Hasegawa, and K.-I. Sato, "Path accommodation design and reconfiguration for different reliability classes in virtualized multi-layer transport network," in *Proceedings of The 20th Opto Electronics and Communications Conference (OECC)*, p. JTuB.24, 2015.

[40] A. Kadohata, T. Tanaka, A. Watanabe, A. Hirano, H. Hasegawa, and K.-I. Sato, "Differential reliability path accommodation design and reconfiguration in virtualized multi-layer transport network," *IEICE Transactions on Communications*, vol. 98, no. 11, pp. 2151–2159, 2015.

[41] M. Fukutoku, T. Ohara, A. Kadohata, A. Hirano, T. Kawai, T. Komukai, M. Suzuki, S. Aisawa, T. Takahashi, M. Tomizawa, *et al.*, "Optimized multi-layer optical network using in-service ODU/wavelength path re-grooming," in *Proceedings of Optical Fiber Communication Conference and Exposition and the National Fiber Optic Engineers Conference (OFC/NFOEC)*, 2011.

[42] K. Zhu and B. Mukherjee, "Traffic grooming in an optical WDM mesh network," *IEEE Journal on Selected Areas in Communications*, vol. 20, no. 1, pp. 122–133, 2002.

[43] T. Ono, T. Ohara, M. Suzuki, S. Aisawa, and M. Tomizawa, "Novel ODU path switching for ODU reallocation without bit disruption using dynamic delay control scheme," in *Proceedings of National Fiber Optic Engineers Conference (NFOEC)*, p. JWA7, 2011.

[44] B. Mukherjee, *Optical WDM networks*. Springer Science & Business Media, 2006.

[45] I. Chlamtac, A. Ganz, and G. Karmi, "Lightpath communications: An approach to high bandwidth optical WAN's," *IEEE Transactions on Communications*, vol. 40, no. 7, pp. 1171–1182, 1992.

[46] Y. Sone, A. Hirano, A. Kadohata, and O. Ishida, "Efficient routing and wavelength assignment algorithm minimizes wavelength fragmentations in WDM mesh networks," in *Proceedings of 16th Opto-Electronics and Communications Conference (OECC)*, 2011.

[47] F. Inuzuka, A. Kadohata, T. Tanaka, Y. Sone, A. Hirano, A. Watanabe, and O. Ishida, "Optical path accommodation efficiency with provisioning order in least fragmentation algorithm," in *Proceedings of 17th Opto-Electronics and Communications Conference (OECC)*, pp. 119–120, 2012.

[48] P. Winzer, "Beyond 100G ethernet," *IEEE Communications Magazine*, vol. 48, no. 7, pp. 26–30, 2010.

[49] E. Modiano, "Traffic grooming in WDM networks," *IEEE Communications Magazine*, vol. 39, no. 7, pp. 124–129, 2001.

[50] M. Zhang, C. You, H. Jiang, Z. Zhu, Y. Yin, L. Liu, and S. Yoo, "Adaptive spectrum defragmentation with intelligent timing and object selection for elastic optical networks with time-varying traffic," in *Proceedings of European Conference and Exposition on Optical Communications (ECOC)*, 2013.

[51] X. Chu, T. Bu, and X.-y. Li, "A study of lightpath rerouting schemes in wavelength-routed WDM networks," in *IEEE International Conference on Communications (ICC)*, pp. 2400–2405, 2007.

[52] M. Nakagawa, H. Hasegawa, K.-I. Sato, R. Sugiyama, T. Takeda, E. Oki, and K. Shiomoto, "New dynamic network design and provisioning algorithms for broadband connection services considering fairness," in *Proceedings of Optical Network Design and Modeling (ONDM) 2009*, pp. 1–6, 2009.

[53] B. Zhou, J. Zheng, and H. T. Mouftah, "Dynamic reconfiguration based on balanced alternate routing algorithm (BARA) for all-optical wavelength-routed WDM networks," in *Proceedings of Global Telecommunications Conference (GLOBECOM)*, vol. 3, pp. 2706–2710, 2002.

[54] E. Bouillet, J.-F. Labourdette, R. Ramamurthy, and S. Chaudhuri, "Lightpath re-optimization in mesh optical networks," *IEEE/ACM Transactions on Networking (TON)*, vol. 13, no. 2, pp. 437–447, 2005.

[55] D. Banerjee and B. Mukherjee, "Wavelength-routed optical networks: Linear formulation, resource budgeting tradeoffs, and a reconfiguration study," *IEEE/ACM Transactions on Networking (TON)*, vol. 8, no. 5, pp. 598–607, 2000.

[56] J. Y. Zhang, O. W. Yang, J. Wu, and M. Savoie, "Optimization of semi-dynamic lightpath rearrangements in a WDM network," *IEEE Journal on Selected Areas in Communications*, vol. 25, no. 9, pp. 3–17, 2007.

[57] F. Cugini, F. Paolucci, G. Meloni, G. Berrettini, M. Secondini, F. Fresi, N. Sambo, L. Poti, and P. Castoldi, "Push-pull defragmentation without traffic disruption in flexible grid optical networks," *Journal of Lightwave Technology*, vol. 31, no. 1, pp. 125–133, 2013.

[58] A. N. Patel, P. N. Ji, J. P. Jue, and T. Wang, "Defragmentation of transparent flexible optical WDM (FWDM) networks," in *Proceedings of Optical Fiber Communication (OFC)*, p. OTuI8, 2011.

[59] M. Saad and Z.-Q. Luo, "Reconfiguration with no service disruption in multifiber WDM networks," *Journal of lightwave technology*, vol. 23, no. 10, p. 3092, 2005.

[60] G. Mohan, P. H. H. Ernest, and V. Bharadwaj, "Virtual topology reconfiguration in IP/WDM optical ring networks," *Computer communications*, vol. 26, no. 2, pp. 91–102, 2003.

[61] A. Narula-Tam and E. Modiano, "Dynamic load balancing in WDM packet networks with and without wavelength constraints," *IEEE Journal on Selected Areas in Communications*, vol. 18, no. 10, pp. 1972–1979, 2000.

[62] F. Solano and M. Pióro, "Lightpath reconfiguration in WDM networks," *Journal of Optical Communications and Networking*, vol. 2, no. 12, pp. 1010–1021, 2010.

[63] N. Jose and A. K. Somani, "Connection rerouting/network reconfiguration," in *Proceedings of Design of Reliable Communication Networks (DRCN)*, pp. 23–30, 2003.

[64] J.-F. P. Labourdette, G. W. Hart, and A. S. Acampora, "Branch-exchange sequences for reconfiguration of lightwave networks," *IEEE Transactions on Communications*, vol. 42, no. 10, pp. 2822–2832, 1994.

[65] Y. Zhang, M. Murata, H. Takagi, and Y. Ji, "Traffic-based reconfiguration for logical topologies in large-scale WDM optical networks," *Journal of lightwave technology*, vol. 23, no. 10, p. 2854, 2005.

[66] R. Martínez, C. Pinart, J. Comellas, and G. Junyent, "Routing issues in transparent optical networks," in *Proceedings of International Conference on Transparent Optical Networks, 2006 International Conference on*, vol. 3, pp. 189–194, 2006.

[67] Y. Huang, J. P. Heritage, and B. Mukherjee, "Connection provisioning with transmission impairment consideration in optical WDM networks with high-speed channels," *Journal of Lightwave Technology*, vol. 23, no. 3, pp. 982–993, 2005.

[68] Y. Sone, A. Kadohata, A. Watanabe, W. Imajuku, K. Matsuda, M. Jinno, T. Takahashi, S. Matsuoka, A. Suzuki, H. Tokuda, *et al.*, "Management and control scheme employing wavelength-grouped transmission-guaranteed link for highly-manageable and cost-efficient transparent optical mesh networks," *Proceedings of European Conference and Exposition on Optical Communications (ECOC)*, 2009.

[69] "Transmission media and optical systems characteristics - Characteristics of optical systems," ITU-T Recommendation G. 680.

[70] M. Pióro and D. Medhi, *Routing, flow, and capacity design in communication and computer networks*. Elsevier, 2004.

[71] D. B. Johnson, "Finding all the elementary circuits of a directed graph," *SIAM Journal on Computing*, vol. 4, no. 1, pp. 77–84, 1975.

[72] T. H. Cormen, *Introduction to algorithms*. MIT press, 2009.

[73] A. Betker, C. Gerlach, R. Hülsermann, M. Jäger, M. Barry, S. Bodamer, J. Späth, C. Gauger, and M. Köhn, "Reference transport network scenarios," *MultiTeraNet Report, July*, 2003.

[74] S. De Maesschalck, D. Colle, I. Lievens, M. Pickavet, P. Demeester, C. Mauz, M. Jaeger, R. Inkret, B. Mikac, and J. Derkacz, "Pan-European optical transport networks: an availability-based comparison," *Photonic Network Communications*, vol. 5, no. 3, pp. 203–225, 2003.

[75] ILOG CPLEX, `http://www-01.ibm.com/software/commerce/optimization/cplex-optimizer/`.

[76] R. Huelsermann, M. Gunkel, C. Meusburger, and D. A. Schupke, "Cost modeling and evaluation of capital expenditures in optical multilayer networks," *Journal of Optical Networking*, vol. 7, no. 9, pp. 814–833, 2008.

[77] W. Yao, G. Sahin, M. Li, and B. Ramamurthy, "Analysis of multi-hop traffic grooming in WDM mesh networks," *Optical Switching and Networking*, vol. 6, no. 1, pp. 64–75, 2009.

[78] H. Alshaer and J. M. Elmirghani, "Multilayer dynamic traffic grooming with constrained differentiated resilience in IP/MPLS-over-WDM networks," *IEEE Transactions on Network and Service Management*, vol. 9, no. 1, pp. 60–72, 2012.

[79] Accedian whitepaper,"The importance of performance assurance in financial services networks," Oct. 2013.

[80] V. Eramo, M. Listanti, R. Sabella, and F. Testa, "Integrated OTN/WDM switching architecture equipped with the minimum number of OTN switches," *Journal of Optical Communications and Networking*, vol. 6, no. 2, pp. 138–151, 2014.

[81] P. Iovanna, F. Testa, R. Sabella, A. Bianchi, M. Puleri, M. R. Casanova, and A. Germoni, "Packet–optical integration nodes for next generation transport networks," *Journal of Optical Communications and Networking*, vol. 4, no. 10, pp. 821–835, 2012.

[82] S. Figuerola and M. Lemay, "Infrastructure services for optical networks [invited]," *Journal of Optical Communications and Networking*, vol. 1, no. 2, pp. A247–A257, 2009.

[83] M. Xia, M. Tornatore, C. U. Martel, and B. Mukherjee, "Service-centric provisioning in WDM backbone networks for the future internet," *Journal of Lightwave Technology*, vol. 27, no. 12, pp. 1856–1865, 2009.

[84] K. Ratnam, M. Gurusamy, and L. Zhou, "Differentiated QoS routing of restorable sub-lambda connections in IP-over-WDM networks using a multi-layer protection approach," in *Proceedings of Broadband Networks (BroadNets)*, pp. 127–136, 2005.

[85] A. Premo, "The use of boolean algebra and a truth table in the formulation of a mathematical model of success," *IEEE Transactions on Reliability*, vol. 3, pp. 45–49, 1963.

[86] L. B. Page and J. E. Perry, "A practical implementation of the factoring theorem for network reliability," *IEEE Transactions on Reliability*, vol. 37, no. 3, pp. 259–267, 1988.

[87] M. Hayashi, "System failure-frequency analysis using a differential operator," *IEEE Transactions on Reliability*, vol. 40, no. 5, pp. 601–609, 1991.

[88] M. Jinno, H. Takara, B. Kozicki, Y. Tsukishima, Y. Sone, and S. Matsuoka, "Spectrum-efficient and scalable elastic optical path network: architecture, benefits, and enabling technologies," *IEEE Communications Magazine*, vol. 47, no. 11, pp. 66–73, 2009.

[89] M. Jinno, B. Kozicki, H. Takara, A. Watanabe, Y. Sone, T. Tanaka, and A. Hirano, "Distance-adaptive spectrum resource allocation in spectrum-sliced elastic optical path network [topics in optical communications]," *IEEE Communications Magazine*, vol. 48, no. 8, pp. 138–145, 2010.

List of Publications

Journal papers

1. (Chapter 4) A. Kadohata, A. Hirano, F. Inuzuka, A. Watanabe, and O. Ishida, "Wavelength path reconfiguration design in transparent optical WDM networks," *IEEE/ OSA J. Commun. Netw.*, vol. 5 , no. 7, pp. 751-761, Jul. 2013.
2. (Chapter 4) A. Kadohata, A. Watanabe, A. Hirano, H. Hasegawa, and K.-I. Sato, "Pre-adjustment rerouting for wavelength defragmentation in optical transparent WDM networks" *IEICE Trans. Commun.*, vol. E98-B, no.10, pp.2014-2021, Oct. 2015.
3. (Chapter 5) A. Kadohata, A. Hirano, M. Fukutoku, T. Ohara, Y. Sone, and O. Ishida, "Multi-layer Greenfield regrooming with wavelength defragmentation," *IEEE Commun. Let.*, vol. 16 , Issue 4, pp. 530-532, April 2012.
4. (Chapter 5) A. Kadohata, A. Watanabe, and A. Hirano, "Sub-lambda and wavelength path reconfiguration in multi-layer transport networks," *IEEE/ OSA J. Commun. Netw.*, vol.7, no.3, pp.A432-A439, Mar. 2015.
5. (Chapter 6) A. Kadohata, T. Tanaka, A. Watanabe, A. Hirano, H. Hasegawa, and K.-I. Sato, "Differential reliability path accommodation design and reconfiguration in virtualized multi-layer transport network," *IEICE Trans. Commun.*, vol. E98-B, no.11, pp.2151-2159, Nov. 2015.

International conferences

1. (Chapter 3) A. Kadohata, A. Watanabe, Y. Sone, T. Sakano, W. Imajuku, and M. Jinno, "Fast and flexible optical path accommodation design based on pre-planning and reconfiguration in transparent optical mesh networks," in *Proc. ONDM2010*, Feb. 2010.
2. (Chapter 4) A. Kadohata, A. Hirano, Y. Sone, and O. Ishida, "Wavelength path reconfiguration to reduce fragmentation and number of operations in WDM mesh networks," in *Proc. ECOC2011*, Mo.1.K, Sept. 2011.
3. (Chapter 4) A. Kadohata, A. Hirano, F. Inuzuka, A. Watanabe, and O. Ishida, "Wavelength defragmentation design for multi-fiber WDM networks," in *Proc. COIN2012*, WA.4, May 2012.
4. (Chapter 4) A. Kadohata, T. Tanaka, A. Watanabe, F. Inuzuka, and A. Hi-

rano, "Wavelength defragmentation algorithm for transparent multi-ring networks with multiple-fibers per Link," in *Proc. OFC/NFOEC 2013*, OW3A.7, Mar. 2013.

5. (Chapter 5) A. Kadohata, "Adaptive reconfiguration of sub-lambda and wavelength paths for unpredictable traffic demands," in *Proc. OFC2014*, W4A.5, pp.1-3, Mar. 2014.
6. (Chapter 6) A. Kadohata, T. Tanaka, A. Watanabe, A. Hirano, H. Hasegawa, and K.-I. Sato, "Path accommodation design and reconfiguration for different reliability classes in virtualized multi-layer transport network," in *Proc. OECC 2015*, JTuB.24, Jun. 2015.

Domestic conferences

1. 門畑顕博, 渡辺篤, 曽根由明, 坂野寿和, 今宿亙, 神野正彦, "トランスペアレント光網における光パス再収容設計方式の提案"　電子情報通信学会 PN 研究会, pp47-52, 2009 年 8 月.
2. 門畑顕博, 渡辺篤, 平野章, 石田修, "迅速で柔軟な設計が可能なトランスペアレント光網光パス収容設計, "　電子情報通信学会総合大会, B-12-3, 2010 年 3 月.
3. 門畑顕博, 平野章, 曽根由明, 石田修, "移設手順量を考慮した光パス再配置方式, "　電子情報通信学会ソサイエティ大会, B-10-69, 2011 年 9 月.
4. 門畑顕博, 平野章, 曽根由明, 石田修, "波長パス再配置方式の検討"　電子情報通信学会 OCS 研究会, 2011 年 10 月.
5. 門畑顕博, 平野章, 犬塚史一, 渡辺篤, 石田修, "マルチファイバ環境における波長パス再配置設計, "　電子情報通信学会ソサイエティ大会, B-10-70, 2012 年 9 月.
6. 門畑顕博, 渡辺篤, 曽根由明, 坂野寿和, 今宿亙, 神野正彦, "波長パスリソース管理に基づいた波長デフラグ"　電子情報通信学会 PN 研究会, pp.53-58, 2013 年 8 月.

Others

Journal papers

1. T. Sakano, A. Kadohata, Y. Sone, A. Watanabe, and M. Jinno, "Multi-layer hypercube photonic network architecture for intra-Datacenter Network," IEICE Transactions on Communications, vol.E94-B, no.4, pp.910-917, April 2011.
2. A. Kadohata, T. Tanaka, W. Imajuku, F. Inuzuka, and A. Watanabe, "Rapid restoration sequence of fiber links and communication paths after catastrophic failure," to be submitted to *IEICE Trans. Commun.*.

International conferences

1. Y. Sone, A. Kadohata, A. Watanabe, W. Imajuku, K. Matsuda, M. Jinno, T. Takahashi, S. Matsuoka, A. Suzuki, and H. Tokuda, "Management and control scheme employing wavelength-grouped transmission-guaranteed link for highly-manageable and cost-efficient transparent optical mesh networks," in *Proc. ECOC2009*, P5. 14, Sept. 2009.
2. T. Sakano, A. Kadohata, A. Watanabe, Y. Sone, and M. Jinno, "Link capacity requirements for a ROADM-based hypercube photonic Network," in *Proc. OECC2010*, pp102-103, Mar. 2010.
3. M. Fukutoku. T. Ohara, A. Kadohata, A. Hirano, T. Kawai, T. Komukai, M. Suzuki, S. Aisawa, T. Takahashi, M. Tomizawa, O. Ishida, and S. Matsuoka, "Optimized multi-layer optical network using in-service ODU / wavelength path re-grooming," in *Proc. OFC/NFOEC 2011*, NMC5, Mar. 2011.
4. Y. Sone, A. Hirano, A. Kadohata, and O. Ishida, "Efficient routing and wavelength assignment algorithm minimizes wavelength fragmentations in WDM mesh networks," in *Proc. OECC2011*, pp.176-177, Mar. 2011.
5. Y. Sone, A. Hirano, A. Kadohata, M. Jinno, and O. Ishida, "Routing and spectrum assignment algorithm maximizes spectrum utilization in optical networks," in *Proc. ECOC2011*, Mo.1.K.3, Sept. 2011.
6. F. Inuzuka, A. Kadohata, T. Tanaka, Y. Sone, A. Hirano, A. Watanabe, and O. Ishida, "Optical path accommodation efficiency with provisioning order in least fragmentation algorithm," in *Proc. OECC2012*, pp.119-120, Mar. 2012.
7. T. Oda, A. Kadohata, A. Watanabe, and A. Hirano, "Optical network optimization considering maintenance-related operational expenditure," in *Proc. ECOC2014*, P. 6. 10, Sept. 2014.

Domestic conferences

1. 門畑顕博, 渡辺篤, 曽根由明, 今宿亙, 神野正彦, "トランスペアレント光網における光パス収容設計方式の比較, " 電子情報通信学会総合大会, B-7-29, 2009 年 3 月.
2. 坂野寿和, 門畑顕博, 曽根由明, 渡辺篤, 神野正彦, "階層化ハイパーキューブ

トポロジをベースとしたフォトニックネットワークアーキテクチャの提案, ” 電子情報通信学会 PN 研究会, pp.13-18, 2009 年 8 月.
3. 坂野寿和, 門畑顕博, 曽根由明, 渡辺篤, 神野正彦, “多階層ハイパーキューブ・フォトニックネットワークの拡張法, ” 電子情報通信学会 PN 研究会, pp.57-62, 2010 年 3 月.
4. 曽根由明, 門畑顕博, 渡辺篤, 曽根由明, 今宿亙, 神野正彦, “伝送保証波長リンクを利用したトランスペアラント光網管理制御, ” 電子情報通信学会総合大会, B-12-34, 2010 年 3 月.
5. 大原拓也, 門畑顕博, 河合武司, 小野 隆, 鈴木昌弘, 小向哲郎, 平野 章, 福徳光師, “光電気ハイブリッドノードの検討, ” 電子情報通信学会 OCS 研究会, pp.57-62, 2011 年 6 月.
6. 犬塚史一, 曽根由明, 門畑顕博, 田中貴章, 渡辺篤, 平野章, 石田修, “光パス波長割当問題における Least Fragmentation 法の評価, ” 電子情報通信学会総合大会, B-10-122, 2012 年 3 月.
7. 大窪洋平, 門畑顕博, 平野章, “光マルチリング網におけるトラヒックグルーミング方式のコスト比較評価,” 電子情報通信学会総合大会, B12-18, 2013 年 3 月
8. 小田拓哉, 門畑顕博, 渡辺篤, 平野章, “保守稼働を考慮した高信頼光リンク構成技術の提案, ” 電子情報通信学会総合大会, B-10-30, 2014 年 3 月.

Patents

1. 今宿亙, 平野章, 高良秀彦, 神野正彦, 曽根由明, 門畑顕博, “光クロスコネクトスイッチ機能部及び光クロスコネクト装置,” 特許 04852491, 2012/01/11.
2. 曽根由明, 今宿亙, 簗島幸男, 門畑顕博,“ノード装置及び通信網及びパス設定方法及びプログラム,” 特許 04852499, 2012/01/11.
3. 門畑顕博, 渡辺篤, 今宿亙, 曽根由明, 神野正彦, “ネットワーク設計管理方法及び装置及び光ネットワークシステム,” 特許 04987023, 2012/07/25.
4. 曽根由明, 今宿亙, 門畑顕博, 渡辺篤, 神野正彦, “通信ノード装置及び通信システム及び通信路制御プログラム,” 特許 05027776, 2012/09/19.
5. 門畑顕博, 曽根由明, 今宿亙, 渡辺篤, 神野正彦, “管理制御システム及び管理装置,” 特許 05090312, 2012/12/05.
6. 門畑顕博, 平野章, 渡辺篤, “パス収容設計方法,” 特許 05419740, 2014/02/19.
7. 曽根由明, 平野章, 門畑顕博, 田中貴章, “光通信網及び通信路設定方法及び光通信網管理システム及び運用システム,” 特許 05455783, 2014/03/26.
8. 平野章, 曽根由明, 門畑顕博, 田中貴章, 松岡伸治, “ネットワーク保守・管理方法及びシステム,” 特許 05492684, 2014/05/14.
9. 平野章, 曽根由明, 門畑顕博, 田中貴章, 松岡伸治, “周波数割当方法および装置,” 特許 05523578(WO12/057095), 2014/06/18.
10. 大原拓也, 福徳光師, 相澤茂樹, 乾哲郎, 河合武司, 平野章, 門畑顕博, 曽根由明, 高橋哲夫, 富沢将人, “マルチレイヤ統合伝送装置及び最適化方法,” 特許 05574491, 2014/08/20.
11. 田中貴章, 曽根由明, 平野章, 門畑顕博, “伝送システム及び伝送方法,” 特許 05583851, 2014/09/03.
12. 田中貴章, 曽根由明, 平野章, 門畑顕博, “通信ノード装置及びパス割当方法,” 特許 05613631, 2014/10/29.

13. 平野章, 福徳光師, 木坂由明, 曽根由明, 門畑顕博, 田中貴章, “ノード装置、通信システム、及び故障切替方法,” 特許 05613633, 2014/10/29.
14. 門畑顕博, 平野章, 曽根由明, 田中貴章, “パス再配置方法及び装置,” 特許 05639550, 2014/12/10.
15. 門畑顕博, 平野章, 曽根由明, 田中貴章, 築島幸男, 平野章, “波長パス再配置方法及び上位レイヤパス再配置方法,” 特許 05687557, 2015/03/18.
16. 門畑顕博, 田中貴章, 犬塚史一, 渡辺篤, 平野章, “通信経路設計装置、通信経路設計方法及び通信経路設計プログラム,” 特許 05748363, 2015/07/15.
17. 田中貴章, 平野章, 門畑顕博, 石田修, “送受信制御装置、送受信制御方法及び送受信制御プログラム,” 特許 05778089, 2015/09/16.

Awards

1. 電子情報通信学会 PN 研究会賞, 2009.
2. NTT 未来ねっと研究所長表彰, 2009.
3. NTT 未来ねっと研究所長表彰, 2013.
4. 電子情報通信学会学術奨励賞, 2013.
5. NTT 先端技術総合研究所長表彰, 2015.